Infrared Finite Amplitudes

A thesis presented for the degree of
Doctor of Philosophy
by

Darren Andrew Forde

Institute for Particle Physics Phenomenology
Department of Physics
University of Durham
August 2004

Abstract

Soft and collinear singularities, known collectively as infrared singularities here, plague the calculation of scattering amplitudes in gauge theories with massless particles such as QCD. The aim of this thesis is to describe methods of deriving amplitudes that are infrared finite and therefore do not suffer from this problem. We begin with an overview of scattering theory which includes a detailed discussion of the source of infrared singularities and outlines approaches that can be used to avoid them. Taking one of these approaches, namely that of dressed states, we give a detailed description of how such states can be constructed. We then proceed to give an explicit example calculation of the total cross section of the process $e^+e^- \to 2$ jets at NLO. In this example we construct dressed amplitudes and demonstrate their lack of infrared singularities and then go on to show that the total cross section is the same as that calculated using standard field theory techniques.

We then move on and attempt to improve the efficiency of calculations using dressed states amplitudes. We describe some of the problems of the method, specifically the large numbers of diagrams produced and the multiple different delta functions present in each amplitude. In attempting to fix these issues we demonstrate the difficulties of producing covariant amplitudes from this formalism. Finally we propose the use of the asymptotic interaction representation as a solution to these difficulties and outline a method of producing covariant infrared finite scattering amplitudes using this.

Declaration

I declare that no material presented in this thesis has previously been submitted for a degree at this or any other university.

The research described in this thesis has been carried out in collaboration with Dr. Adrian Signer and parts of Chapter 4 were also done in collaboration with Mark Morley-Fletcher. Chapter 3 is derived from the following publication,

- *Infrared-finite amplitudes for massless gauge theories.* D.A. Forde and A. Signer, Nucl. Phys. B 684, 125-161.

Contents

List of Figures

Chapter 1

Introduction

1.1 Physical observables

The aim of all theoretical calculations is to produce predictions for the outcome of experimental processes. Particle physics experiments at colliders produce large amounts of data which can be analysed in many different ways. Quantities known as *physical observables* are then calculated from this analysis. Theoretical calculations must therefore produce predictions of these physical observables. This is usually achieved by perturbatively expanding and then calculating scattering elements, known as amplitudes, of the field theory describing the physics of the experiment, for example QED or QCD. The modulus squared of these amplitudes is then integrated over the entire allowed region of their parameter space. This is known as integrating over the *phase space*. To calculate a specific physical observable this integral is then weighted by some function describing the physical observable for which a prediction is required. Schematically this calculation takes the form,

$$\int dLips(k_i, ...)|\mathcal{A}|^2 \times J(k_i, ...) \tag{1.1}$$

Where *dLips* represents the phase space integral measure, $J(k_i, ...)$ is the weighting function and $\mathcal{A}$ is the amplitude.

The weighting function given by $J(k_i, ...)$ can have many forms. The simplest of which is when it is taken to be equal to one, this gives us the total cross section, a quantity which is very difficult to measure experimentally. Therefore more complicated weighting functions for easier measurements are required, for example jet definitions and thrust.

The important part of Eq.(1.1) as far as this thesis will be concerned with, is the amplitude $\mathcal{A}$. This contains all the details of the physics of the theory being used to describe the experiment. The rest of this thesis deals with defining new methods of calculating this quantity.

1.2 Quantum field theory calculations

We want to be able to calculate $\mathcal{A}$, given in Eq.(1.1). The starting point of all field theory calculations is a Lagrangian describing the theory in which we wish to calculate. This usually takes the form of a kinetic part (also known as the free part) and an interaction part, for example the Lagrangian of massless QED is given by [1],

$$\begin{aligned}\mathcal{L} &= \mathcal{L}_{kinetic} + \mathcal{L}_{int} \\ &= \overline{\psi}(x) i \not{\partial} \psi(x) - \frac{1}{4} \left(\partial_\mu A_\nu(x) - \partial_\nu A_\mu(x) \right) \left(\partial^\mu A^\nu(x) - \partial^\nu A^\mu(x) \right) \\ &\quad - e \overline{\psi}(x) \not{A}(x) \psi(x) \end{aligned} \tag{1.2}$$

Here the $\psi(x)$ are the fermionic electron fields at x and $A^\mu(x)$ is the vector photon field also at x. We want to work with a quantum field theory and so we will need to quantise the theory described by our chosen Lagrangian. Here and for the rest of this thesis we will assume that canonical quantisation has been used. Quantisation using this method involves promoting all the fields and their conjugate momenta to operators [1, 2, 3]. Commutation relations for integer spin fields and their conjugate moments are then defined on points of a particular space-time surface. Similarly for half-integer spin fields we have anti-commutation relations. Traditionally field theory commutation (or anti-commutation) relations are defined to exist between fields at equal times. This is not the only choice that could be made, other space-time surfaces can also be used. For example the surface of the light cone is used in light cone quantisation [4].

To compute $\mathcal{A}$ from the quantised theory we are then led to calculate the overlap of the *in* states with the *out* states [1]. These states describe the incoming and outgoing particle content of the system respectively. For example we could have,

$$\mathcal{A} \equiv {}_{out}\langle q(p_1)\overline{q}(p_2)|q(p_3)\overline{q}(p_4)\rangle_{in} \tag{1.3}$$

This would describe the overlap of two incoming "quarks" (with momenta p_3 and p_4), which are fields of the full Lagrangian, with two outgoing "quarks" (with momenta p_1 and p_2), which are also fields of the full Lagrangian. What is meant by a "quark" depends upon the theory we are calculating with.

There are multiple ways of calculating this quantity $\mathcal{A}$. The main method which will be used throughout this thesis is that of scattering theory, this method will be discussed in detail in Chapter 2. An alternative technique which we will describe here and use in Chapter 4 is to relate the overlap of *in* and *out* states to time ordered correlation functions. The calculation of the overlap of the *out* states with momentum q_i, to the *in* states with momentum p_i is related to the S-Matrix (see Section 2.1.8). We can then use the LSZ reduction formulation [1], to relate these S-Matrix elements to the expectation value of a time ordered product (denoted by $T\{...\}$) of fields ψ of the full theory at x_i and y_i in a correlation function,

$$\begin{aligned}
&{}_{out}\langle p_1, ..., p_n|q_1, ..., q_m\rangle_{in} \\
&= \; {}_{in}\langle p_1, ..., p_n|S|q_1, ..., q_m\rangle_{in} \\
&= \; Z^{-\frac{n+m}{2}} \int d^4x_1...d^4x_n d^4y_1...d^4y_m e^{i\sum p_i.y_i} e^{-i\sum q_i.x_i} \\
&\quad \times \Box_{y_1}...\Box_{y_n}\Box_{x_1}...\Box_{x_m}\langle 0|T\{\psi(y_1)...\psi(y_n)\psi(x_1)...\psi(x_m)\}|0\rangle
\end{aligned} \tag{1.4}$$

Here Z is a renormalisation factor [1] which relates the full fields ϕ to the *in* and *out* fields $\phi_{in/out}$ at $t \to \pm\infty$ via,

$$\psi(x) \equiv Z^{\frac{1}{2}}\psi_{in/out}(x) \tag{1.5}$$

From Eq.(1.4) we see that the S-Matrix is the residue of the multi-particle pole when when all the external particles go on-shell (i.e $p_i^2 = m^2$) in the correlation function.

Currently we cannot analytically solve these correlation functions for any "realistic" theories[1]. Only solutions for free field theories (i.e. $\mathcal{L}_{int} = 0$) exist. This is due to the complexity of the Lagrangian's involved. Progress is being made though with numerical attempts to calculate these quantities. This process is known as lattice theory, where the space-time in which the Lagrangian sits is discretised as a set of points, i.e. a lattice. This lattice can then be numerically modelled with the accuracy of the final results being then limited by the available computing power. This thesis will not be involved with numerical solutions of this sort. Instead to solve these correlation functions we will be forced to use perturbation theory.

Perturbation theory usually involves relating the full fields of the theory to the fields of the free theory (i.e. the theory given when $\mathcal{L}_{int} = 0$ in the Lagrangian of the full theory). To do this we must switch the full fields into the interaction picture using evolution operators (see Section 2.1.7). Using these we can then relate the correlation function of the full fields ψ, to fields ψ_I, which evolve in time with only the free part of the Hamiltonian [1],

$$\langle 0|T\{\psi(x_1)...\psi(x_n)\}|0\rangle = \frac{\langle 0|T\{\psi_I(x_1)...\psi_I(x_n)\exp\left(-i\int d^4x\mathcal{L}_{int}\right)\}|0\rangle}{\langle 0|T\{\exp\left(-i\int d^4x\mathcal{L}_{int}\right)\}|0\rangle} \quad (1.6)$$

This perturbative expansion now consists of correlation functions containing only fields which evolve in time in the same way as free fields. Therefore the problem of calculating the overlap of states has been reduced to that of calculating the correlation functions of time ordered products of free fields.

Wicks theorem can then be used to replace these time ordered correlation functions with free field propagators [1, 2]. This whole procedure can be encapsulated by the method of Feynman diagrams. If we want to calculate an amplitude at a particular order n in perturbation theory we can draw all topologically different ways of connecting, with lines, the incoming and outgoing particles with n vertices. Each diagram produced in this way will

[1]These are theories we would use, for example, to make predictions for collider experiments, such theories include QED, QCD etc.

then correspond to one of the ways of replacing the time ordered product of fields in the free field correlation functions with propagators. The vertices in the Feynman diagrams therefore represent interactions and any internal lines represent propagators between these interactions, for example see Figure 1.1. The sum of all Feynman diagrams with n vertices is therefore the entire perturbative amplitude at order n.

1.3 Perturbative calculations

The calculation of an amplitude $\mathcal{A}$ is split up order by order in a perturbation series. Different Feynman diagrams can be used to describe the contributions to these amplitudes. The *order* of a contribution to a process is determined by counting the power of the coupling constant in the contributing amplitude. If this power is the same as that of the lowest order diagram that contributes to that process then the contribution is known as *leading order* (LO). The topological structure of Feynman diagrams contributing at LO is usually that of a tree diagram. The next order above this is known as the *next-to-leading order* (NLO). This will have one power more in the coupling constant than the LO contribution and therefore must have an extra vertex but no new external legs. Hence NLO contributions must have an extra loop compared to the leading order diagrams. This means that NLO contributions usually have the topology of a single loop, this would be a one-loop Feynman diagram. Similarly the next order higher, which is known as *next-to-next-to-leading order* (NNLO) will consist of one further loop in the topology and so is usually given by two-loop Feynman diagrams.

As we are working with a perturbation series we will therefore also calculate the physical observables Eq.(1.1) to a particular order. The physical observable contains the modulus squared of the amplitude. So the contributions to the physical observable at a particular order will come from the multiplication of amplitudes at different orders. For a general physical observable σ_J, at order n we will have,

$$\sigma_J\Big|_n = \int dLips(p_1,...,p_m)\mathcal{A}_1^* \times \mathcal{A}_{n-1}\, J(p_1,...,p_m)$$

$$+\int dLips(p_1,...,p_{m+1})\mathcal{A}_2^* \times \mathcal{A}_{n-2}\, J(p_1,...,p_{m+1})$$
$$+...+\int dLips(p_1,...,p_m)\mathcal{A}_{n-1}^* \times \mathcal{A}_1\, J(p_1,...,p_m) \qquad (1.7)$$

Here $Lips(p_1,...,p_j)$ is the phase space associated with integrating over the momentum $p_1,...,p_j$ of the external particles in the amplitudes given by $\mathcal{A}_i$, which contributes at order i in the coupling. For example the term $\mathcal{A}_{n-1}$ would contain the diagram consisting of $n-1$ vertices where n is the order at which we are calculating the physical observable. Finally $J(p_1,...,p_j)$ is the weighting function for the physical observable, this also depends upon the momenta of the external particles. So to calculate a process up to NNLO for example, we would need LO, NLO and NNLO amplitudes to get the complete result (see the example in Section 1.4 for an NLO process). The sum of amplitudes here is an incoherent sum as the amplitudes at different orders contain different numbers of incoming and outgoing states. Correspondingly each piece will in general have a different phase space integral. The complete sum of pieces will contain all physically indistinguishable contributions to that process at the specified order.

To proceed further the contributing amplitudes would have to be calculated. It is at this point that we run into calculational difficulties. Beyond tree level the majority of Feynman diagrams are divergent. There are two types of divergence that are encountered. The first are ultraviolet (UV) singularities. These are caused by high momentum modes appearing in the integrals over the momentum of internal loops. These can be systematically dealt with by firstly regularising the integral in some way, the most common method used being that of dimensional regularisation. Then using the procedure of renormalisation the singularities can be systematically removed. Renormalisation relates the quantities in the Lagrangian, such as those labelled as the mass and interaction coupling to the renormalised mass and coupling of the theory in some renormalisation scheme. Any UV divergences are removed in this procedure as the difference between the renormalised quantities of the theory and the quantities in the Lagrangian is infinite.

The second type of divergence that we meet are the so called infrared (IR) divergences[2]. These arise in the low momentum modes of loop integrals in amplitudes and also in the phase space integrals of Eq.(1.7). They manifest themselves in two different ways, the first occurs when a particle emitted from an initial or final state particle goes soft (i.e. its energy goes to zero). The second occurs when a particle goes collinear to one of the external particles. Renormalisation does not remove these singularities as their root cause is very different from that of UV singularities (see Section 2.2).

The problems of IR divergences limits the type of quantities that we can calculate with a perturbation theory. We are forced to only deal with physical observables which can be defined in an infrared safe way [3, 5]. These IR safe quantities are such that they do not depend on the long range behaviour of the theory. This can be stated equivalently (see Section 2.2) as that IR safe quantities do not depend on whether or not a parton emits an arbitrarily soft gluon and also do not depend on whether or not a parton splits into two collinear partons.

To handle the IR divergences we must regulate the amplitudes in some way. The simplest method being to introduce a mass for any massless fields in the Lagrangian. Amplitudes thus regulated will now contain logarithms of the mass which diverge as the mass regulator is taken to zero. More commonly dimensional regularisation can be used, whereby the amplitudes are evaluated in $D \equiv 4 - 2\epsilon$ dimensions. The infrared singularities then reveal themselves as poles in $1/\epsilon$. Dimensional regularisation has also the added advantage of simultaneously regularising the UV divergences. So one regulator can be used for all the divergences in the amplitude. The UV poles will arise as $1/\epsilon^n$ factors for n-loop amplitudes and IR poles will arise as $1/\epsilon^{2n}$ factors for n-loop amplitudes, in the integrated results. The poles from the two types of singularities will therefore mix together. This mixing however does not cause any problems with UV renormalisation.

If we were now to use our IR regulated amplitudes to calculate an IR safe quantity then we will get a completely finite result when we combine all the pieces of Eq.(1.7) except in one significant case [5, 6, 7, 8]. Any parts

[2] We use the terms "infrared divergences" and "infrared singularities" for both, soft and collinear singularities throughout this thesis.

of amplitudes contributing to Eq.(1.7) which would give a divergence, if the IR regulator were to be removed, will cancel between other such terms. The regulator can then be safely removed leaving us with an infrared finite result. The one exception to this result is the case when we have initial state collinear singularities. In this situation all the initial state singularities do not cancel and instead are absorbed into the definition of what are known as parton distribution functions (PDF's) [7]. The PDF's describe the probability of finding a certain type of parton within an incoming particle. The factorisation theorem [7, 8] then informs us that we can separate out the long distance behaviour, including the collinear singularities and non-perturbative effects, into these PDF's. The short distance behaviour then has no initial state infrared divergences and can be calculated perturbatively.

1.4 An example IR safe quantity calculation

To demonstrate this cancellation of IR divergences in the calculation of IR safe quantities we will now give a simple example of how this occurs. This example is the calculation of the total cross section for $e^+e^- \to 2$ jets at NLO. We will have to compute two amplitudes for this process. The first amplitude that contributes is commonly known as the virtual contribution because the IR singularities arise from the loop integrals. It contains an incoming photon and an outgoing quark and anti-quark, this is shown in Figure 1.1. The amplitude for this is given by,

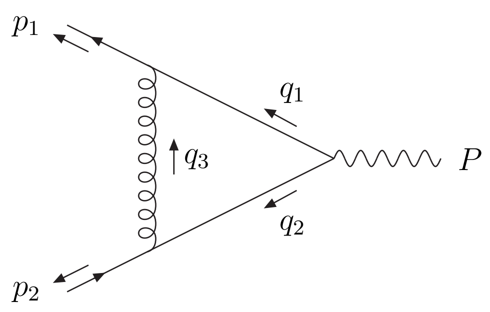

Figure 1.1: The vertex correction diagram

$$\begin{aligned}\mathcal{A}(q_{p1}, \bar{q}_{p2}; \gamma(P)) = \\ e\mathcal{A}_{0,1}(q_{p1}, \bar{q}_{p2}; \gamma(P)) + eg^2\mathcal{A}_{2,1}(q_{p1}, \bar{q}_{p2}; \gamma(P)) + \mathcal{O}(g^4)\end{aligned} \tag{1.8}$$

where $\mathcal{A}_{0,1}$ contains a single quark-antiquark-photon vertex and $\mathcal{A}_{2,1}$ contains a single quark-antiquark-photon vertex and two quark-antiquark-gluon vertices. Here e is the electromagnetic coupling constant and g is the strong coupling constant.

The second amplitude which contributes to this is commonly known as the real emission because the IR singularities arise from external particles going soft and/or collinear in the phase space integration. It contains an incoming photon and an outgoing quark, anti-quark and gluon, this is shown in Figure 1.2. The amplitude for this is given by,

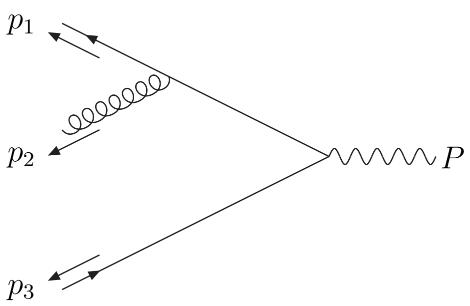

Figure 1.2: The one-gluon emission diagram.

$$\mathcal{A}(q_{p1}, \bar{q}_{p2}, g_{p3}; \gamma(P)) = eg\mathcal{A}_{1,1}(q_{p1}, \bar{q}_{p2}, g_{p3}; \gamma(P)) + \mathcal{O}(g^3) \tag{1.9}$$

Here $\mathcal{A}_{1,1}$ indicates that this amplitude has a single quark-antiquark-photon vertex and a single quark-antiquark-gluon vertex. We can write Eq.(1.7) for this process at order e^2g^2 as,

$$\sigma_J\Big|_{e^2g^2} = \lim_{\epsilon\to 0}\left(\int dLips(p_1, p_2)|\mathcal{A}^*_{2,1} \times \mathcal{A}_{0,1}|J(p_1, p_2)\right.$$

$$+\int dLips(p_1,p_2,p_3)|\mathcal{A}_{1,1}|^2 J(p_1,p_2,p_3)$$
$$+\int dLips(p_1,p_2)|\mathcal{A}^*_{0,1}\times\mathcal{A}_{2,1}|J(p_1,p_2)\Big) \quad (1.10)$$

where ϵ is the regulator in dimensional regularisation. For σ_J to be an IR safe observable we then require that the weighting function $J(p_1,...)$ satisfies the following conditions in the soft and collinear limits,

$$\begin{aligned} J(p_1,p_2,p_3) &\rightarrow J(p_1,p_2,0)=J(p_1,p_2)\\ J(p_1,p_2,p_3) &\rightarrow J((1-\lambda)p_1,p_2,\lambda p_1)=J(p_1,p_2)\\ J(p_1,p_2,p_3) &\rightarrow J(p_1,(1-\lambda)p_2,\lambda p_2)=J(p_1,p_2) \end{aligned} \quad (1.11)$$

These conditions can be generalised for processes which contain greater numbers of external particle momenta.

For the case of the total cross section we set $J=1$ and so the conditions in Eq.(1.11) are trivially met. Upon performing the integration over the phase space we obtain,

$$\sigma\equiv\sigma_{J=1}=\int d\sigma_0+\lim_{\epsilon\rightarrow 0}\int\left(e^2g^2d\sigma_{q\bar{q}}+e^2g^2d\sigma_{q\bar{q}g}\right)+\mathcal{O}(g^4) \quad (1.12)$$

where,

$$d\sigma_0 \sim |\mathcal{A}_{0,1}(q_{p1},\bar{q}_{p2};\gamma(P))|^2 \quad (1.13)$$
$$d\sigma_{q\bar{q}} \sim 2\mathrm{Re}\left[\mathcal{A}_{0,1}(q_{p1},\bar{q}_{p2};\gamma(P))\mathcal{A}^*_{2,1}(q_{p1},\bar{q}_{p2};\gamma(P))\right] \quad (1.14)$$
$$d\sigma_{q\bar{q}g} \sim |\mathcal{A}_{1,1}(q_{p1},\bar{q}_{p2},g_{p3};\gamma(P))|^2 \quad (1.15)$$

The virtual cross section, $d\sigma_{q\bar{q}}$ and the real cross section, $d\sigma_{q\bar{q}g}$ both contain infrared singularities and only when combined to form an infrared safe observable do these divergences cancel. So for the total cross section calculated here we obtain,

$$\sigma_0 = \frac{4\pi\alpha^2_{\mathrm{em}}e^2_qN_c}{3s} \quad (1.16)$$

$$\sigma_{q\bar{q}} = \sigma_0\, C_F \frac{\alpha_s}{\pi} c_\Gamma \left(\frac{1}{\epsilon^2} + \frac{3}{2\epsilon} + \frac{19}{4} - \frac{\pi^2}{2} \right) + \mathcal{O}(\epsilon) \quad (1.17)$$

$$\sigma_{q\bar{q}g} = \sigma_0\, C_F \frac{\alpha_s}{\pi} c_\Gamma \left(-\frac{1}{\epsilon^2} - \frac{3}{2\epsilon} - 4 + \frac{\pi^2}{2} \right) + \mathcal{O}(\epsilon) \quad (1.18)$$

where $c_\Gamma = 1 + \mathcal{O}(\epsilon)$ and $C_F = (N_c^2 - 1)/(2N_c) = 4/3$. Thus, at next to leading order the total cross section is given after setting ϵ to zero by,

$$\sigma = \sigma_{q\bar{q}} + \sigma_{q\bar{q}g} = \sigma_0 \left(1 + \frac{\alpha_s}{4\pi}\, 3C_F \right) \quad (1.19)$$

and we see that all dependence on ϵ has vanished and therefore the regulator can be removed.

1.5 General methods for dealing with IR singularities

In the example in the previous section we saw that IR divergences cancel between different physically indistinguishable contributions after the phase space integration has been performed. These different phase space integrals generally contain different numbers of particles. Therefore we cannot combine all the contributing terms before performing these integrals. This would then appear to preclude the use of an entirely numerical approach for the calculation of these quantities. For simple leading order calculations this is not such a problem, but as we attempt to gain greater accuracy by going to higher orders in the perturbation series, the complexity of the amplitudes makes analytic progress difficult.

To surmount this problem much theoretical work has gone into developing techniques where the integration can be split up in such away as the singular regions can be analytically integrated, whilst the rest of the amplitude is calculated numerically. There are two such methods, the first of which is known as the phase space *slicing* method [9] and the second is known as the *subtraction* method [10, 11].

Both techniques have been generalised to processes involving any number of jets involving both lepton and hadron collisions at the NLO level. The subtraction procedure at NLO works as follows [11]. We start with the total contribution to an observable at NLO. This can be split up into a real piece $d\sigma_R$ (e.g. Eq.(1.9)) and a virtual piece $d\sigma_V$ (e.g. Eq.(1.8)). The calculation can then be rewritten as follows,

$$\begin{aligned}\sigma_{NLO} &= \int_{m+1} d\sigma_R + \int_m d\sigma_V \\ &= \int_{m+1} (d\sigma_R - d\sigma_S) + \int_{m+1} d\sigma_S + \int_m d\sigma_V \\ &= \int_{m+1} (d\sigma_R - d\sigma_S) + \int_m \left(d\sigma_V + \int_1 d\sigma_S \right) \end{aligned} \tag{1.20}$$

where the subscript on the integrals indicates the number of external particles which are to be integrated over in the phase space integrals. Here $d\sigma_S$ is an approximation of $d\sigma_R$ such that it contains the same soft and/or collinear singularity structure in the IR regulator. The first term in Eq.(1.20) is now IR finite as the $d\sigma_S$ acts as a counter term to cancel any singularities. The regulator can therefore be removed from this term and it can be numerically integrated. We now need to be able to perform the single analytical integral over $d\sigma_S$ in the second term of Eq.(1.20). If this is possible then the poles given in terms of the regulator will cancel with those in $d\sigma_V$. The regulator can then be removed from these two terms and the rest of the phase space integrals performed numerically.

The crucial part of the above procedure is that we can chose a form for $d\sigma_S$ such that it can be integrated over analytically. A general method for generating $d\sigma_S$ for any process contributing at NLO was developed in [11]. Furthermore the virtual piece can, if we choose suitable counter-terms $d\sigma_S$, also be numerically integrated over the internal one-loop integral [12]. This means that it should be possible to completely numerically integrate any NLO observable.

Although great progress has been made with NLO calculations if we want to increase the accuracy of our theoretical predictions we will require NNLO results. Unfortunately the amplitudes required will be more complex. These will now include two-loop contributions as well as one-loop and tree contributions. The greater complexity of the amplitudes combined with the greater complexity of the phase space integrals has made progress slow in this area.

To move ahead then with NNLO calculations there has been great focus into two main areas. The first is that of the calculation of the amplitudes themselves. Much work has been devoted to the development of general methods for the calculation of the two-loop integrals involved [13] and the use of these in explicit amplitudes [14]. Work is also being directed towards the necessary one-loop and tree contributing amplitudes at NNLO.

The second region of development has been in the area of the phase space integrals of the amplitudes required at NNLO. This has lead to attempts to derive a general subtraction procedure for NNLO processes. The starting point of such a subtraction procedure involves understating and being able to generate in a general form the soft and collinear singularities of the various amplitudes involved. For the two-loop virtual correction a general form of these poles has been given in [15, 16]. Further work also includes explicit derivations of the forms for the splitting functions and soft limits for quarks and gluons [17, 18]. Factorisation formula for the soft and collinear singularities of real emissions at NNLO in one-loop and tree diagrams are also being produced [19, 20, 21, 22]. These have then been used to examine explicit processes [23, 24]. However the difficulty of integrating over the IR divergent phase spaces of the amplitudes involved is still a bottleneck to the further calculation NNLO physical observables.

1.6 Infrared finite amplitudes

Even though we can make headway in performing calculations using the usual approaches described above the difficulties that exist suggest that new methods of avoiding the problem of infrared singularities at the amplitude level would be of benefit. It is therefore useful to investigate the origin of these singularities in order to explore the possibility of avoiding them altogether. The origin of the problem lies in the long-range nature of the interactions. As a consequence the usual in and out states do not evolve in time asymptotically according to the free Hamiltonian. It is this breakdown of the standard assumption that results in the non-existence of the scattering operator (this will be discussed in detail in chapter 2). Thus, if we want to avoid infrared singularities from the outset we have to construct an S-Matrix that successfully maps the full states of the theory to the asymptotic states we want to calculate with.

Previous work in this area has been split between the use of two types of state. The first type of states used are the true *asymptotic* states of the full theory. Transition amplitudes are then calculated between these asymptotic states with a modified S-Matrix (see Section 2.3) [25, 26, 27]. The second types of states used are called *dressed* states, transition amplitudes can then be calculated using the normal S-Matrix between these modified states. Work in this area has been carried out initially for QED with massive fermions [28, 29] and then many steps have been made to extend it to soft singularities in non-abelian theories [30, 31, 32]. It is possible to construct dressed states (also known as generalised coherent states) which include multiple soft gluon emission to all orders in the coupling [33]. It can be shown that the S-matrix between such states is free of soft singularities [34, 35].

Apart from the more complicated structure of the soft singularities due to the self-interaction of the gauge bosons there is the additional complication of collinear singularities in a non-abelian gauge theory. Due to the collinear singularities the asymptotic Hamiltonian is more complicated [27, 36, 37, 38] and the prospect of being able to include these effects to all orders in perturbation theory is not very promising. But the idea of constructing an asymptotic Hamiltonian that takes into account the asymptotic dynamics and using the corresponding evolution operator to either construct asymptotic states or to dress the usual states [39, 40] can still be applied and is not tied to any particular theory. In particular, four-point interactions that are present in non-abelian gauge theories can be incorporated [41].

1.7 Overview of the contents of this thesis

In this thesis we investigate the practical feasibility of constructing scattering amplitudes that are free from soft and collinear singularities. We are not so much interested in general considerations but rather try to establish a method to define and explicitly compute infrared finite amplitudes order-by-order in perturbation theory. Apart from the conceptional advantage of avoiding divergent amplitudes such a method would have a variety of practical advantages. Obviously, the finiteness of the amplitudes would facilitate a completely numerical approach to the calculation of amplitudes. This also applies to the combination of fixed order results with parton shower Monte Carlo programs.

The structure of the rest of thesis will then be as follows. Chapter 2 will begin with an overview of scattering theory and then explicitly highlight the source of infrared singularities. The chapter concludes with basic outlines of the different methods of deriving scattering amplitudes which are free of infrared singularities and will be the basis of the calculations performed in chapters 3 and 4. Chapter 3 then contains a detailed discussion of the use of *dressed* states and gives an explicit example of the calculation of the total cross section for $e^+e^- \to 2$ jets at NLO. The technical details of this calculation are relegated to Appendix A. Chapter 4 will be split into two halves the first half highlights the difficulties in simplifying the calculational process involved in the use of dressed state infrared finite scattering amplitudes. This will focus around the issues of producing covariant amplitudes and the conservation of energy across the whole amplitude. The second part of the chapter will focus on the use of the asymptotic interaction picture to solve the issues discussed in the first half of the chapter. Finally Chapter 5 will summarise the different ideas and techniques presented in this thesis and give an outlook to future work.

Chapter 2

Scattering Theory

In the previous chapter we gave an overview of how scattering amplitudes in field theories are usually derived. This involved using the LSZ reduction formula and switching into the interaction picture. We could then define a covariant perturbative expansion which could be calculated using Feynman diagrams. Amplitudes calculated in this way contain infrared singularities which are a major stumbling block to higher order calculations.

The aim of this chapter is to present an alternative method of deriving a perturbative expansion for scattering amplitudes. This method is usually known as scattering theory or the Hamiltonian formalism. We will start as before from the overlap of the initial and final states of the process being calculated. From this we derive a form for the amplitudes in time ordered perturbation theory instead of covariant perturbation theory as in the last chapter. During this derivation the fundamental causes of infrared singularities will become apparent. The amplitudes generated in this way will be equivalent to those of the previous chapter and so also contain infrared singularities. The advantage of using the Hamiltonian formalism though is that the intricacies of the infrared divergences are most apparent here. This allows us greater control in developing a formalism for avoiding them in the calculation of scattering amplitudes. We will therefore conclude this chapter with an overview of the different methods of modifying the above procedure to produce amplitudes that are completely free of infrared singularities.

2.1 The S-Matrix and in & out states

We want to be able to calculate the amplitude $\mathcal{A}$ given in Eq.(1.1) using scattering theory [42]. This requirement can be translated into the need to calculate the overlap of the initial and final states of the theory we are calculating with. So we have as our starting point,

$$\mathcal{A} = \langle \Psi_\beta(t) | \Psi_\alpha(t) \rangle \tag{2.1}$$

We will see how this form of $\mathcal{A}$ relates to that of Eq.(1.3) in Section 2.1.6. The states $|\Psi_i(t)\rangle$ are full states of the theory i.e. they satisfy the Schrodinger equation,

$$i\frac{\partial}{\partial t}|\Psi_i(t)\rangle = H_f|\Psi_i(t)\rangle \tag{2.2}$$

Here H_f is the full Hamiltonian of the theory being calculated. The states consist of a complete set of quantum numbers i which are eigenvalues of operators which commute with H_f. These quantum numbers describe all the properties of the states such as the particle content and spin.

As these states satisfy the Schrodinger equation Eq.(2.2) they evolve in time according to the full Hamiltonian. It is currently not possible to diagonalise H_f for the type of process's we will want to calculate in this thesis. Therefore we cannot calculate $\mathcal{A}$ directly from the evolution of these states. We must instead use perturbation theory and attempt to calculate this quantity approximately.

2.1.1 Green's functions

If we are to perturbatively expand $\mathcal{A}$ we will find it useful to define the Green's functions. These describe how states propagate through time. We define G^- as the advanced Green's function which describes the evolution of a state backwards in time. Similarly we define G^+ as the retarded Green's function which describes the evolution of the states forwards in time. They are given by the following [42],

$$
\begin{aligned}
G_i^+(t-t') &= -i\theta(t-t')e^{-iH_i(t-t')} \\
G_i^-(t-t') &= i\theta(t'-t)e^{-iH_i(t-t')}
\end{aligned}
\tag{2.3}
$$

where H_i is the Hamiltonian of the theory the states are evolving with, for example $H_i = H_f$ for the Green's functions of the full states of the theory, G_f.

The Green's functions describe how the states evolve or propagate through time because they are solutions of the equation,

$$\left(i\frac{\partial}{\partial t} - H_i\right) G_i^{(\pm)}(t) = \mathbf{1}\delta(t) \tag{2.4}$$

with the initial conditions,

$$
\begin{aligned}
G_i^+(t) = 0 \quad \text{for} \quad t < 0 \\
G_i^-(t) = 0 \quad \text{for} \quad t > 0
\end{aligned}
$$

So we can describe a state of the Hamiltonian H_i, at time t' where $t' > t$ in terms of the state at t using,

$$|\Psi_\alpha(t')\rangle = iG_i^+(t'-t)|\Psi_\alpha(t)\rangle \tag{2.5}$$

and similarly describe the evolution to a time t' where $t' < t$ using,

$$|\Psi_\alpha(t')\rangle = -iG_i^-(t'-t)|\Psi_\alpha(t)\rangle \tag{2.6}$$

We can easily see that the Green's functions are hermitian and so we have,

$$\left(G_i^+(t)\right)^\dagger = G_i^-(-t) \tag{2.7}$$

2.1.2 In & out states

We require a form for $\mathcal{A}$ with which we can calculate. To do this we will need to relate a subset of the eigenstates $|\Psi_\alpha(t)\rangle$ of the Hamiltonian of the full theory H_f, to a new subset of eigenstates of the Hamiltonian of a second theory. We will be using a scattering theory formalism and so the Hamiltonian of this second theory should be the asymptotic theory of the full system H_{asym}. The states of this asymptotic theory $|\phi_{A,\alpha}(t)\rangle$, satisfy a Schrodinger equation for which the Hamiltonian H_{asym}, is equivalent to that of the full theory in the remote past and future. The usual form taken for H_{asym} is H_0, the Hamiltonian of the free theory (this is discussed in more detail in Section 2.1.4).

These asymptotic states evolve in time according to their own set of Green's functions which are given by,

$$\begin{aligned} G^{+}_{asym}(t-t') &= -i\theta(t-t')e^{-iH_{asym}(t-t')} \\ G^{-}_{asym}(t-t') &= i\theta(t'-t)e^{-iH_{asym}(t-t')} \end{aligned} \tag{2.8}$$

Using these we initially define,

$$|\phi_{A,\alpha}(t)\rangle \equiv iG^{+}_{asym}(t-t')|\Psi_{\alpha}(t')\rangle \tag{2.9}$$

This describes a state $|\phi_{A,\alpha}(t)\rangle$ which has evolved from time t' to t according to the asymptotic Hamiltonian and looked like the state $|\Psi_\alpha(t')\rangle$ at time t'. If we now take $t' \to -\infty$ then the asymptotic state $|\phi_{A,\alpha}(t)\rangle$ will have evolved from the full state which existed in the infinite past. So if we assume that the states of the full theory in the remote past were equivalent to those of the asymptotic theory, then we say that the state $|\phi_{A,\alpha}(t)\rangle$ is the *in* state of the theory at time t. This is given by,

$$|\phi_{in}(t)\rangle = \lim_{t' \to -\infty} iG^{+}_{asym}(t-t')|\Psi_{\alpha}(t')\rangle \tag{2.10}$$

Similarly we can define an *out* state by assuming that the states of the full theory will be equivalent to the asymptotic theory in the infinite future,

$$|\phi_{out}(t)\rangle = \lim_{t' \to \infty} -iG^{-}_{asym}(t-t')|\Psi_{\alpha}(t')\rangle \tag{2.11}$$

Although suppressed in the definitions of Eq.(2.10) and Eq.(2.11) the *in* and *out* states carry with them the same quantum numbers as the full states. These quantum numbers are eigenvalues of operators which now must commute with H_{asym}.

We can think of the *in* state as being prepared or controlled in the infinite past as an eigenstate with eigenvalues α of operators which commute with H_{asym}. This *in* state then evolves through time eventually becoming an *out* state, which is then not controlled but determined by its evolution through time according to the full theory. Throughout this we should really take the *in* states as being initially described by well separated wave packets in the far past [43]. These then evolve through time to collide in some interaction region and then separate out to become *out* states in the remote future. In explicit calculations though we can usually "get away" with treating the *in* states as an incoming monochromatic beam (i.e. a state with an energy which is an exact eigenvalue of the system and not a distribution) and avoid any issues with convergence [42, 43].

Unless otherwise stated we will use for the rest of this thesis the labels *in* and *out* on the states $|\phi\rangle$ to refer to wave-packets containing a distribution of asymptotic states. Then states $|\phi_i\rangle$ which have a specified eigenvalue label i, are exact eigenstates of H_{asym} with a single energy eigenvalue E_i. When performing calculations with the wave-packet states $|\phi_{in/out}\rangle$ we will though always assume that we can take the idealised situation of a monochromatic beam and use a state with a single energy eigenvalue, $|\phi_i\rangle$.

2.1.3 Møller operators

Now that we have related the full states of the theory to the asymptotic theory in the remote past and future we would like to be able to relate the full fields at any time t to the asymptotic states. We can do this by defining Møller operators. The first definition is given by [42],

$$|\Psi_\alpha(t)\rangle = \Omega_f^{(+)}|\phi_{in}(t)\rangle \tag{2.12}$$

So $\Omega_f^{(+)}$ maps a state of the full theory, with Hamiltonian H_f, at time t onto that of an *in* state at time t. The $(+)$ superscript on the Ω indicates the type of Green's function involved in the definition of the *in* state. In this case the advanced Green's function was used. Similarly we can define a second Møller operator,

$$|\Psi_\alpha(t)\rangle = \Omega_f^{(-)}|\phi_{out}(t)\rangle \tag{2.13}$$

Here $\Omega_f^{(-)}$ maps the *out* state at time t to a state of the full theory also at time t. The $(-)$ superscript indicates the use of the retarded Green's function to define the *out* state. As in the last section we have suppressed the eigenvalue label from the *in* and *out* states in the definitions above.

Only a subset of the full states of the theory can be mapped using these Møller operators. The states which can be mapped are known as the *scattering states* because they can be represented by superpositions of the asymptotic states. Any states of the full theory which cannot be mapped in this way are known as a *bound states* of the theory and their interactions cannot be described using scattering theory.

Due to the hermiticity of the Green's functions Eq.(2.7), we can define a reverse mapping for Eq.(2.12) and Eq.(2.13) respectively, these are given by,

$$|\phi_{in}(t)\rangle = \Omega_f^{(+)\dagger}|\Psi_\alpha(t)\rangle \tag{2.14}$$
$$|\phi_{out}(t)\rangle = \Omega_f^{(-)\dagger}|\Psi_\alpha(t)\rangle \tag{2.15}$$

We can use the Møller operators therefore to map all the states of the full theory which are of interest in scattering experiments onto those of the asymptotic theory. The hope then is that we can perform any calculations required in the asymptotic theory.

2.1.4 The free states as the asymptotic states

Clearly from the discussion in the last section the choice of which asymptotic Hamiltonian we use is very important. Usually field theory calculations are done by choosing the free Hamiltonian as the asymptotic Hamiltonian. This free Hamiltonian is defined as the Hamiltonian of the full theory without any of its interaction terms. So we have,

$$H_f = H_0 + H_{int} \tag{2.16}$$

where H_0 is the free Hamiltonian and H_{int} contains all the interaction terms. The free Hamiltonian therefore only contains the kinetic energy terms for the fields and any mass terms. Of course for our purposes for the rest of this thesis we will assume that any masses are all set to zero, as we are interested in massless theories.

The choice $H_{asym} = H_0$ is usually made because it is assumed that the interactions die off quickly enough that outside of the interaction region of the wave packets their effects are negligible. Therefore the full states of the theory should resemble non-interacting free states. Furthermore a theory with no interactions can be completely diagonalised and so it is possible to perform the types of calculations we will require using such eigenstates.

Calculations will require the use of normalised states and so we have to define a normalisation for the states. We start from,

$$\begin{aligned} \langle \phi_{0,\beta}(E') | \phi_{0,\alpha}(E) \rangle &= N^2 \delta(E - E') \delta_{\beta\alpha} && (2.17) \\ \langle \Psi_\beta(E') | \Psi_\alpha(E) \rangle &= M^2 \delta(E - E') \delta_{\beta\alpha} && (2.18) \end{aligned}$$

where the states $|\phi_{0,\alpha}(E)\rangle$ are eigenstates of H_0 with a set of eigenvalues α and the states $|\Psi_\alpha(E)\rangle$ are eigenstates of H_f with eigenvalues α. We have also replaced the time dependence of these states by Fourier transforming them so as to explicitly refer to their energy dependence instead (see Section 2.1.6). As we can solve the free theory exactly and we would want to work with eigenstates of this theory we will choose the boundary conditions such that the normalisation of the free states gives $N^2 = 1$. Now we would naively think that because of the properties of the Møller operators that we would have,

$$\begin{aligned} \langle \Psi_\beta(E') | \Psi_\alpha(E) \rangle &= \langle \phi_\beta(E') | \Omega_f^{(\pm)\dagger} \Omega_f^{(\pm)} | \phi_\alpha(E) \rangle \\ &= \langle \phi_\beta(E') | \phi_\alpha(E) \rangle = \delta(E - E') \delta_{\beta\alpha} && (2.19) \end{aligned}$$

and therefore that $M^2 = 1$. This is not the case though for field theory calculations, instead we will have $M^2 = Z^{-1}$. The reason for this is that the fields and parameters in the Lagrangian of the free theory are in fact completely different from those of the full theory. This difference arises from the self-interactions of the fields due to the interaction terms in the full Hamiltonian. Instead Eq.(2.19) must be written as,

$$\begin{aligned} \langle Z^{-\frac{1}{2}}\Psi_\beta(E')|Z^{-\frac{1}{2}}\Psi_\alpha(E)\rangle &= Z^{-1}\langle\phi_\beta(E')|\Omega_f^{(\pm)\dagger}\Omega_f^{(\pm)}|\phi_\alpha(E)\rangle \\ &= Z^{-1}\langle\phi_\beta(E')|\phi_\alpha(E)\rangle = Z^{-1}\delta(E-E')\delta_{\beta\alpha} \end{aligned} \tag{2.20}$$

where Z represents a multiplicative factor containing all the various renormalisation terms required to relate the full fields to the free fields (see Section 1.2). In perturbative calculations therefore we will also have to include these factors which themselves will also be determined perturbatively.

Finally because we have set $N^2 = 1$, we will then also have,

$$\sum_c |\phi_{0,c}\rangle\langle\phi_{0,c}| \equiv 1 \tag{2.21}$$

This relation expresses the fact that the free states are a complete set and span the entire Hilbert space.

2.1.5 Properties of the Møller operators

We can easily see from Eq.(2.12) and Eq.(2.14) that,

$$|\phi_{in}(t)\rangle = \Omega_f^{(+)\dagger}\Omega_f^{(+)}|\phi_{in}(t)\rangle \tag{2.22}$$

Now we know that the *in* and *out* must span the entire Hilbert space and so we can conclude that the Møller operators are isometric,

$$\Omega_f^{(+)\dagger}\Omega_f^{(+)} = 1 \tag{2.23}$$

In general the converse is not true, i.e.

$$\Omega_f^{(+)}\Omega_f^{(+)\dagger} \neq 1 \tag{2.24}$$

because the full states of the theory (as described in Section 2.1.3) can contain bound states and therefore the Møller operators do not span the entire Hilbert space of the full theory. This means that the Møller operators are not unitary (if there are no bound states then the Møller operators will be unitary). We will find though that fixed order perturbative forms of the Møller operators will act in a unitary way. This occurs because the fixed order perturbative forms of the Møller operators will only act on a reduced closed subspace of the full space of the full theory and hence appear unitary.

As the Møller operators are isometric we therefore have,

$$\begin{aligned} H_f\Omega_f^{(\pm)} &= \Omega_f^{(\pm)}H_{asym} \\ \Omega_f^{(\pm)\dagger}H_f &= H_{asym}\Omega_f^{(\pm)\dagger} \end{aligned} \tag{2.25}$$

This allows us to demonstrate that every eigenvalue of H_{asym} is also an eigenvalue of H_f,

$$\begin{aligned} H_f|\Psi_\alpha(t)\rangle &= H_f\Omega^{(+)}|\phi_\alpha(t)\rangle = \Omega^{(+)}H_{asym}|\phi_\alpha(t)\rangle = E_\alpha\Omega^{(+)}|\phi_\alpha(t)\rangle \\ &= E_\alpha|\Psi_\alpha(t)\rangle \end{aligned} \tag{2.26}$$

where we have dropped the *in* label from the *in* state and replaced it with its explicit eigenvalue label. The converse that every eigenvalue of H_f is an eigenvalue of H_{asym} is not true as there is no reverse form of Eq.(2.25).

As the mapping provided by the Møller operators is isometric this implies that we require a one-to-one relation between the states of the full theory and those of the asymptotic theory. This translates to the requirement that the asymptotic space which the Møller operator acts upon cannot contain degenerate states. Otherwise we cannot uniquely define the mapping between the spaces.

2.1.6 The time-independent form of the Møller operators

In order to proceed further we will need explicit forms for the Møller operators. We can derive an explicit time-independent form for Eq.(2.12) if we take,

$$|\Psi_\alpha(t)\rangle = \lim_{t'\to-\infty} iG_f^+(t-t')|\phi_{in}(t')\rangle \tag{2.27}$$

the reversed form of Eq.(2.10) and differentiate with respect to t',

$$\begin{aligned} &i\frac{\partial}{\partial t'}\left(G_f^+(t-t')|\phi_{in}(t')\rangle\right) \\ &\quad = -\delta(t-t')|\phi_{in}(t')\rangle - G_f^+(t-t')(H_f - H_{asym})|\phi_{in}(t')\rangle \end{aligned} \tag{2.28}$$

Where the states $|\phi_{in}\rangle$ are the eigenstates of H_{asym}. Integrating with respect to t' and using Eq.(2.27) then gives,

$$|\Psi_\alpha(t)\rangle = |\phi_{in}(t)\rangle + \int_{-\infty}^{\infty} dt' G_f^+(t-t')(H_f - H_{asym})|\phi_{in}(t')\rangle \tag{2.29}$$

Using the Green's function of the free theory we can write this as,

$$\begin{aligned} &\Omega_f^{(+)}|\phi_\alpha(t)\rangle \\ = \quad &|\phi_\alpha(t)\rangle - i\int_{-\infty}^{\infty} dt' G_f^+(t-t')(H_f - H_{asym})G_{asym}^-(t'-t)|\phi_\alpha(t)\rangle \end{aligned} \tag{2.30}$$

Comparing this with Eq.(2.12) then shows that,

$$\Omega_f^{(+)} = 1 - i\int_{-\infty}^{\infty} dt' G_f^+(t-t')(H_f - H_{asym})G_{asym}^-(t'-t) \tag{2.31}$$

A time independent form of this Møller operator can then be derived by using the explicit form of the Green's functions given in Eq.(2.3) on Eq.(2.29).

This gives,

$$|\phi_\alpha(t)\rangle - i\int_{-\infty}^{\infty} dt'\theta(t-t')e^{-iH_f(t-t')}(H_f - H_{asym})|\phi_\alpha(t')\rangle \qquad (2.32)$$

Now the theta function bounds this integral from above, so the upper limit becomes t and the lower limit of the integral is unbounded. We can easily see that the exponential will not converge in this lower limit of $t \to -\infty$ by itself. The Møller operator though is defined to be isometric and so we should assume that this integral does in-fact converge at the lower limit.

We can make this integral converge by regulating it in some way, the most common form of this is to use what is called *adiabatic* switching. Here we add to the integral in Eq.(2.32) an extra exponential factor containing a parameter ϵ. This extra exponential factor then makes the integral converge and we expect to be able to safely set $\epsilon \to 0$ at the end of the calculation. So we now have,

$$|\phi_\alpha(t)\rangle - i\int_{-\infty}^{\infty} dt'\theta(t-t')e^{-iH_f(t-t')}e^{-|\epsilon|(t-t')}(H_f - H_{asym})|\phi_\alpha(t')\rangle \quad (2.33)$$

To get a time independent form we now Fourier transform this,

$$\begin{aligned}
&\int_{-\infty}^{\infty} dte^{iE_\alpha t}|\phi_\alpha(t)\rangle \\
&\qquad -i\int_{-\infty}^{\infty} dtdt'\theta(t-t')e^{-i(H_f-E_\alpha-i\epsilon)(t-t')}(H_f - H_{asym})e^{iE_\alpha t'}|\phi_\alpha(t')\rangle \\
&= \quad |\phi_\alpha(E)\rangle - i\int_{-\infty}^{\infty} dt\theta(-t)e^{i(H_f-E_\alpha-i\epsilon)t}|\phi_\alpha(E)\rangle \qquad (2.34)
\end{aligned}$$

Performing the time integrals then gives the time independent form for the Møller operator as,

$$\Omega_f^{(+)}|\phi_\alpha(E)\rangle = \left(1 + \frac{1}{E_\alpha - H_f + i\epsilon}(H_f - H_{asym})\right)|\phi_\alpha(E)\rangle \qquad (2.35)$$

Similarly we also have,

$$\langle\phi_\alpha(E)|\Omega_f^{(+)\dagger} = \langle\phi_\alpha(E)|\left(1 + (H_f - H_{asym})\frac{1}{E_\alpha - H_f - i\epsilon}\right) \tag{2.36}$$

The forms of $\Omega_f^{(-)}$ and $\Omega_f^{(-)\dagger}$ are the same as Eq.(2.35) and Eq.(2.36) but with $+i\epsilon \rightarrow -i\epsilon$ in the denominator of Eq.(2.35) and $-i\epsilon \rightarrow +i\epsilon$ in the denominator of Eq.(2.36).

For these relations to be of any use we would need to be able to diagonalise H_f, which as stated before we do not know how to do. These definitions therefore need to be perturbatively expanded. We can do this using [43],

$$\frac{1}{E - H \pm i\epsilon} = \frac{1}{E - K \pm i\epsilon} + \frac{1}{E - K \pm i\epsilon}(H - K)\frac{1}{E - H \pm i\epsilon} \tag{2.37}$$

where K is an arbitrary operator. If we choose $K = H_{asym}$ then Eq.(2.35) becomes,

$$\begin{aligned}\Omega_f^{(+)}|\phi_\alpha(E)\rangle \;\; = \;\; & \Bigg(1 + \frac{1}{E_\alpha - H_{asym} + i\epsilon}(H_f - H_{asym}) \\ & + \frac{1}{E_\alpha - H_{asym} + i\epsilon}(H_f - H_{asym})\frac{1}{E_\alpha - H_{asym} + i\epsilon} \\ & \times (H_f - H_{asym}) + ...\Bigg)|\phi_\alpha(E)\rangle\end{aligned} \tag{2.38}$$

We can derive similar perturbative forms for $\Omega_f^{(+)\dagger}$, $\Omega_f^{(-)}$ and $\Omega_f^{(-)\dagger}$. We are free to choose any K to perturbatively expand with, the choice being determined by the K which is the most useful to perform calculations with. From this we can see that in a fixed order perturbative calculation we have the initial state evolving with the asymptotic Hamiltonian until the time of its first interaction. After this interaction it then evolves with the asymptotic Hamiltonian up until its next interaction. It then repeats this process for each interaction, the total number of interactions being equal to the order calculated.

By relating the asymptotic states isometrically to the full states we see that the Møller operators are defining a basis for the full states. As stated in Section 2.1.3 the space the Møller operators span is not the entire space of the full states. This means that the Møller operators provide a basis for only the scattering states of the full theory. Furthermore as there are two forms of the Møller operators, the $\Omega^{(+)}$ and the $\Omega^{(-)}$, then there will be two different basis of the scattering states. These will differ only in the way they converge in the far past and future. They are given by,

$$|\Psi_\alpha^+\rangle = \Omega_f^{(+)}|\phi_\alpha\rangle \tag{2.39}$$
$$|\Psi_\alpha^-\rangle = \Omega_f^{(-)}|\phi_\alpha\rangle \tag{2.40}$$

The $\pm$ superscript on the $|\Psi\rangle$ states indicates which Møller operator was used to define that basis, and through this the type of basis it defines.

The $|\Psi_\alpha^+\rangle$ describes a state which was initially a well defined *in* state wave-packet with eigenvalues specified by α. Therefore the α in $|\Psi_\alpha^+\rangle$ relates to a set of eigenstates of operators which commute with H_{asym} and not with H_f. This state then evolves forward in time scattering until it leaves the interaction region and becomes an *out* state. At this point it is no longer in a controlled state with definite eigenvalues α but instead has deviated from the *in* state by an amount determined by the details of the interaction.

Similarly $|\Psi_\alpha^-\rangle$ describes a state which was initially a well defined *out* state wave-packet with eigenvalues α. Again the α in $|\Psi_\alpha^-\rangle$ refers to a set of eigenvalues of operators which commute with H_{asym}. This can then be evolved backwards in time until the wave-packet leaves the interaction region and becomes an *in* state. This *in* state is not well defined and has indefinite eigenvalues α. Instead it is altered from the *out* state by an amount determined by the interaction.

As we are interested in calculating the interactions of scattering states we can use these basis' to replace the appropriate full states used in the definition given in Eq.(2.1). So instead we will now calculate,

$$\mathcal{A} = \langle\Psi_\beta^-|\Psi_\alpha^+\rangle \tag{2.41}$$

The choice of basis used for this replacement is determined by what we are calculating. So the initial state being well defined must be represented by a basis of + states. Similarly the − basis must be used for the outgoing states as these have a well defined form in the far future. We can now see from this choice how this definition relates to Eq.(1.3), the state Ψ_α^+ become the *in* states of Eq.(1.3) and the state Ψ_β^- becomes the *out* states of Eq.(1.3).

2.1.7 Time-dependent Møller operators

We will now derive a time dependent form for the Møller operators. The time dependence of operators in quantum mechanics can be dealt with in many equivalent ways. Initially we have given all the time dependence of the eigenstates and the Møller operators in the Schrodinger picture. This means that the states evolve in time with the full Hamiltonian H_f whilst the operators do not evolve in time at all. So we can describe the evolution of a state $|\Psi_S(t)\rangle$ and a general operator $O_S(t)$, both in the Schrodinger picture as [44],

$$i\frac{\partial}{\partial t}|\Psi_S(t)\rangle = H_f|\Psi_S(t)\rangle, \qquad i\frac{\partial O_S(t)}{\partial t} = 0$$

$$\Rightarrow |\Psi_S(t)\rangle = e^{-iH_f(t-t_0)}|\Psi(t_0)\rangle = U_{S,f}(t,t_0)|\Psi(t_0)\rangle \tag{2.42}$$

The operator $U_{S,f}(t,t_0)$ is then the evolution operator in the Schrodinger picture. We could have equally well defined everything in the Heisenberg picture. Here all the operators now evolve in time with the same full theory Hamiltonian H_f as the Schrodinger picture and the states instead are stationary. The evolution of a state $|\Psi_H(t)\rangle$ and a general operator $O_H(t)$, both in the Heisenberg picture, is then given by,

$$i\frac{\partial}{\partial t}|\Psi_H(t)\rangle = 0, \qquad i\frac{\partial O_H(t)}{\partial t} = [O_H(t), H_f]$$

$$\begin{aligned} \Rightarrow O_H(t) &= e^{iH_f(t-t_0)}O(t_0)e^{-iH_f(t-t_0)} \\ &= U^\dagger_{H,f}(t,t_0)O(t_0)U_{H,f}(t,t_0) \end{aligned} \tag{2.43}$$

where $U_{H,f}(t,t_0)$ is the evolution operator in the Heisenberg picture. The pictures are equivalent to each other at $t = t_0$ and any calculation of an amplitude or expectation value performed using either picture will be equivalent because of the unitarity of the evolution operators. This can be seen in the following,

$$\begin{aligned}
\langle\Psi_S(t)|O_S|\Psi_S(t)\rangle &= \langle\Psi(t_0)|U^\dagger_{S,f}(t,t_0)O(t_0)U_{S,f}|\Psi(t_0)\rangle \\
&\equiv \langle\Psi(t_0)|U^\dagger_{H,f}(t,t_0)O(t_0)U_{H,f}|\Psi(t_0)\rangle \\
&= \langle\Psi_H|O_H(t)|\Psi_H\rangle \qquad (2.44)
\end{aligned}$$

In both of the above pictures we must evolve either the states or the operators with the full Hamiltonian, which as stated at the beginning of Section 2.1 we do not know how to do. To avoid this problem we will instead define a third picture which will be part way between the previous two. We define this picture by performing the following transformation upon the states and operators,

$$U_{H_{asym}}(t,t_0) = e^{-iH_{asym}(t-t_0)} \qquad (2.45)$$

in such a way as that the states now evolve only with $H_{A,int} = H_f - H_{asym}$ whilst the operators evolve with H_{asym}. So we have states $|\Psi_A(t)\rangle$ and general operators $O_A(t)$, both in what is called the asymptotic interaction picture [27, 45], given by,

$$\begin{aligned}
|\Psi_A(t)\rangle &= U^\dagger_{H_{asym}}(t,t_0)|\Psi_S(t)\rangle = U^\dagger_{H_{asym}}(t,t_0)U_{S,f}(t,t_0)|\Psi(t_0)\rangle \\
&= U_A(t,t_0)|\Psi(t_0)\rangle \\
O_A(t) &= U^\dagger_{H_{asym}}(t,t_0)O(t_0)U_{H_{asym}}(t,t_0) \\
&= U^\dagger_{H_{asym}}(t,t_0)U_{H,f}(t,t_0)O_H(t)U^\dagger_{H,f}(t,t_0)U_{H_{asym}}(t,t_0) \\
&= U_A(t,t_0)O_H(t)U^\dagger_A(t,t_0) \qquad (2.46)
\end{aligned}$$

Where we now have an asymptotic evolution operator U_A (which is defined in Eq.(2.49) below). If we were to take the usual choice of $H_{asym} = H_0$ then,

$$H_{A,int} = H_f - H_0 = H_{int} \tag{2.47}$$

and this becomes the normal interaction picture [42], with an evolution operator given by,

$$U_I(t,t') = e^{iH_0(t-t')}e^{-iH_f(t-t')} \tag{2.48}$$

This is used to define the fields ψ_I in Eq.(1.6).

The asymptotic interaction picture evolution operator as defined in Eq.(2.46) is given by,

$$U_A(t,t') = e^{iH_{asym}(t-t')}e^{-iH_f(t-t')} \tag{2.49}$$

and must satisfy the Schrodinger equation,

$$i\frac{\partial}{\partial t}U_A(t,t_0) = H_{A,int}(t)U_A(t,t_0) \tag{2.50}$$

where,

$$H_{A,int}(t) = U^{\dagger}_{H_{asym}}(t,t_0)(H_f(t_0) - H_{asym}(t_0))U_{H_{asym}}(t,t_0) \tag{2.51}$$

We can solve this differential equation along with the boundary condition $U_A(t_0,t_0) = 1$ (i.e. this picture should be equivalent to the others at time t_0) to get the following perturbative form for $U_A(t,t_0)$,

$$\begin{aligned} U_A(t,t_0) &= 1 + (-i)\int_{t_0}^{t} dt_1 H_{A,int}(t_1) \\ &\quad +(-i)^2\int_{t_0}^{t} dt_1 \int_{t_0}^{t_1} dt_2 H_{A,int}(t_1)H_{A,int}(t_2) + ... \\ &= 1 + (-i)\int_{-\infty}^{\infty} dt_1 F_{tt_1} H_{A,int}(t_1) \\ &\quad +(-i)^2\int_{-\infty}^{\infty} dt_1 \int_{-\infty}^{\infty} dt_2 F_{tt_1}F_{t_1t_2}H_{A,int}(t_1)H_{A,int}(t_2) \\ &\quad +... \end{aligned} \tag{2.52}$$

where,

$$F_{t_i t_j} = \theta(t_i - t_j)\theta(t_j - t_0) - \theta(t_0 - t_i)\theta(t_i - t_j) \tag{2.53}$$

The evolution operators have the following useful properties,

$$U_A(t,t') = U_A(t,t_1)U_A(t_1,t') \tag{2.54}$$

for $t \geq t_1 \geq t'$ and also,

$$U_A^\dagger(t,t') = U_A(t',t) \tag{2.55}$$

Now we can take the form of the Møller operator given in Eq.(2.30) and rewrite it to get [42],

$$\begin{aligned}
\Omega_f^{(+)} &= \lim_{t\to-\infty} e^{iH_f(t-t_0)}e^{-iH_{asym}(t-t_0)} \\
&= \lim_{t\to-\infty} U_A^\dagger(t,t_0) \\
&\equiv U_A^\dagger(-\infty,t_0)
\end{aligned} \tag{2.56}$$

Therefore we can derive a time-dependent perturbative form for the Møller operators in the asymptotic interaction picture from the asymptotic evolution operators. The Møller operator $\Omega_f^{(+)}$ then has the form,

$$\begin{aligned}
\Omega_f^{(+)} &= U_A^\dagger(-\infty,t_0) = U_A(t_0,-\infty) \\
&= 1 + (-i)\int_{-\infty}^{t_0} dt_1 H_{A,int}(t_1) \\
&\quad +(-i)^2\int_{-\infty}^{t_0} dt_1 \int_{-\infty}^{t_1} dt_2 H_{A,int}(t_1)H_{A,int}(t_2) + ... \\
&= 1 + (-i)\int_{-\infty}^{\infty} dt_1 \theta(t_0 - t_1)H_{A,int}(t_1) \\
&\quad +(-i)^2\int_{-\infty}^{\infty} dt_1 \int_{-\infty}^{\infty} dt_2 \theta(t_0 - t_1)\theta(t_1 - t_2)H_{A,int}(t_1)H_{A,int}(t_2) \\
&\quad +...
\end{aligned} \tag{2.57}$$

Similarly we have,

$$
\begin{aligned}
\Omega_f^{(+)\dagger} &= U_A(-\infty, t_0) = U_A^\dagger(t_0, -\infty) \\
&= 1 + (+i)\int_{-\infty}^{\infty} dt_1 \theta(t_0 - t_1) H_{A,int}(t_1) \\
&\quad +(+i)^2 \int_{-\infty}^{\infty} dt_1 \int_{-\infty}^{\infty} dt_2 \theta(t_0 - t_2)\theta(t_2 - t_1) H_{A,int}(t_1) H_{A,int}(t_2) \\
&\quad +... \qquad (2.58)
\end{aligned}
$$

$$
\begin{aligned}
\Omega_f^{(-)} &= U_A(\infty, t_0) \\
&= 1 + (+i)\int_{-\infty}^{\infty} dt_1 \theta(t_0 - t_1) H_{A,int}(t_1) \\
&\quad +(+i)^2 \int_{-\infty}^{\infty} dt_1 \int_{-\infty}^{\infty} dt_2 \theta(t_2 - t_1)\theta(t_1 - t_0) H_{A,int}(t_1) H_{A,int}(t_2) \\
&\quad +... \qquad (2.59)
\end{aligned}
$$

$$
\begin{aligned}
\Omega_f^{(-)\dagger} &= U_A^\dagger(\infty, t_0) \\
&= 1 + (-i)\int_{-\infty}^{\infty} dt_1 \theta(t_0 - t_1) H_{A,int}(t_1) \\
&\quad +(-i)^2 \int_{-\infty}^{\infty} dt_1 \int_{-\infty}^{\infty} dt_2 \theta(t_1 - t_2)\theta(t_2 - t_0) H_{A,int}(t_1) H_{A,int}(t_2) \\
&\quad +... \qquad (2.60)
\end{aligned}
$$

These perturbative definitions for the Møller operators can easily be seen to be unitary as well as isometric. The difference between the $\pm$ Møller operators is now encapsulated in the different theta functions and the regularisation which would be required for the convergence of the integrals. If we were to perform the time integrals in these definitions we would find that we get the form for the time-independent Møller operators given in Eq.(2.38), as expected. The choice of the picture we choose to calculate the time dependence of the Møller operators in is then related to our choice of which Hamiltonian we choose for K when we perform the perturbative expansion in Eq.(2.37).

2.1.8 The S-Matrix

We are now in a position to calculate Eq.(2.41). Using the Møller operators we have [42],

$$\mathcal{A} = \langle \Psi_\beta^-(t)|\Psi_\alpha^+(t)\rangle = \langle \phi_{out}(t)|\Omega_f^{(-)\dagger}\Omega_f^{(+)}|\phi_{in}(t)\rangle = \langle \phi_\beta(t)|S|\phi_\alpha(t)\rangle \quad (2.61)$$

where we have replaced the *in* and *out* labels with the states explicit eigenvalue dependence in the last step. We have therefore defined,

$$S = \Omega_f^{(-)\dagger}\Omega_f^{(+)} \quad (2.62)$$

which is known as the S operator. When the S operator is placed between *in* and *out* states as in Eq.(2.61) we can write,

$$\mathcal{A} = S_{\beta\alpha} = \langle \phi_\beta(t)|S|\phi_\alpha(t)\rangle \quad (2.63)$$

where $S_{\beta\alpha}$ is known as the S-Matrix and $\mathcal{A}$ is called the scattering matrix element or S-Matrix element. We can replace the Møller operators in this definition with the evolution operators given in the last section. So we now have,

$$S = U_A(\infty, t_0)U_A^\dagger(-\infty, t_0) \equiv U_A(\infty, -\infty) \quad (2.64)$$

Therefore using Eq.(2.57) we can write a perturbative expansion of the S operator in a time dependant form in the asymptotic interaction picture as,

$$\begin{aligned} S_A &= 1 + (-i)\int_{-\infty}^{\infty} dt_1 H_{A,int}(t_1) \\ &\quad + (-i)^2 \int_{-\infty}^{\infty} dt_1 \int_{-\infty}^{t_1} dt_2 H_{A,int}(t_1)H_{A,int}(t_2) + ... \\ &= 1 + (-i)\int_{-\infty}^{\infty} dt_1 H_{A,int}(t_1) \\ &\quad + (-i)^2 \int_{-\infty}^{\infty} dt_1 \int_{-\infty}^{\infty} dt_2 \theta(t_1 - t_2) H_{A,int}(t_1)H_{A,int}(t_2) + ... \end{aligned} \quad (2.65)$$

Again if we were to take $H_{asym} = H_0$ we would get S_I, the usual S operator given in the interaction picture. The different forms for the S-Matrix in the different time pictures are all unitarily equivalent to each other[1].

The S operator maps the *in* states onto the *out* states and so we have,

$$|\phi_{out}\rangle = S|\phi_{in}\rangle = \Omega_f^{(-)\dagger}\Omega_f^{(+)}|\phi_{in}\rangle \tag{2.66}$$

From this and using Eq.(2.25) we can easily see that the S operator commutes with the Hamiltonian H_{asym},

$$[S, H_{asym}] = 0 \tag{2.67}$$

This implies that scattering elements will conserve energy, i.e. they will be of the form,

$$\langle\phi_\beta(t)|S|\phi_\alpha(t)\rangle \propto \delta(\omega_\beta - \omega_\alpha) \tag{2.68}$$

where the ω_i are eigenvalues of H_{asym}. The S operator can also be shown to be unitary as we have,

$$|\phi_{in}\rangle = S^\dagger|\phi_{out}\rangle = \Omega_f^{(+)\dagger}\Omega_f^{(-)}|\phi_{out}\rangle \tag{2.69}$$

and as the *in* and *out* states span the entire Hilbert space we therefore have,

$$S^\dagger S = 1 \tag{2.70}$$

2.2 Infrared divergences

As stated in Section 2.1.4 traditionally we take $H_{asym} = H_0$, so that the *in* and *out* states are eigenstates of the free Hamiltonian, H_0. The S-Matrix is given by S_I and is defined in the interaction picture with $H_{int} = H_f - H_0$.

[1]This is only true when all the Møller operators for the different pictures are isometric, in the case of $H_{asym} = H_0$ this is not usually true and so we would need to regularise any infrared divergences before we regain this unitarity. We will discus this further in Section 2.3

In deriving the S-Matrix we have assumed that the Møller operators were isometric. With the choice of H_0 for the asymptotic Hamiltonian we must now check that this assumption is valid. This means that we must investigate whether the mapping of the full scattering states $|\Psi_\alpha\rangle$, onto the free states $|\phi_\alpha\rangle$, given by $\Omega_f^{(\pm)}$, involves any mappings onto degenerate states. Usually we hope that the set of quantum numbers α is enough to remove any such degeneracies. This may not always be the case though. If the spectrum of any of the eigenvalues is degenerate when all the other eigenvalues are fixed then the possibility of degenerate states exists.

We can immediately see that such a degenerate subspace of eigenvalues could exist. The spectrum of H_0 can contain energy degenerate subspaces and so different states with the same energy may exist. Such states are known as *soft* and/or *collinear* states. States which contain soft particles (i.e. they have zero energy and no mass), have the same energy as the same state without the soft particles. Collinear states occur when we have two collinear particles both of which are massless. This state will then have the same energy as that of just a single massless particle. Furthermore the particle number of these free H_0 states is not a conserved quantum number, as it is not an observable quantity. Therefore as there are no other good quantum numbers with which we can distinguish between the states which contain energy degenerate soft and/or collinear particles then we have degenerate subspaces of states in the spectrum of H_0. These types of states would only be a problem though if the Møller operator maps full states of the theory onto more than one state in any set of degenerate states in the spectrum of H_0.

The soft and collinear states consist of fields which are never well separated and therefore the initial state wave-packets never leave the interaction region. This clearly contradicts the requirement of scattering theory that the final state wave-packets are well separated and would be the consequence of the loss of isometry of the Møller operators. Therefore we can translate the need for the Møller operator to not map states in the degenerate subspaces to the equivalent statement that we need the *interaction* to *"turn off"* at infinity. Otherwise we will have initial and final states that will have energies in the subspace of the energy degenerate soft and collinear states.

If all the fields in the free Hamiltonian are massive then there will clearly be no degenerate states as each state will have a different mass and therefore the Møller operators will be isometric. If though there are massless fields in H_0 then we need to investigate $\Omega_f^{(\pm)}$ further. We can begin by taking the time dependent form for the Møller operator $\Omega_f^{(+)}$, given in Eq.(2.57). Next we place the interaction Hamiltonian H_{int} between H_0 states. We assume here that H_{int}, just for the simplicity of the argument, contains a single term. This single term corresponds to an interaction between three or more fields and has a coupling constant g (for example the three gluon vertex in QCD). Here we only want to investigate the weak convergence of the Møller operators and not a strong operator convergence to avoid any spurious regions of IR singularities [41]. The perturbative expansion at order g^n in the coupling of the interaction then looks like,

$$g^n \int_{-\infty}^{\infty} dt_1 \langle \phi_{out} | H_{int} | \phi_{0,a_1} \rangle e^{-it_1(\omega_{a_1} - \omega_{out})} \times ... \times \int_{-\infty}^{t_{n-1}} dt_n \langle \phi_{0,a_{n-1}} | H_{int} | \phi_{in} \rangle e^{-it_n(\omega_{in} - \omega_{a_{n-1}})} \quad (2.71)$$

For the perturbative expansion to make sense the time integrals in Eq.(2.71) must converge. Now the only limits of this integral which could cause convergence problems are the lower $-\infty$ limit of the right most integral and the upper ∞ limit of the left most integral. All other integrals are bounded from above or below by either of these limits.

Usually we would now assume that these integrals must converge and therefore use *adiabatic* switching to guarantee this. Instead we will look at the details of the convergence of these limits more closely. If $\omega_{out} - \omega_{a_1} \equiv 0$ or $\omega_{a_{n-1}} - \omega_{in} \equiv 0$ for any values of ω_{out}, ω_{a_1}, $\omega_{a_{n-1}}$ or ω_{in} within the support of the wave-packets of the *in* or *out* states then we will have,

$$\exp(-it_1(\omega_{a_1} - \omega_{out})) \to 1 \quad \text{or} \quad \exp(-it_1(\omega_{in} - \omega_{a_{n-1}})) \to 1 \quad (2.72)$$

and clearly the integral in Eq.(2.71) will diverge.

The conditions under which $\omega_{out} - \omega_{a_1} \equiv 0$ or $\omega_{a_{n-1}} - \omega_{in} \equiv 0$ occurs will depend upon the type of interaction contained in H_{int}. For example in QED the three point interaction can give us energy factors of the type,

$$e \int d\vec{x} \, : \overline{\Psi}(p_1)\gamma^{\mu}\Psi(p_2) : A_{\mu}(p_3) \Rightarrow \exp\left(it\left(\omega_{\vec{p_1}-\vec{p_3}} + \omega_{\vec{p_3}} - \omega_{\vec{p_1}}\right)\right) \tag{2.73}$$

which corresponds to the diagram in Figure 2.1. In the massless case of the

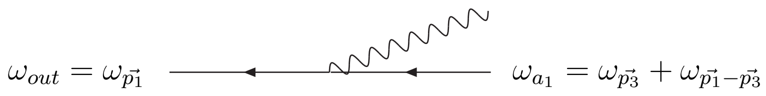

Figure 2.1: Diagram showing the absorption of a photon.

three point interaction there are two types of solution for,

$$\omega_{\vec{p_1}-\vec{p_3}} + \omega_{\vec{p_3}} - \omega_{\vec{p_1}} = 0 \tag{2.74}$$

The first is in the case that the photon goes soft so that $\omega_{\vec{p_3}} \rightarrow 0$ and therefore,

$$\omega_{\vec{p_1}-\vec{p_3}} + \omega_{\vec{p_3}} - \omega_{\vec{p_1}} \rightarrow \omega_{\vec{p_1}} - \omega_{\vec{p_1}} = 0 \tag{2.75}$$

Secondly when the photon becomes collinear to the quark we have $\vec{p_3} \equiv \lambda\vec{p_1}$, and so we get,

$$\omega_{\vec{p_1}-\vec{p_3}} + \omega_{\vec{p_3}} - \omega_{\vec{p_1}} \rightarrow |1-\lambda|\omega_{\vec{p_1}} + |\lambda|\omega_{\vec{p_1}} - \omega_{\vec{p_1}} = 0 \text{ for } \lambda \geq 0 \tag{2.76}$$

The support of the *in* or *out* state wave-packets does not exclude soft or collinear regions and therefore the Møller operator clearly maps full states onto the sets of energy degenerate free states. So we can say that the interaction does not *"turn off"* at infinity and the cause of this is that the Møller operator is not isometric in this case. Breaking this basic requirement then manifests itself in the divergences that appear when we try to perform calculation using these Møller operators. These divergences are collectively known as infrared singularities as they only occur when we have initial and final state energy configurations that contain soft and/or collinear states. Similar divergences will also appear in QCD and in many other theory involving massless fields.

2.2.1 Regularised Møller operators

The usual solution to the problems of infrared divergences is to take the amplitudes containing such divergences and then regulate them in some way. In the case of a mass regulator we can easily see from the last section that this removes the energy degeneracy between the states. Therefore the Møller operator is rendered isometric and hence the amplitudes will be finite. Similarly dimensional regularisation alters the dimensions within the integral of the four-momenta such that the result is now finite. In general therefore the regulator makes the Møller operators isometric and consequentially we can use the S-Matrix to perform calculations.

When calculating IR safe quantities, we know from Section 1.3 that all dependence on the regulator cancels. This cancellation occurs when we sum up all physically relevant amplitudes squared. This happens because all the H_0 states which make up the real state of the full theory, that were mistakingly split up by the non-isometric Møller operator, are recombined. So when this summing occurs in Eq.(1.7) all the necessary terms will have been combined such that we have made the mapping between the two spaces of states isometric. Hence the result will be finite and the regulator can be removed. An explicit example of this cancellation is given in Section 1.4.

2.3 A better asymptotic Hamiltonian

In Section 2.2 we saw that the traditional choice of H_0 as the asymptotic Hamiltonian led to the derivation of Møller operators that broke the fundamental assumption of isometry. The problem with the H_0 basis is that the energy of the state $|p_1, p_3\rangle$ with $\omega_{\vec{p_3}} \to 0$ and/or $\omega_{\vec{p_3}} \to \lambda\omega_{\vec{p_1}}$ is degenerate with that of the state $|p_1\rangle$. By relating the full states of the theory to *in* and *out* states which are eigenstates of H_0 we mistakingly map onto different states the same state of the full theory. A better choice for the asymptotic Hamiltonian would therefore be one which does satisfy the one-to-one mapping requirement.

Our choice of asymptotic Hamiltonian requires only that an isometric mapping can be made. For practical purposes only, we would also realistically want the Møller operators relating the two spaces to be expandable perturbatively and also that we can use the eigenvalues and eigenstates of that Hamiltonian to perform calculations.

The problem H_0 states occur when they contain soft and/or collinear particles which never fully separate. This suggests that these should be combined along with "bare" H_0 states to get a true asymptotic state. We denote the Hamiltonian of which these new asymptotic states are eigenstates as the asymptotic Hamiltonian H_A. A form for this can be derived by splitting up the interaction piece H_{int}, of the full Hamiltonian given in Eq.(2.16) into a *soft* piece and a *hard* piece. So we have,

$$\begin{aligned} H_f &= H_0 + H_{int} \\ &= H_0 + H_S(\Delta) + H_H(\Delta) \end{aligned} \tag{2.77}$$

and therefore the asymptotic Hamiltonian, H_A is given by,

$$H_A(\Delta) = H_0 + H_S(\Delta) \tag{2.78}$$

The split between the *soft* and *hard* Hamiltonians is not unique. So we include a parameter Δ to define where we perform this split. The only requirement on Δ is that $H_S(\Delta)$ includes all the true long-range interactions. Thus, the emission of a soft gauge boson and the splitting of a parton into two collinear partons has to be included. But there is a lot of freedom on how precisely we make the split between soft and hard interactions. Throughout the rest of this thesis we will call $H_\Delta \equiv H_S(\Delta)$ the soft Hamiltonian, even though it does include *all* long-range interactions that potentially give rise to infrared singularities. In particular, the soft Hamiltonian also includes the splitting of a parton into two collinear partons.

As we have included all the parts of the interaction Hamiltonian that give rise to long-range interactions into $H_A(\Delta)$, then there will be no degeneracy in its eigenstate spectrum. This can be seen if we imagine expanding the $H_A(\Delta)$ states in terms of H_0 states. An eigenstate of $H_A(\Delta)$ with energy ω_a will then be a combination of the infinite sum of all possible soft and collinear H_0 states which have the same energy ω_a. We will denote such an eigenstate as $|\phi_{A,\alpha}\rangle$. A simple pictorial perturbative representation of such an H_A state in terms of H_0 states is shown in Figure 2.2. This lack of energy degenerate subspaces now means that the Møller operators relating the space of full states to these asymptotic states will be isometric. This implies there will be no infrared divergences in the amplitudes.

$|\phi_{A,\alpha}\rangle \equiv$

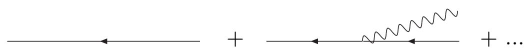

Figure 2.2: Pictorial representation of a simple H_A state.

We now need to derive the form for the Møller operators for $H_A(\Delta)$ and then consequentially the S-Matrix. We can do this easily by placing the time-dependent Møller operators from Section 2.1.7 in the asymptotic interaction picture, as given in Eq.(2.57). The *in* and *out* states and the energies of these states are therefore eigenstates and eigenvalues respectively of $H_A(\Delta)$. Equally in the time-independent formalism from Section 2.1.6 we would use $K = H_A(\Delta)$ in the perturbative expansion relation Eq.(2.37) to derive Eq.(2.38) in the correct form. This gives us a new Møller operator,

$$|\Psi_\alpha\rangle = \Omega_A^{(+)}|\phi_{A,in}\rangle \tag{2.79}$$

and similarly we also have, $\Omega_A^{(+)\dagger}$, $\Omega_A^{(-)}$ and $\Omega_A^{(-)\dagger}$.

We can now use these new Møller operators to derive the S-Matrix for the new asymptotic states. This new S-Matrix will be denoted by S_A and its form will be given by Eq.(2.65) where we will have,

$$H_{A,int} \equiv H_H(\Delta) \tag{2.80}$$

The properties of the S_A-Matrix as given in Section 2.1.8 all still hold. This implies we will have,

$$[S_A, H_A(\Delta)] = 0 \tag{2.81}$$

So now the energy of the system given by $H_A(\Delta)$ commutes with the asymptotic S_A-Matrix, so in the same way as for the H_0 basis, energy is conserved at the amplitude level.

We can check that this basis will in fact be free of infrared singularities by examining Eq.(2.71) using the new $H_A(\Delta)$ basis of asymptotic states. We can immediately see that for $\omega_{out} - \omega_{a_1} = 0$ we would need to have two states $|\phi_{A,out}\rangle$ and $|\phi_{A,a_1}\rangle$ with the same energy. The new asymptotic basis though contains no energy degenerate subspaces of states and as the energy factors come from either side of an interaction then $|\phi_{A,out}\rangle$ can never equal $|\phi_{A,a_1}\rangle$. Therefore we will never have,

$$\exp(-it(\omega_{out} - \omega_{a_1})) \to 1 \tag{2.82}$$

This therefore means that the integral will converge at its upper limit. A similar argument can be used for the $\exp(-it(\omega_{a_{n-1}} - \omega_{in}))$ factor. Therefore the Møller operator is finite and isometric.

If we are to perform calculations using these states then we need a form for the eigenstates of $H_A(\Delta)$. Unfortunately as this basis contains interactions terms we do not know how to solve it exactly. The most straightforward approach is therefore is try to relate these asymptotic basis states to a set of states which we do know how to calculate. Of course the only states we can solve exactly are the free eigenstates of H_0. So we will want an operator which can relate the new asymptotic basis to the basis of free states. As we cannot diagonalise $H_A(\Delta)$ this implies that this relation will have to be perturbative.

The most obvious way of doing this would be to use a Møller operator which relates the eigenstates of H_0 to those of $H_A(\Delta)$. This would be,

$$|\phi_{A,\alpha}\rangle = \Omega_\Delta |\phi_{0,\alpha}\rangle \tag{2.83}$$

If we write the Møller operator in the time-dependent general form between free states as,

$$\langle\phi_{0,\beta}|\Omega_\Delta|\phi_{0,\alpha}\rangle = \delta_{\beta\alpha} + (-i)\int_{-\infty}^{\infty} dt_1 e^{-it_1(\omega_\alpha-\omega_\beta)}\langle\phi_{0,\beta}|H_s(\Delta)|\phi_{0,\alpha}\rangle + ... \quad (2.84)$$

We see that again we will have to deal with the issue of convergence at the upper and lower limits of these time integrals. So these Møller operators will, as before, have to be made convergent. If we assume that they are convergent we can regulate then using *adiabatic* switching and then as before we find that we have two such basis'. A + basis denoted by, $|\phi^+_{A,\alpha}\rangle$ with the corresponding Møller operator $\Omega^{(+)}_\Delta$ and a $-$ basis $|\phi^-_{A,\alpha}\rangle$ with the corresponding Møller operator $\Omega^{(-)}_\Delta$. Of course these integrals are not really convergent and so these changes of basis suffer from the same infrared divergences that plagued the traditional H_0 basis in Section 2.2. We would need to use some further form of regularisation to make these integrals convergent, which removes the benefit of using the correct asymptotic basis in the first place.

Furthermore if all of the Møller operators were isometric we would have,

$$\begin{aligned} S_A = \Omega^{(-)\dagger}_A\Omega^{(+)}_A &\equiv \Omega^{(-)}_\Delta\Omega^{(-)\dagger}_\Delta\Omega^{(-)\dagger}_A\Omega^{(+)}_A\Omega^{(+)}_\Delta\Omega^{(+)\dagger}_\Delta \\ &\equiv \Omega^{(-)}_\Delta\Omega^{(-)\dagger}_f\Omega^{(+)}_f\Omega^{(+)\dagger}_\Delta \\ &\equiv \Omega^{(-)}_\Delta S_I\Omega^{(+)\dagger}_\Delta \end{aligned} \quad (2.85)$$

where we have taken $\Omega^{(-)\dagger}_\Delta\Omega^{(-)\dagger}_A \equiv \Omega^{(-)\dagger}_f$ and $\Omega^{(+)}_A\Omega^{(+)}_\Delta \equiv \Omega^{(+)}_f$. So if we were to then calculate S-Matrix elements of this we would find,

$$\langle\phi_{A,out}|S_A|\phi_{A,in}\rangle = \langle\phi_{out}|\Omega^{(-)\dagger}_\Delta\Omega^{(-)}_\Delta S\Omega^{(+)\dagger}_\Delta\Omega^{(+)}_\Delta|\phi_{in}\rangle = \langle\phi_{out}|S_I|\phi_{in}\rangle \quad (2.86)$$

The matrix elements of S_A on asymptotic states would therefore be the same as those of S_I on free states. So we see that if we were to regularise the infrared divergent Ω_Δ Møller operators to make them unitary we would be effectively just recalculating traditional regularised S_I matrix elements in a more convoluted way. To sidestep the problems discussed here we will investigate working with eigenstates of $H_A(\Delta)$ directly in the asymptotic interaction picture in Chapter 4.

2.4 Dressed states

In Section 2.2 the basis of free H_0 states contained energy degenerate subspaces which the Møller operator mapped states of the full theory into, rendering the transformation divergent. In Section 2.3 we looked at modifying the asymptotic basis we used, using eigenstates of $H_A(\Delta)$ instead of eigenstates of H_0. The Møller operators related to this new basis of asymptotic states then did not lead to infrared divergences in the scattering amplitudes. Now instead of making this change in the basis of the asymptotic states used we will look at modifying the Møller operators independently of the basis they map between. If we could alter the Møller operators such that they excluded the degenerate subspaces of the H_0 energy spectrum, then such a Møller operator would also be isometric and consequentially free from infrared divergences.

A Møller operator of this form can be defined. We do this by taking the usual Møller operator $\Omega_f^{(+)}$, relating the full theory and the free states, and applying the transformation $\Omega_\Delta^{(+)\dagger}$ to it. So we now have,

$$\Omega^{(+)} \equiv \Omega_f^{(+)}\Omega_\Delta^{(+)\dagger} \tag{2.87}$$

We can see that this will generate a new infrared finite Møller operator $\Omega^{(+)}$ because as in Section 2.1.5 the energy eigenvalues of H_0 will also be energy eigenvalues of $H_A(\Delta)$. So $\Omega_\Delta^{(+)}$ takes any H_0 energy degenerate state and relates it to a *single* eigenstate of $H_A(\Delta)$ with the same energy eigenvalue as the original degenerate state. We then only require that the $H_A(\Delta)$ eigenstate to which $\Omega_\Delta^{(+)}$ maps the H_0 states to can in turn always be related to a *single* eigenstate of H_0. This will always be the case for the situations we will consider here and so the energy degenerate subspaces of states which $\Omega_f^{(+)}$ maps to are always then mapped onto a single H_0 state. Hence this Møller operator is infrared finite. A more detailed investigation into the infrared finiteness of these states is given in [34]. A pictorial representation of the different degenerate H_0 eigenstates being mapped to a single H_0 eigenstate is shown in Figure 2.3. This result is confirmed to third order in the perturbative expansion of H_{int} in Section 3.1.5.

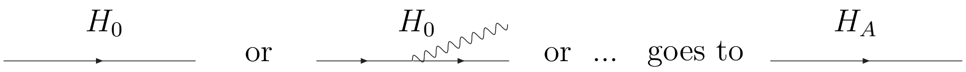

Figure 2.3: Schematic representation of the mapping of different energy degenerate H_0 states on the LHS to a single H_0 state on the RHS.

To calculate scattering matrix elements we would then have,

$$\begin{aligned} \langle \phi_{out} | \Omega^{(-)\dagger} \Omega^{(+)} | \phi_{in} \rangle &= \langle \phi_{out} | \Omega_\Delta^{(-)} \Omega_f^{(-)\dagger} \Omega_f^{(+)} \Omega_\Delta^{(+)\dagger} | \phi_{in} \rangle \\ &\equiv \langle \phi_{out} | \Omega_\Delta^{(-)} S_I \Omega_\Delta^{(+)\dagger} | \phi_{in} \rangle \end{aligned} \tag{2.88}$$

or equally well we could write,

$$\begin{aligned} \langle \phi_{out} | \Omega^{(-)\dagger} \Omega^{(+)} | \phi_{in} \rangle &= \langle \phi_{out} | \Omega_\Delta^{(-)} \Omega_\Delta^{(-)\dagger} \Omega_A^{(-)\dagger} \Omega_A^{(+)} \Omega_\Delta^{(+)} \Omega_\Delta^{(+)\dagger} | \phi_{in} \rangle \\ &\equiv \langle \phi_{out} | S_A | \phi_{in} \rangle \end{aligned} \tag{2.89}$$

The form in Eq.(2.89) differs from the scattering matrix elements of Eq.(2.86) in that we calculate S_A on the H_0 states rather than on the H_A states. So amplitudes derived from this new Møller operator will no longer be unitarily equivalent to the usual amplitudes. It will though give equivalent results at the physical observable level once we have summed over the correct *in* and *out* states. The states that must be summed over will be identical to those that are required when we calculate infrared safe observables from amplitudes using the usual Møller operator $\Omega_f^{(\pm)}$. We can check this using Eq.(1.1) to calculate a physical observable. So if we were to sum over all possible initial and final states we have schematically,

$$\sum_{in,out} \int |A|^2 \times J = \sum_{in,out} \int \langle \phi_{out} | \Omega_{I,A}^\dagger S \Omega_{I,A} | \phi_{in} \rangle \langle \phi_{in} | \Omega_{I,A}^\dagger S^\dagger \Omega_{I,A} | \phi_{out} \rangle \times J$$

$$= \sum_{in,out} \int Tr\left[\Omega^{\dagger}_{I,A} S \Omega_{I,A} \Omega^{\dagger}_{I,A} S \Omega_{I,A}\right] \times J$$
$$= \sum_{in,out} \int Tr\left[S S^{\dagger}\right] \times J \qquad (2.90)$$

This is equivalent to the result we would have for the usual scattering matrix elements from Section 2.2. So after we have summed up all terms contributing to a particular order we expect to get the same results as those achieved using the usual amplitudes. The key difference here is that these new amplitudes are infrared finite before we perform the sum over states and so can be calculated numerically. This potentially simplifies the calculation required to produce a prediction of a physical observable.

There are now two ways that we could proceed to take to calculate the scattering elements. We could use the form given in Eq.(2.88), which would involve calculating the S-Matrix in the usual manner and then *dressing* the states with the $\Omega^{(\pm)}_{\Delta}$ operators. This can be written as,

$$\langle \phi_{out} | \Omega^{(-)}_{\Delta} S_I \Omega^{(+)\dagger}_{\Delta} | \phi_{in} \rangle = \langle \{\phi_{out}\} | S_I | \{\phi_{in}\} \rangle \qquad (2.91)$$

The states $|\{\phi_{\alpha}\}\rangle$ are then known as *dressed states*. When suitably regularised they contain divergences which cancel those in the S_I matrix. Amplitudes of this form will consist of the sum of pieces from the dressed states and from the S-Matrix. Only the sum of these pieces would be infrared finite, the individual pieces would not necessarily have to be. This is the form we will use to perform calculations in Chapter 3. This will be used there because of the greater clarity it gives in demonstrating the infrared finite nature of the amplitudes.

Alternatively we can calculate scattering elements from Eq.(2.89). To do this we would need to derive a form for S_A, this operator will be completely free of infrared singularities throughout the entire calculation. To derive S_A we start by expressing the Møller operators in a time dependent form. We can derive explicit time dependent forms for Eq.(2.87) in two different ways.

As,

$$\Omega^{(+)} \equiv \Omega_f^{(+)}\Omega_\Delta^{(+)\dagger} \equiv \Omega_A^{(+)} \tag{2.92}$$

we could take $\Omega_A^{(+)}$ in the explicit form given by Eq.(2.57) with $H_{A,int} = H_A(\Delta)$ so that we would then be in the asymptotic interaction picture. Then S_A would be given by Eq.(2.65) with $H_{A,int} = H_A(\Delta)$. Using this form would require though the use of an asymptotic basis. Alternatively we could combine the interaction picture forms of $\Omega_f^{(+)}$ and $\Omega_\Delta^{(+)\dagger}$ together directly to derive a perturbative definition for $\Omega^{(+)}$ in the interaction picture. We could then go on to derive a perturbative form for S_A, this approach will be taken in Section 4.1.

The disadvantage of using these Møller operators to derive dressed state amplitudes is that because we are now expanding S_A on a basis of H_0 states then,

$$[S_A, H_0] \neq 0 \tag{2.93}$$

Therefore we will lose energy conservation at the amplitude level. We are though calculating S_A perturbatively and so we will have,

$$S_A \equiv \Omega_\Delta^{(-)} S_I \Omega_\Delta^{(+)\dagger} \tag{2.94}$$

and will hence get an energy delta function from the H_0 states acting on S_I. So instead of having a single energy delta function multiplying the amplitudes, as in Eq.(2.68), there will be an energy delta function that conserves energy across only the S_I part of the amplitude. There will be no delta function coming from the dressing factors. This occurs for both forms of the scattering elements Eq.(2.88) and Eq.(2.89). This will lead to difficulties when attempting to calculate physical observables in Chapter 3.

2.5 Conclusion

In this chapter we have given an overview of the subject of scattering theory. It has particularly highlighted the source of the infrared divergences. They occur when we break the isometry of the Møller operators. This is done when we make the standard assumption that the asymptotic Hamiltonian is equal to the free field Hamiltonian and leads to divergences in the soft and collinear regions of the scattering amplitudes. From this knowledge we have been able to suggest two main solutions to this problem, the first is the asymptotic interaction picture and this will be investigated in Chapter 4. The second method is that of dressed states which we will now look at in greater detail in the next chapter.

Chapter 3

Calculations Using Dressed States

In the previous chapters we have shown how gauge theories with massless fermions are plagued by infrared singularities. Infrared singularities are related to either arbitrarily soft gauge bosons or arbitrarily collinear gauge bosons and/or fermions. More precisely, if we define our external states in the usual way by acting with creation operators on the vacuum, then higher-order S-matrix elements between such external states contain infrared divergences.

Many attempts have been made to define amplitudes that are well defined, i.e. do not contain such singularities. However, most attempts were restricted to soft singularities. In particular it has been shown that in an abelian gauge theory with massive fermions it is possible to define external states whose S-matrix elements are free from infrared singularities to all orders in perturbation theory [28].

An abelian gauge theory with massive fermions does not contain collinear singularities. This simplifies the situation considerably. As soon as we consider the non-abelian case, however, we cannot avoid the appearance of collinear divergences. The reason is that in the non-abelian case a massless gauge boson can split into two arbitrarily collinear gauge bosons. Such a splitting results in a collinear singularity. Thus, giving the fermions a mass does not protect us from collinear singularities.

The aim of this chapter will be to investigate the possibility of defining infrared-finite amplitudes for a massless, non-abelian gauge theory using the method of *dressed* states as defined in the previous chapter. The application of these amplitudes would then, of course, be QCD. In most applications of perturbative QCD the quarks (at least the light flavors) are treated as massless. Since we will have to deal with collinear singularities anyway in a non-abelian theory, we might as well take the common approach and treat the quarks as massless.

We will begin this chapter by giving a detailed definition of what we mean by dressed states and outline how we can construct amplitudes using them. We then discuss some of the calculational techniques we will require. Finally we give an explicit example demonstrating the cancellation of IR singularities within these amplitudes. The example given is that of the total cross section for $e^+e^- \to 2$ jets at NLO.

3.1 Infrared-finite amplitudes using dressed states

In order to obtain infrared-finite amplitudes we will use the formalism of dressed states as described in section 2.4, more specifically we will take the form of the amplitudes given in Eq.(2.88). Measurable cross sections are then constructed out of these infrared-finite matrix elements using eq.(1.1).

The dressed states are denoted as $|\{\phi_\alpha\}\rangle$ and are not eigenstates of $H_A(\Delta)$. This is because the operator generating these states is $\Omega_\Delta^{(+)\dagger}$ and not $\Omega_\Delta^{(+)}$, as it would need to be if it were to be an eigenstate of $H_A(\Delta)$. These states can only be described in a perturbative way and so we will never be able to describe bound states. At each order in perturbation theory though the states $|\{\phi_\alpha\}\rangle$ will correspond to some sort of "jet-like" structure. In particular, these states are coloured and will have to be related to hadronic states using a hadronization model. This is as in the cross-section approach and is an issue that we do not address in this thesis.

From eq.(2.88) we are then led to compute matrix elements

$$\mathcal{M}_{fi} \equiv \langle \phi_{out} | S_A(\Delta) | \phi_{in} \rangle \equiv \langle \{\phi_{out}\} | S_I | \{\phi_{in}\} \rangle \tag{3.1}$$

order by order in perturbation theory and relate them to physical (infrared safe) cross sections. It has been argued previously that matrix elements as given in Eq. (3.1) are also free of soft singularities [34, 35]. In the present chapter we extend this to include collinear singularities (see also [27]). For more details on this issue we refer to Section 3.1.5.

3.1.1 Notation and conventions

Before we proceed let us fix our notation and conventions. Whereas part of the discussion so far was done in the Schrödinger picture we will now turn to the interaction picture. Thus all operators and states are now to be understood to be given in the interaction picture.

To start with we construct the usual states of the Fock space[1]

$$|q_i(p_i) \ldots \bar{q}_j(p_j) \ldots g_k(p_k) \ldots \rangle \equiv \prod_i b^\dagger(p_i) \prod_j d^\dagger(p_j) \prod_k a^\dagger(p_k) \, |0\rangle \tag{3.2}$$

where $b^\dagger$, $d^\dagger$ and $a^\dagger$ denote the creation operators for fermions, anti-fermions and gauge bosons respectively and we suppressed the helicity labels. We will generically denote such states by $|i\rangle$ and $\langle f|$. Of course, we have to keep in mind that the states as given in Eq. (3.2) are not normalisable and we tacitly assume they have been smeared with test functions. Thus, we are really concerned with wave packets. However, we assume they are sharply peaked around a certain value of the momentum such as to represent a particle beam with (nearly) uniform, sharp momentum.

The creation and annihilation operators satisfy the usual (anti)commu-

[1] We should note here that the notation used in Eq.(3.2) should not be confused with the notation of Eq.(1.3) where we used full states, here and from now on such states will be free fields.

tation relations

$$\begin{aligned}
[a(\lambda_1,\vec{k}_1), a^\dagger(\lambda_2,\vec{k}_2)] &= -(2\pi)^3 2\omega(\vec{k}_1) g_{\lambda_1\lambda_2}\,\delta(\vec{k}_1-\vec{k}_2) && (3.3)\\
\{b(r_1,\vec{k}_1), b^\dagger(r_2,\vec{k}_2)\} &= (2\pi)^3 2\omega(\vec{k}_1)\delta_{r_1 r_2}\,\delta(\vec{k}_1-\vec{k}_2) && (3.4)\\
\{d(r_1,\vec{k}_1), d^\dagger(r_2,\vec{k}_2)\} &= (2\pi)^3 2\omega(\vec{k}_1)\delta_{r_1 r_2}\,\delta(\vec{k}_1-\vec{k}_2) && (3.5)
\end{aligned}$$

with $\omega(\vec{k}_i)\equiv|\vec{k}_i|$. Note that the ordering used in Eq. (3.2) implies a certain phase convention. Of course, all amplitudes are only defined up to such a convention.

The field operators are given by

$$\begin{aligned}
\Psi_\alpha &= \int \mathrm{d}\widetilde{k}\,\left(u_\alpha(r,\vec{k})\,b(r,\vec{k})\,e^{-ikx} + v_\alpha(r,\vec{k})\,d^\dagger(r,\vec{k})\,e^{+ikx}\right) && (3.6)\\
\overline{\Psi}_\alpha &= \int \mathrm{d}\widetilde{k}\,\left(\bar{u}_\alpha(r,\vec{k})\,b^\dagger(r,\vec{k})\,e^{+ikx} + \bar{v}_\alpha(r,\vec{k})\,d(r,\vec{k})\,e^{-ikx}\right) && (3.7)\\
A_\mu &= \int \mathrm{d}\widetilde{k}\,\left(\varepsilon_\mu(\lambda,\vec{k})\,a(\lambda,\vec{k})\,e^{-ikx} + \varepsilon^*_\mu(\lambda,\vec{k})\,a^\dagger(\lambda,\vec{k})\,e^{+ikx}\right) && (3.8)
\end{aligned}$$

where we defined

$$\mathrm{d}\widetilde{k} \equiv \frac{d^{D-1}\vec{k}}{(2\pi)^{D-1}2\omega(\vec{k})}\sum_{1,2} \tag{3.9}$$

and the sum is over the two helicities of the fermions or gauge bosons respectively.

Once the interaction Hamiltonian is given we can compute the evolution operator as a time ordered exponential and obtain in the interaction picture

$$U_I(t,t_0) \equiv T\,\exp\left(-i\int_{t_0}^{t} dt\,H_I(t)\right) \tag{3.10}$$

which can be shown to be the same as $U_I(t,t_0)$ generated from Eq.(2.48). The Møller operators are then given by $\Omega^{(\pm)}_{full} = U_I(t_0,\mp\infty)$ in the interaction picture and, thus, the scattering operator S is related to the evolution operator

$$S = \Omega^{(-)\dagger}_{full}\Omega^{(+)}_{full} = U_I(+\infty,t_0)U_I(t_0,-\infty) \tag{3.11}$$

This allows us to find the S-matrix elements between some initial and final state

$$\langle f|S|i\rangle = \langle f|T\ \exp\left(-i\int_{-\infty}^{+\infty} dt\, H_I(t)\right)|i\rangle \tag{3.12}$$

where $|i\rangle$ and $\langle f|$ are states as defined in Eq. (3.2). Inserting the explicit form of H_I into Eq. (3.12) allows us to compute S-matrix elements. Of course, in practise such a calculation is nothing but the computation of the corresponding Feynman diagrams.

3.1.2 Definition of infrared-finite amplitudes

In analogy to Eq. (3.10) we define a form for the soft evolution operator as,

$$U_\Delta(t,t_0) \equiv T\ \exp\left(-i\int_{t_0}^{t} dt\, H_\Delta(t)\right) \tag{3.13}$$

where we only include the soft Hamiltonian $H_\Delta(t) \equiv H_S(\Delta, t)$. Acting on a certain state, the soft evolution operator modifies this state by allowing for soft and collinear emissions. Then, the usual Feynman-Dyson scattering matrix S can be decomposed as,

$$S_I = U_I(+\infty, t_0)U_I(t_0, -\infty) \equiv \Omega_\Delta^{(-)\dagger} S_A(\Delta)\Omega_\Delta^{(+)} \tag{3.14}$$

where we have introduced the soft Møller operators $\Omega_\Delta^{(\pm)} \equiv U_\Delta(t_0, \mp\infty)$, see also eq.(2.85). More explicitly, we have

$$\begin{aligned}
\Omega_\Delta^{(-)\dagger} &\equiv T\ \exp\left(-i\int_0^\infty dt H_\Delta(t)\right) \qquad (3.15)\\
&= 1 - i\int_0^\infty dt\, H_\Delta(t) + (-i)^2\int_0^\infty dt\int_0^t dt'\, H_\Delta(t)H_\Delta(t') + \ldots\\
&= 1 - i\int_0^\infty dt\, H_\Delta(t) + \frac{(-i)^2}{2!}\int_0^\infty dt\int_0^\infty dt'\, T\{H_\Delta(t)H_\Delta(t')\} + \ldots
\end{aligned}$$

where we set $t_0 = 0$ here and for the rest of this chapter. Eq. (3.14) defines a modified scattering operator $S_A(\Delta)$. This operator has the crucial property that it includes at least one hard interaction and, therefore, matrix elements $\langle f|S_A(\Delta)|i\rangle$ of this operator with ordinary external initial and final states as defined in Eq. (3.2) have no infrared singularities. If we define dressed initial and final states, $|\{i\}\rangle$ and $\langle\{f\}|$ according to

$$\begin{aligned} |\{i\}\rangle &\equiv \Omega_\Delta^{(+)\dagger}|i\rangle && (3.16)\\ \langle\{f\}| &\equiv \langle f|\Omega_\Delta^{(-)} && (3.17)\end{aligned}$$

then

$$\langle\{f\}|S|\{i\}\rangle = \langle f|S_A(\Delta)|i\rangle \tag{3.18}$$

Thus, the S-matrix elements of dressed states are free of infrared singularities. We should stress that dressed states are not asymptotic states, i.e. they are not eigenstates of the asymptotic Hamiltonian.

Let us look at a dressed final state somewhat more carefully. We obtain a dressed final state by acting with $\Omega_\Delta^{(-)}$ on a final state as defined in Eq. (3.2). We denote this dressed state by adding curly brackets.

$${}_f\langle\{q(p_i)\ldots\bar{q}(p_j)\ldots g(p_k)\ldots\}| = \langle q(p_i)\ldots\bar{q}(p_j)\ldots g(p_k)\ldots|\Omega_\Delta^{(-)} \tag{3.19}$$

Once the asymptotic Hamiltonian is fixed Eq. (3.19) is a unique relation, order by order in perturbation theory, between an ordinary final state $\langle f|$ and the corresponding dressed final state $\langle\{f\}|$. A similar relation holds for dressed initial states.

$$|\{q(p_i)\ldots\bar{q}(p_j)\ldots g(p_k)\ldots\}\rangle_i = \Omega_\Delta^{(+)\dagger}|q(p_i)\ldots\bar{q}(p_j)\ldots g(p_k)\ldots\rangle \tag{3.20}$$

In what follows we will suppress the labels f and i but keep in mind that the states $|\{q(p_i)\ldots\bar{q}(p_j)\ldots g(p_k)\ldots\}\rangle$ and $\langle\{q(p_i)\ldots\bar{q}(p_j)\ldots g(p_k)\ldots\}|$ are not conjugates of each other. Also, we would like to stress that all these states are states in the usual Fock space. Of course, this implicitly assumes that we use some kind of regularisation for the infrared singularities in intermediate steps.

The soft Møller operators dress the usual non-interacting external states with a cloud of soft and collinear partons. Since the infrared behaviour of H_Δ and the full interaction Hamiltonian are the same by construction, this dressing generates infrared singularities that cancel those generated by the full scattering operator.

There are two main differences between the soft(/collinear) Møller operator, Eq. (3.15), and the usual scattering operator, Eq. (3.12). Firstly, $\Omega_\Delta^{(\pm)}$ involve only the soft part H_Δ of the interaction Hamiltonian. Secondly, the time integration in the soft Møller operator runs only from 0 to ∞ rather than from $-\infty$ to ∞.

The fact that the time integration is restricted to $t > 0$ is related to the loss of Lorentz invariance in the amplitudes $\mathcal{M}_{fi}$, Eq. (3.1). This is to be expected since S_A does not commute with H_0 and, therefore, $\mathcal{M}_{fi}$ is generally not proportional to an energy conserving $\delta(E_i - E_f)$. Instead, individual parts of the amplitude will have δ-functions with different energy arguments (see Eq. (3.29)). The difference between these arguments determines the amount by which energy conservation can be violated in $\mathcal{M}_{fi}$ and is related to the parameter Δ. In the limit $\Delta \to 0$ the amount by which energy can be violated tends to 0. Thus, the parameter Δ determines how much the initial wave packets are distorted through the evolution with the soft Møller operators. We will come back to these issues in Section 3.1.7.

3.1.3 Factorisation of modified S-matrix elements

We now turn to the question on how to compute the infrared-finite amplitudes defined in Eq. (3.18) and how they are related to ordinary amplitudes.

A possible approach is to start from the right hand side of Eq. (3.18). This would involve using the explicit form of S_A, given below in Eq. (3.29) to compute the amplitudes. As we argue in Section 3.1.5 the structure of S_A is such that no infrared singularities occur. This opens up the possibility of evaluating the amplitudes numerically. We have to keep in mind, however, that there are still ultraviolet singularities which will have to be removed by renormalisation. In order to take an entirely numerical approach the renormalisation procedure would have to be done at the integrand level [12].

We will take a somewhat different approach in that we start from the left hand side of Eq. (3.18). We relate the infrared finite amplitude to ordinary amplitudes by inserting a complete set of states twice

$$\langle\{f\}|S|\{i\}\rangle = \langle f|\Omega_\Delta^{(-)}\, S\, \Omega_\Delta^{(+)\dagger}|i\rangle = \langle f|\Omega_\Delta^{(-)}|f'\rangle \otimes \langle f'|S|i'\rangle \otimes \langle i'|\Omega_\Delta^{(+)\dagger}|i\rangle \quad (3.21)$$

Note that in the final expression all states are ordinary Fock space states as defined in Eq. (3.2). In this way, the infrared finite amplitude is split into three pieces. First, there is an ordinary S-matrix element, $\langle f'|S|i'\rangle$. The other two factors are dressing factors for the initial and final state. All these pieces are infrared divergent and only the complete amplitude is infrared finite, order by order in perturbation theory. The ultraviolet singularities appear only in $\langle f'|S|i'\rangle$ and are dealt with as usual by renormalisation. The symbol $\otimes$ denotes integration over all momenta and summation over all helicities of the state under consideration. Thus, for say $\langle f'| = \langle q(p_1,r_1)\bar{q}(p_2,r_2)g(p_3,r_3)| \equiv \langle q_{p1}\bar{q}_{p2}g_{p3}|$ we have

$$|f'\rangle \otimes \langle f'| = \sum_{r_1\, r_2\, r_3} \int \mathrm{d}\widetilde{p}_1 \mathrm{d}\widetilde{p}_2 \mathrm{d}\widetilde{p}_3\; |q_{p1}\bar{q}_{p2}g_{p3}\rangle\, \langle q_{p1}\bar{q}_{p2}g_{p3}| \qquad (3.22)$$

We should stress that Eq. (3.21) implies that the dressing is not done for each external parton separately. The dressing factors $\langle f|\Omega_{\Delta-}|f'\rangle$ do contain terms that factorise into separate contributions for each parton, but they also contain colour correlated contributions.

3.1.4 Dressing factors

As we have seen in Eq. (3.21) infrared-finite amplitudes are composed of three factors. First, there is an ordinary amplitude, $\langle f'|S|i'\rangle$, computed in the usual way using ordinary Feynman rules. Then there are the two dressing factors, one for the initial and one for the final state. The calculation of these dressing factors is somewhat different from the calculation of ordinary amplitudes and it is useful to look at this in some more detail.

For concreteness we consider the calculation of a final state dressing factor. The starting point is Eq. (3.15). Let us stress again that since the time integration in Eq. (3.21) is from 0 to ∞ we break Lorentz invariance right from the beginning. Of course, in the final result for a physical quantity

Lorentz invariance will be restored. In fact, the calculation has many features of (old-fashioned) time-ordered perturbation theory. Most notably, all particles will be on-shell. Three-momentum will be conserved in all vertices, but energy will not be conserved.

A typical term of the (asymptotic) Hamiltonian that gives rise to an n-point interaction has the form

$$\int \mathrm{d}\vec{x} \int \prod_{i=1}^{n} \mathrm{d}\widetilde{k}_i \; V(\vec{k}_i)\Theta(\Delta)\, e^{i\vec{x}\cdot\sum\sigma_i\vec{k}_i} e^{-it\sum\sigma_i\omega(\vec{k}_i)} \tag{3.23}$$

where $\omega(\vec{k}_j) \equiv |\vec{k}_j|$ denotes the energy of the particles and the sign σ_i is positive (negative) for incoming (outgoing) particles. $V(\vec{k}_i)$ is made up of creation and annihilation operators, eventually accompanied by spinors and/or polarisation vectors and a certain power of the coupling constant. The range of integration over the momenta is restricted to the singular regions. This is indicated in the notation by $\Theta(\Delta)$. The precise form of this function is not important at the moment. After performing the $\mathrm{d}\vec{x}$ integration we obtain the momentum conserving delta function $(2\pi)^{D-1}\delta^{(D-1)}(\sum\sigma_i\vec{k}_i)$. However, since the t integration is restricted to $t \geq 0$ we do not obtain an energy conserving δ function. Rather we have to introduce the usual adiabatic factor $0^+ > 0$ and use

$$\int_0^\infty \mathrm{d}t\, e^{-i\omega t} \to \int_0^\infty \mathrm{d}t\, e^{-i\omega t} e^{-t0^+} = \frac{-i}{\omega - i0^+} \tag{3.24}$$

Of course, if the t integration was restricted to $t \leq 0$ we would have

$$\int_{-\infty}^0 \mathrm{d}t\, e^{-i\omega t} \to \int_{-\infty}^0 \mathrm{d}t\, e^{-i\omega t} e^{+t0^+} = \frac{i}{\omega + i0^+} \tag{3.25}$$

and the sum of Eq. (3.24) and Eq. (3.25) indeed results in $2\pi\delta(\omega)$.

To summarise, for an n-point vertex in the calculation of a dressing factor for a final state we have to use

$$\int \prod_{i=1}^{n} \mathrm{d}\widetilde{k}_i\, (2\pi)^{D-1}\delta^{(D-1)}(\sum\sigma_i\vec{k}_i)\, \frac{\Theta(\Delta)}{\sum\sigma_i\omega(\vec{k}_i) - i0^+}\, V(\vec{k}_i) \tag{3.26}$$

Were it not for the $\Theta(\Delta)$ function and the restriction of the t-integration to

$t \geq 0$ this would lead to the standard Feynman rule.

3.1.5 Finiteness of modified S-matrix elements

In this subsection we substantiate our claim that matrix elements as defined in Eq. (3.1) or Eq. (3.18) are free from collinear and soft singularities. We start from the definition

$$S_A(\Delta) = \Omega_\Delta^{(-)} S \, \Omega_\Delta^{(+)\dagger} \tag{3.27}$$

and use the explicit form of the soft Møller operator and S to express $S_A(\Delta)$ in terms of H_Δ and H_H. Furthermore, we observe that according to Eq. (3.23) the time dependence of the Hamiltonian $H(t_j)$ is given by

$$H_H(t_j) = h_j \, e^{-it_j \varpi_j}; \quad H_\Delta(t_j) = s_j \, e^{-it_j \varpi_j} \tag{3.28}$$

where $\varpi_j \equiv \sum \sigma_i \omega(\vec{k}_i)$ is the sum of the energies of the particles associated with the corresponding n-point vertex and h_j and s_j are time independent. Performing the algebra and the t-integrations we obtain up to third order

$$\begin{aligned} S_A &= 1 - 2i\pi \, h_1 \, \delta(\varpi_1) \\ &+ 2i\pi \, h_1 h_2 \, \frac{\delta(\varpi_1 + \varpi_2)}{\varpi_1} + 2i\pi \, [h_1, s_2] \, \frac{\delta(\varpi_1) - \delta(\varpi_1 + \varpi_2)}{\varpi_2} \\ &+ 2i\pi \, h_1(h_2 + s_2)h_3 \, \frac{\delta(\varpi_1 + \varpi_2 + \varpi_3)}{\varpi_1 \varpi_3} \\ &- 2i\pi \, [[h_1, s_2], s_3] \left(\frac{\delta(\varpi_1 + \varpi_2) - \delta(\varpi_1 + \varpi_2 + \varpi_3)}{\varpi_1 \varpi_3} + \frac{\delta(\varpi_1)}{\varpi_2(\varpi_2 + \varpi_3)} \right) \\ &- 2i\pi \, s_1 h_2 h_3 \, \frac{\delta(\varpi_2 + \varpi_3) - \delta(\varpi_1 + \varpi_2 + \varpi_3)}{\varpi_1 \varpi_3} \\ &- 2i\pi \, h_1 h_2 s_3 \, \frac{\delta(\varpi_1 + \varpi_2) - \delta(\varpi_1 + \varpi_2 + \varpi_3)}{\varpi_1 \varpi_3} \end{aligned} \tag{3.29}$$

First of all we notice that all the purely soft terms $s_1 s_2 \ldots$ vanish. This holds to all orders and is crucial to ensure that S_A is free from infrared singularities. Infrared singularities potentially arise if $\varpi_i \to 0$. This corresponds to either a soft or collinear emission at the corresponding vertex. Let us now go through the terms in Eq. (3.29) and check that for none of them such a singularity can occur. For this to be true we have to define h_i such that it vanishes for $\varpi_i \to 0$. This can be achieved by choosing the $\Theta(\Delta)$ in Eq. (3.23) accordingly.

We start by looking at the second order terms, given in the second line of Eq. (3.29). The only potential singularity in the first term is $\varpi_1 \to 0$. This is harmless since $h_1 = 0$ in this limit. In the second term we have the potential singularity $\varpi_2 \to 0$ which is not prevented by s_2. However, in this limit the term is proportional to $\delta(\varpi_1)$ and the same argument as for the first order term applies.

The arguments for the third order terms, given in the third to sixth line of Eq. (3.29) are similar. The only dangerous limits in the third line term for example are $\varpi_1 \to 0$ and $\varpi_3 \to 0$. Both of these are prevented by the presence of h_1 and h_3. Considering the term in the fourth line, we first note that $\delta(\varpi_1)h_1 = 0$. As a result there is no problem with the limit $\varpi_2 \to 0$ and $\varpi_2 \to -\varpi_3$. Furthermore, the singularity in the limit $\varpi_1 \to 0$ is prevented by the presence of h_1 and the limit $\varpi_3 \to 0$ is made harmless by the combination of δ functions. Similarly, the terms in the fifth and sixth line are finite in the limit $\varpi_1 \to 0$ and $\varpi_3 \to 0$. Thus we see that (up to this order) there are no singularities in S_A as long as h_i is chosen to vanish for $\varpi_i \to 0$.

We mention again that S_A does not only contain terms proportional to $\delta(\varpi_1+\varpi_2+\varpi_3)$ but also terms with "incomplete" δ-functions. These are the energy violating terms mentioned above. We also remark that the absence of terms containing $1/(\varpi_i+\varpi_j)$ in S_A (the corresponding term in the fourth line of Eq. (3.29) vanishes) justifies our initial claim that all infrared singularities are related to limits $\varpi_i \to 0$.

3.1.6 Construction of infrared finite amplitudes

The expression given in Eq. (3.21) is a (double) sum over all possible intermediate states $|f'\rangle\langle f'|$ and $|i'\rangle\langle i'|$. However, if we compute the amplitude to a certain order in the coupling constant, only a very limited number of intermediate states contribute. It is for example clear that at order $\mathcal{O}(g^0)$ the dressing factor $\langle f|\Omega_\Delta^{(-)}|f'\rangle$ is zero, unless $f = f'$. From this we see that at leading order in perturbation theory the amplitude $\langle \{f\}|S|\{i\}\rangle$ is the same as $\langle f|S|i\rangle$.

Including higher-order corrections this identity will, of course, not hold any longer. At order $\mathcal{O}(g^1)$ the states f and f' can be different. To get a non-vanishing contribution they must be related either by adding a (soft or collinear) gluon or by exchanging a quark-antiquark pair by a gluon.

In order to illustrate this in more detail, let us consider a concrete process. To simplify matters we consider a case with no partons in the initial state. What we have in mind is for example the process $e^+e^- \to \gamma \to$ jets. As long as we treat this process at leading order in the electromagnetic coupling but at higher order in the strong coupling, g, we encounter only final state singularities. Thus, for the purpose of understanding how the dressing removes the infrared singularities we can restrict ourselves to the final state partons and treat the initial state simply as $|0\rangle$.

Before writing down Eq. (3.21) more explicitly for the process under consideration, let us introduce a somewhat more compact notation. We will denote the momenta and helicities of the partons in the intermediate state f' by q_i and s_i respectively and use the notation $q_{qi} \equiv q(\vec{q}_i, s_i)$ etc. The momenta and helicities of the partons in the final state f on the other hand will be denoted by p_i and r_i and we use $q_{pi} \equiv q(\vec{p}_i, r_i)$. The order $\mathcal{O}(g^n)$ terms of the dressing factors are then denoted by

$$\begin{aligned} & g^n\, \mathcal{W}^{(n)}(q_{p1}, \bar{q}_{p2}, g_{p3} \ldots; q_{q1}, \bar{q}_{q2} \ldots) \equiv \\ & \qquad \langle q(\vec{p}_1, r_1)\bar{q}(\vec{p}_2, r_2)g(\vec{p}_3, r_3)\ldots|\Omega_\Delta^{(-)}|q(\vec{q}_1, s_1)\bar{q}(\vec{q}_2, s_2)\ldots\rangle\Big|_{g^n} \end{aligned} \tag{3.30}$$

Similarly, we denote the order $\mathcal{O}(g^n)$ terms of the amplitude by

$$\begin{aligned} & g^n\, \mathcal{A}^{(n)}(q(\vec{q}_1, s_1), \bar{q}(\vec{q}_2, s_2), g(\vec{q}_3, s_3)\ldots; \gamma) \equiv \\ & \qquad \langle q(\vec{q}_1, s_1)\bar{q}(\vec{q}_2, s_2)g(\vec{q}_3, s_3)\ldots|S|0\rangle\Big|_{g^n} \equiv g^n\, \mathcal{A}^{(n)}(q_{q1}, \bar{q}_{q2}, g_{q3}\ldots; \gamma) \end{aligned} \tag{3.31}$$

and we introduce a notation for the infrared finite amplitudes

$$g^n\, \mathcal{A}^{(n)}(\{q_1(\vec{p}_1, r_1), \bar{q}_2(\vec{p}_2, r_2), g_3(\vec{p}_3, r_3)\ldots\}; \gamma) \equiv \tag{3.32}$$

$$\langle\{q(\vec{p}_1,r_1)\bar{q}(\vec{p}_2,r_2)g(\vec{p}_3,r_3)\ldots\}|S|0\rangle\Big|_{g^n} \equiv g^n\,\mathcal{A}^{(n)}(\{q_{p1},\bar{q}_{p2},g_{p3}\ldots\};\gamma)$$

We always make use of the convention that the helicity associated with momentum $\vec{p}_i$ is r_i whereas the helicity associated with momentum $\vec{q}_i$ is s_i.

Let us now use Eq. (3.21) to write down the infrared finite amplitude $\langle\{q(p_1,r_1)\bar{q}(p_2,r_2)\}|S|0\rangle$ order by order in perturbation theory. At leading order we have

$$\begin{aligned} \mathcal{A}^{(0)}(\{q_{p1},\bar{q}_{p2}\};\gamma) &\equiv \langle\{q(p_1,r_1)\bar{q}(p_2,r_2)\}|S|0\rangle\Big|_{g^0} \\ &= \mathcal{W}^{(0)}(q_{p1},\bar{q}_{p2};q_{q1},\bar{q}_{q2})\otimes\mathcal{A}^{(0)}(q_{q1},\bar{q}_{q2};\gamma) \\ &= \mathcal{A}^{(0)}(q_{p1},\bar{q}_{p2};\gamma) \end{aligned} \tag{3.33}$$

where in the last step we used

$$\begin{aligned} &\mathcal{W}^{(0)}(q_{p1},\bar{q}_{p2};q_{q1},\bar{q}_{q2}) = \\ &\quad (2\pi)^3 2\omega(\vec{p}_1)\delta_{r_1s_1}\delta(\vec{p}_1-\vec{q}_1)\ (2\pi)^3 2\omega(\vec{p}_2)\delta_{r_2s_2}\delta(\vec{p}_2-\vec{q}_2) \end{aligned} \tag{3.34}$$

Eq. (3.34) is simply obtained by noting that $\Omega_{\Delta-}=1$ at $\mathcal{O}(g^0)$, Eq. (3.15), and using the (anti)commutation relations Eqs.(3.3), (3.4) and (3.5).

At $\mathcal{O}(g)$ the amplitude is zero because for every intermediate state f' either the dressing factor $\langle f|\Omega_{\Delta-}|f'\rangle$ or the amplitude $\langle f'|S|0\rangle$ vanishes.

At $\mathcal{O}(g^2)$ the situation is more interesting. We have

$$\begin{aligned} \mathcal{A}^{(2)}(\{q_{p1},\bar{q}_{p2}\};\gamma) &\equiv \langle\{q(p_1,r_1)\bar{q}(p_2,r_2)\}|S|0\rangle\Big|_{g^2} \\ &= \mathcal{W}^{(0)}(q_{p1},\bar{q}_{p2};q_{q1},\bar{q}_{q2})\otimes\mathcal{A}^{(2)}(q_{q1},\bar{q}_{q2};\gamma) \\ &+ \mathcal{W}^{(2)}(q_{p1},\bar{q}_{p2};q_{q1},\bar{q}_{q2})\otimes\mathcal{A}^{(0)}(q_{q1},\bar{q}_{q2};\gamma) \\ &+ \mathcal{W}^{(1)}(q_{p1},\bar{q}_{p2};q_{q1},\bar{q}_{q2},g_{q3})\otimes\mathcal{A}^{(1)}(q_{q1},\bar{q}_{q2},g_{q3};\gamma) \end{aligned} \tag{3.35}$$

The first term on the right hand side of Eq. (3.35) is nothing but the usual one-loop amplitude multiplied by the $\mathcal{O}(g^0)$ dressing factor and, using Eq. (3.34), can be written as

$$\mathcal{W}^{(0)}(q_{p1},\bar{q}_{p2};q_{q1},\bar{q}_{q2})\otimes\mathcal{A}^{(2)}(q_{q1},\bar{q}_{q2};\gamma) = \mathcal{A}^{(2)}(q_{p1},\bar{q}_{p2};\gamma) \tag{3.36}$$

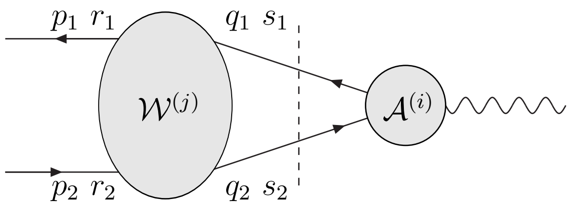

Figure 3.1: Cut diagrams for 2-particle intermediate state. The term $\mathcal{W}^{(0)} \otimes \mathcal{A}^{(2)}$ of Eq. (3.36) corresponds to $j = 0, i = 2$ and $\mathcal{W}^{(2)} \otimes \mathcal{A}^{(0)}$ corresponds to $j = 2, i = 0$.

The second term is also a two-particle cut term, but this time it is the usual tree-level amplitude multiplied by the next-to-leading order dressing factor. These two terms are shown in Figure 3.1.

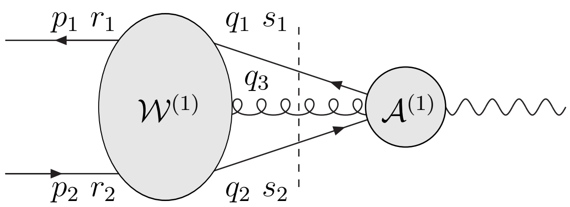

Figure 3.2: Cut diagram for 3-particle intermediate state.

The third term in Eq. (3.35) is of a somewhat different nature as it is a three-particle cut diagram, as illustrated in Figure 3.2. The dressing factor $\mathcal{W}^{(1)}(q_{p1}, \bar{q}_{p2}; q_{q1}, \bar{q}_{q2}, g_{q3})$ is zero unless the gluon g_{q3} is either soft or collinear to the quark or antiquark. Thus, the dressing factor projects out the infrared singular piece of the bremsstrahlung amplitude. This is exactly the piece that is needed to render the full amplitude $\mathcal{A}^{(2)}(\{q_{p1}, \bar{q}_{p2}\}; \gamma)$ finite.

In the next section we will calculate this amplitude explicitly and check that the infrared singularities present in the three terms of Eq. (3.35) cancel in the sum.

The construction of the amplitude at higher orders in g follows the same pattern. For any odd power of g the amplitude vanishes for the same reason as it vanishes at $\mathcal{O}(g)$. At $\mathcal{O}(g^4)$ it is given by

$$
\begin{aligned}
\mathcal{A}^{(4)}(\{q_{p1}, \bar{q}_{p2}\}; \gamma) = & \qquad\qquad\qquad\qquad\qquad\qquad\qquad\qquad\qquad (3.37)\\
& \mathcal{W}^{(0)}(q_{p1}, \bar{q}_{p2}; q_{q1}, \bar{q}_{q2}) \otimes \mathcal{A}^{(4)}(q_{q1}, \bar{q}_{q2}; \gamma) \\
+ & \mathcal{W}^{(2)}(q_{p1}, \bar{q}_{p2}; q_{q1}, \bar{q}_{q2}) \otimes \mathcal{A}^{(2)}(q_{q1}, \bar{q}_{q2}; \gamma) \\
+ & \mathcal{W}^{(4)}(q_{p1}, \bar{q}_{p2}; q_{q1}, \bar{q}_{q2}) \otimes \mathcal{A}^{(0)}(q_{q1}, \bar{q}_{q2}; \gamma) \\
+ & \mathcal{W}^{(1)}(q_{p1}, \bar{q}_{p2}; q_{q1}, \bar{q}_{q2}, g_{q3}) \otimes \mathcal{A}^{(3)}(q_{q1}, \bar{q}_{q2}, g_{q3}; \gamma) \\
+ & \mathcal{W}^{(3)}(q_{p1}, \bar{q}_{p2}; q_{q1}, \bar{q}_{q2}, g_{q3}) \otimes \mathcal{A}^{(1)}(q_{q1}, \bar{q}_{q2}, g_{q3}; \gamma) \\
+ & \mathcal{W}^{(2)}(q_{p1}, \bar{q}_{p2}; q_{q1}, \bar{q}_{q2}, g_{q3}, g_{q4}) \otimes \mathcal{A}^{(2)}(q_{q1}, \bar{q}_{q2}, g_{q3}, g_{q4}; \gamma) \\
+ & \mathcal{W}^{(2)}(q_{p1}, \bar{q}_{p2}; q_{q1}, \bar{q}_{q2}, q_{q3}, \bar{q}_{q4}) \otimes \mathcal{A}^{(2)}(q_{q1}, \bar{q}_{q2}, q_{q3}, \bar{q}_{q4}; \gamma)
\end{aligned}
$$

The separate terms in Eq. (3.37) are infrared divergent but in the sum all these divergences cancel. This can be seen by looking at a particular Feynman diagram, for example the one shown in Figure 3.3, and realising that Eq. (3.37) is nothing but the sum over all possible cuts. Since the dressing factors are constructed such that in the infrared limit they correspond to the usual amplitudes it is clear that the infrared singularities in $\mathcal{A}^{(4)}(\{q_{p1}, \bar{q}_{p2}\}; \gamma)$ have to cancel in the same way as they cancel in ordinary cut diagrams. The first term of Eq. (3.37) corresponds to the ordinary two-loop amplitude and is represented by cut 1. The other two-particle cuts, the second and third term, are represented by cut 2 and 3. There are two three-particle cut terms, term 4 and 5. Finally, for the diagram under consideration, there is one four-particle cut contribution, namely term 6. For a certain Feynman diagram not all terms of Eq. (3.37) are present. In our case, the last term of Eq. (3.37) which is another four-particle cut contribution is missing.

We should stress that our approach to construct infrared finite amplitudes is by no means restricted to amplitudes with final state singularities only. Initial state singularities are dealt with by dressing the initial state, as can be seen in Eq. (3.21).

In fact, the dressing of the initial state would even be needed for processes as discussed above, i.e. with say only a γ in the initial state. Above and in

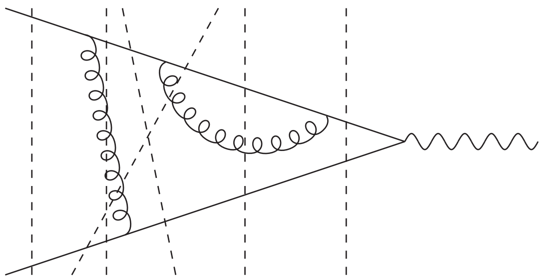

Figure 3.3: All possible cuts of a Feynman diagram representing the various terms of Eq. (3.37).

the rest of this paper we have excluded any QED vertices from the soft Hamiltonian even though there is a potential collinear singularity at this vertex. We do this because we treat the incoming photon as off-shell and so it will generate no infrared singularities.

If we were to include such vertices in the soft Hamiltonian then we would generate many more diagrams with non-vanishing initial-state dressing factors such as $\mathcal{W}(q(\vec{q}_1, s_1), \bar{q}(\vec{q}_2, s_2), g(\vec{q}_3, s_3); \gamma)$. We would find though, that all such extra contributes would cancel as all diagrams with purely soft vertices cancel as described in Section 3.1.5.

3.1.7 From amplitudes to cross sections

Once the infrared finite amplitudes have been computed, they can be used to compute cross sections for observables related to these amplitudes. The procedure to obtain cross sections from amplitudes depends to some extent on the external states we use and deserves some further considerations.

In the cross-section approach we usually deal with amplitudes that are proportional to a four-dimensional delta function. Upon taking the absolute value squared, this leaves us with the problem of interpreting the square of a delta function. Usually this is dealt with in a rather non-rigorous manner by putting the system in a four dimensional box of size $V \cdot T$. The square of the delta function is then interpreted as $V \cdot T$ times a single delta function.

The factor $V \cdot T$ is cancelled by taking into account the normalisation of the states and the flux factor, which leaves us with a cross section proportional to a single four-dimensional delta function, expressing conservation of four momentum.

The appearance of the square of the delta function is of course related to the fact that we usually work with non-normalisable states with a sharp value of momentum and energy. In a more rigorous treatment within the cross-section approach the in and out states would have to be written as wave packets, sharply peaked around a certain value of momentum and energy. It can then be shown that the spreading of the wave packet during the scattering process can be safely neglected [43]. As mentioned in Section 2.2.1 the precise definition of the measurable quantity is given in terms of a measurement function. This is a function of the partonic momenta. If we are dealing with wave packets rather than sharp-momentum states, the measurement function has to be defined in terms of these wave packets. However, as long as we deal with wave packets whose spread is well below any experimental resolution, we can simply use the normal measurement function with the partonic momentum replaced by the central value of the wave packet and we get the same result as in the above mentioned, less rigorous approach [43].

Let us now turn to the situation we encounter if we work with infrared-finite amplitudes, defined in Eq. (3.1). As mentioned before, the amplitude is then not proportional to an energy conserving delta function, even if we were to start with the usual non-normalisable states. Following the proper treatment with wave packets, we think of the states $|i\rangle$ and $\langle f|$ (or $|\Phi_i\rangle$ and $\langle\Phi_f|$) as sharply peaked wave packets. The states $|\{i\}\rangle$ and $\langle\{f\}|$ as defined in Eqs. (3.16) and (3.17) are also wave packets. Through the action of the Møller operators, their spread is larger than the spread of $|i\rangle$ and $\langle f|$ and depends crucially on the parameter Δ. If we choose Δ small enough such that the spread of the wave packets related to the states $|\{i\}\rangle$ and $\langle\{f\}|$ is still smaller than any experimental resolution, we can still compute any measurable cross section by using the standard measurement function with the partonic momenta replaced by the central value of the wave packet.

The important point is that we must be able to express any measurable quantity in terms of the states $|\{i\}\rangle$ and $\langle\{f\}|$. However, since the states $|\{i\}\rangle$ and $\langle\{f\}|$ differ from $|i\rangle$ and $\langle f|$ only by soft and collinear interactions, this is nothing but the requirement that the quantity we are dealing with is infrared safe. Indeed, the requirement of infrared safety states that the quantity must not depend on whether or not a parton emits another arbitrarily soft or collinear parton. But in the limit $\Delta \to 0$ the soft Møller operators do precisely this. Thus, choosing Δ small enough ensures that the construction of the measurable quantity in terms of the partonic momenta is not affected by the soft Møller operators.

This solves the problem on how to obtain differential cross sections, once the infrared-finite amplitudes are known, in principle. In practise, the explicit implementation of this programme is far from trivial and requires further investigations. We mention for example that choosing Δ very small might result in numerical problems, similar to the so called binning problem in the standard approach. If, on the other hand, we choose Δ too large (relative to the experimental resolution) the infrared-finite amplitudes are too inclusive to allow the computation of any possible physical quantity. It has been advocated before that the most convenient choice of H_A is the one that precisely corresponds to the experimental resolution [27]. While this might be true in principle, we think that this is not a practicable way to proceed, since then the asymptotic Hamiltonian would depend on the details of the experiment.

3.2 An example $e^+e^- \to$ 2 jets at NLO

We consider the process $e^+e^- \to \gamma(P) \to 2$ jets. At leading order there is only one partonic process that contributes, $e^+e^- \to q\bar{q}$. However, at next-to-leading order there is also the process $e^+e^- \to q\bar{q}g$. Since the initial state does not interact strongly we can restrict our considerations to the process $\gamma^*(P) \to 2$ jets. An example of how this process is calculated in the usual approach is given in section 1.4.

3.2.1 The infrared finite amplitudes

In terms of infrared finite amplitudes, at next-to-leading order a cross section is also made up of two contributions. The two amplitudes that contribute are those with the final states $\langle\{q_{p1}\bar{q}_{p2}\}|$ and $\langle\{q_{p1}\bar{q}_{p2}g_{p3}\}|$. However, the crucial point is that both these amplitudes are infrared finite. Up to the order in g required they are given by

$$\begin{aligned}
\mathcal{A}(\{q_{p1},\bar{q}_{p2}\};\gamma) \equiv \langle\{q_{p1}\bar{q}_{p2}\}|S|0\rangle = & \qquad\qquad (3.38)\\
\int \mathrm{d}\widetilde{q}_1\mathrm{d}\widetilde{q}_2\ & \mathcal{W}^{(0)}(q_{p1},\bar{q}_{p2};q_{q1},\bar{q}_{q2}) \times \mathcal{A}^{(0)}(q_{q1},\bar{q}_{q2};\gamma(P))\\
+ \int \mathrm{d}\widetilde{q}_1\mathrm{d}\widetilde{q}_2\ & g^2\,\mathcal{W}^{(0)}(q_{p1},\bar{q}_{p2};q_{q1},\bar{q}_{q2}) \times \mathcal{A}^{(2)}(q_{q1},\bar{q}_{q2};\gamma(P))\\
+ \int \mathrm{d}\widetilde{q}_1\mathrm{d}\widetilde{q}_2\ & g^2\,\mathcal{W}^{(2)}(q_{p1},\bar{q}_{p2};q_{q1},\bar{q}_{q2}) \times \mathcal{A}^{(0)}(q_{q1},\bar{q}_{q2};\gamma(P))\\
+ \int \mathrm{d}\widetilde{q}_1\mathrm{d}\widetilde{q}_2\mathrm{d}\widetilde{q}_3\ & g^2\,\mathcal{W}^{(1)}(q_{p1},\bar{q}_{p2};q_{q1},\bar{q}_{q2},g_{q3})\\
& \times \mathcal{A}^{(1)}(q_{q1},\bar{q}_{q2},g_{q3};\gamma(P)) \ +\ \mathcal{O}(g^4)
\end{aligned}$$

and

$$\begin{aligned}
\mathcal{A}(\{q_{p1},\bar{q}_{p2},g_{p3}\};\gamma) \equiv \langle\{q_{p1}\bar{q}_{p2}g_{p3}\}|S|0\rangle = & \qquad\qquad (3.39)\\
\int \mathrm{d}\widetilde{q}_1\mathrm{d}\widetilde{q}_2\ & g\,\mathcal{W}^{(1)}(q_{p1},\bar{q}_{p2},g_{p3};q_{q1},\bar{q}_{q2}) \times \mathcal{A}^{(0)}(q_{q1},\bar{q}_{q2};\gamma(P))\\
+ \int \mathrm{d}\widetilde{q}_1\mathrm{d}\widetilde{q}_2\mathrm{d}\widetilde{q}_3\ & g\,\mathcal{W}^{(0)}(q_{p1},\bar{q}_{p2},g_{p3};q_{q1},\bar{q}_{q2},g_{q3})\\
& \times \mathcal{A}^{(1)}(q_{q1},\bar{q}_{q2},g_{q3};\gamma(P)) \ +\ \mathcal{O}(g^3)
\end{aligned}$$

where a sum over the spin/helicities of the intermediate particles is understood to be included in $\int \mathrm{d}\widetilde{q}_i$, Eq. (3.9).

3.2.2 The asymptotic Hamiltonian

Before we can proceed with the calculation of the infrared finite amplitudes we have to define the asymptotic Hamiltonian H_Δ. Once we have H_Δ we can obtain the Møller operator, Eq. (3.15), and use it to construct the dressed states, Eq. (3.19), order by order in perturbation theory.

The only condition on H_Δ is that it includes all long-range interactions from the original Hamiltonian. In order to separate these long range soft and collinear emission terms from the hard emission terms we need to introduce (at least) one parameter which we denote by Δ. The dependence of the asymptotic Hamiltonian on this parameter is indicated in the notation H_Δ. Once these terms are incorporated into the asymptotic Hamiltonian we are free to include any other terms from the original Hamiltonian that we wish, as these will only produce finite Δ-dependent contributions to the two final amplitudes. It is clear from Eq. (3.21) that for the final result this Δ dependence has to cancel.

In our case the only term of the interaction Hamiltonian we wish to include in H_Δ is the quark gluon interaction vertex,

$$H_I \equiv g \int d\vec{x}\ :\overline{\Psi} T^a \gamma^\mu \Psi : A_\mu^a \tag{3.40}$$

Using Eqs. (3.6,3.7) and (3.8) we see that H_I consists of eight terms

$$\begin{aligned} H_I \;\; &= \;\; g\, T^a \int \mathrm{d}\widetilde{k}_1 \mathrm{d}\widetilde{k}_2 \mathrm{d}\widetilde{k}_3 \sum_{i=1}^{8} V_i(\vec{k}_1, \vec{k}_2, \vec{k}_3) \qquad (3.41) \\ & \qquad \times \exp\left(-it \sum_{j=1}^{3} \sigma_{ij}\omega(\vec{k}_j)\right) \delta^{(D-1)}\left(\sum_{j=1}^{3} \sigma_{ij}\vec{k}_j\right), \end{aligned}$$

where (suppressing the helicity and colour labels)

$$\begin{aligned}
V_1 &= b^\dagger(\vec{k}_1) b(\vec{k}_2) a(\vec{k}_3) \cdot \bar{u}(\vec{k}_1) \not{\epsilon}(\vec{k}_3) u(\vec{k}_2), \\
V_2 &= b^\dagger(\vec{k}_1) d^\dagger(\vec{k}_2) a(\vec{k}_3) \cdot \bar{u}(\vec{k}_1) \not{\epsilon}(\vec{k}_3) v(\vec{k}_2), \\
V_3 &= d(\vec{k}_1) b(\vec{k}_2) a(\vec{k}_3) \cdot \bar{v}(\vec{k}_1) \not{\epsilon}(\vec{k}_3) u(\vec{k}_2), \\
V_4 &= -d^\dagger(\vec{k}_1) d(\vec{k}_2) a(\vec{k}_3) \cdot \bar{v}(\vec{k}_2) \not{\epsilon}(\vec{k}_3) v(\vec{k}_1), \\
V_5 &= b^\dagger(\vec{k}_1) b(\vec{k}_2) a^\dagger(\vec{k}_3) \cdot \bar{u}(\vec{k}_1) \not{\epsilon}^*(\vec{k}_3) u(\vec{k}_2), \\
V_6 &= d(\vec{k}_1) b(\vec{k}_2) a^\dagger(\vec{k}_3) \cdot \bar{v}(\vec{k}_1) \not{\epsilon}^*(\vec{k}_3) u(\vec{k}_2), \\
V_7 &= b^\dagger(\vec{k}_1) d^\dagger(\vec{k}_2) a^\dagger(\vec{k}_3) \cdot \bar{u}(\vec{k}_1) \not{\epsilon}^*(\vec{k}_3) v(\vec{k}_2),
\end{aligned}$$

$$V_8 \;=\; -d^\dagger(\vec{k}_1)d(\vec{k}_2)a^\dagger(\vec{k}_3)\cdot\bar{v}(\vec{k}_2)\not{\epsilon}^*(\vec{k}_3)v(\vec{k}_1) \tag{3.42}$$

The sign factors σ_{ij} are $+1$ (-1) for incoming (outgoing) particles.

As we only have to include terms in H_Δ that contribute in the singular regions we are free to exclude the V_i in Eq. (3.42) for which $\sum \sigma_i\omega(\vec{k}_i)$ can never equal zero with all $\omega(\vec{k}_i) \geq 0$ such that not all of the $\omega(\vec{k}_i) = 0$. We can see from Eq. (3.26) that such terms will always be finite. From the remaining terms we choose only those that give a singularity in the physically relevant soft or collinear regions. This means that for our example we can exclude V_2 and V_6, as these only go singular when the two incoming or outgoing quarks from the vertex are collinear. We emphasise that for more general processes these terms have to be included in the asymptotic Hamiltonian.

We can confine the remaining terms even further as we are free to choose the form of the finite part of H_Δ. We restrict the integration of the momenta $\vec{k}_1, \vec{k}_2$ and $\vec{k}_3$ to just the potentially singular regions. This restriction is achieved here by including a theta function, $\Theta(\Delta_i(\vec{k}_1,\vec{k}_2,\vec{k}_3))$ in each V_i from Eq. (3.42) which will appear in H_Δ. The form of $\Delta_i(\vec{k}_1,\vec{k}_2,\vec{k}_3)$ is completely arbitrary as long as $\Theta \to 1$ in the soft and collinear limits.

The form of the Θ function that we will take for this example is,

$$\Theta(\Delta_i(\vec{k}_1,\vec{k}_2,\vec{k}_3)) \equiv \Theta(\Delta - |\sum_j \sigma_{ij}\omega(\vec{k}_j)|). \tag{3.43}$$

This choice of $\Delta(\vec{k}_1,\vec{k}_2,\vec{k}_3)$ is particularly appropriate because as we see in Eq. (3.26), $\sum_j \sigma_{ij}\omega(\vec{k}_j)$ is the exact form that the singular terms take. This theta function therefore restricts the integral to just the regions close to these singular limits.

By splitting up the covariant vertex into pieces and restricting the integration to just the singular regions we are removing the manifest Lorentz and gauge invariance from the amplitudes. Physical observables will though be Lorentz and gauge invariant as we are effectively just performing a unitary transformation (as we have regulated the $\Omega_\pm$ operators) on a known Lorentz and gauge invariant result.

To summarise, for our asymptotic Hamiltonian we take just the vertices

V_1, V_4, V_5 and V_8, giving,

$$\begin{aligned} H_\Delta &= g \int \mathrm{d}\widetilde{k}_1 \mathrm{d}\widetilde{k}_2 \mathrm{d}\widetilde{k}_3 \sum_{i=1,4,5,8} \left\{ V_i(\vec{k}_1, \vec{k}_2, \vec{k}_3) \exp\left(-it \sum_{j=1}^{3} \sigma_{ij} \omega(\vec{k}_j) \right) \right. \\ &\qquad \left. \delta^{(D-1)} \left(\sum_{j=1}^{3} \sigma_{ij} \vec{k}_j \right) \Theta(\Delta - | \sum_j \sigma_{ij} \omega(\vec{k}_j)|) \right\}. \qquad (3.44) \end{aligned}$$

3.2.3 Diagrammatic rules for the asymptotic regions

We can now take Eq. (3.44) and use it in Eq. (3.15) to form the asymptotic operator. We could then go on to calculate the dressed states of Eq. (3.30) with this operator defined between suitable in and out states by using the commutation relations between a, b, d, $a^\dagger$, $b^\dagger$, $d^\dagger$ and time-ordered perturbation theory. However it can be shown that there are a set of diagrammatic rules for the asymptotic region which behave in a similar way to Feynman diagrams in normal perturbative field theory. Using these we rules we can simplify the calculation.

These diagrammatic rules consist of vertex and propagator 'like' objects, but unlike normal Feynman diagrams we must take all time orderings of the vertices into account. This is because we base the evaluation of the amplitude in the asymptotic region on time ordered perturbation theory. As mentioned before energy is not conserved at each vertex and since the range of the time integration in the Møller operators is from 0 to ∞ there is no overall energy conservation.

As there is a time ordering to the vertices we have both absorption and emission rules. These are defined in Figure 3.4 with time flowing from right to left.

We form propagator 'like' objects from the spin sums of fermion spinors and an associated energy denominator. Although they are not real propagators in the normal field theory sense of inverted off-shell two-point Green functions, they do represent the transition from one vertex to another. The rules for these are shown in Figure 3.5, where $\overline{p}^\mu \equiv (p^0, -\vec{p})$.

As with ordinary field theory we must integrate over all internal momenta and so for each propagator in the asymptotic region we must integrate over

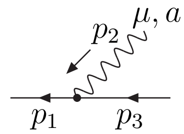

$$\equiv (ig)T^a\gamma^\mu \frac{\delta^{(3)}(\vec{p}_3+\vec{p}_2-\vec{p}_1)}{\omega(\vec{p}_3)+\omega(\vec{p}_2)-\omega(\vec{p}_1)-i0^+} \times \Theta(\Delta - |\omega(\vec{p}_3)+\omega(\vec{p}_2)-\omega(\vec{p}_1)|)$$

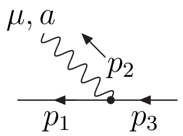

$$\equiv (-ig)T^a\gamma^\mu \frac{\delta^{(3)}(\vec{p}_1+\vec{p}_2-\vec{p}_3)}{\omega(\vec{p}_1)+\omega(\vec{p}_2)-\omega(\vec{p}_3)-i0^+} \times \Theta(\Delta - |\omega(\vec{p}_1)+\omega(\vec{p}_2)-\omega(\vec{p}_3)|)$$

Figure 3.4: The diagrammatic rules for vertices.

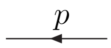

$$\equiv \frac{i\not{p}}{2\omega(\vec{p})}.$$

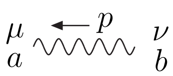

$$\equiv \frac{\delta^{ab}}{2\omega(\vec{p})}\left(-g_{\mu\nu} + \frac{p_\mu \overline{p}_\nu + p_\nu \overline{p}_\mu}{(p\overline{p})}\right).$$

Figure 3.5: The diagrammatic rules for propagators.

its momentum $\int d^{D-1}p/(2\pi)^{D-1}$ in $D-1 = 3-2\epsilon$ dimensions. The rules for external particles are exactly the same as for QED or QCD and so do not need to be reproduced here. Finally we must include a factor of $1/n!$ with each diagram, where n represents the order in the coupling in the asymptotic region.

As stated before the soft Møller operators are not necessarily gauge invariant nor Lorentz invariant. Infrared singularities though will only occur in the region where $\varpi = \sum \sigma_i \omega(\vec{k}_i) = 0$. In this limit Lorentz invariance is restored and so the structure of the singularities will also be Lorentz invariant. Given that our amplitudes will not be gauge invariant, we will perform all calculations including the second term of the gluon propagator which ensures that we sum over physical polarisations only.

3.2.4 The amplitude $\mathcal{A}(\{q(p_1), \bar{q}(p_2)\}; \gamma)$

Let us start with the amplitude $\mathcal{A}(\{q_{p1}, \bar{q}_{p2}\}; \gamma)$ given in Eq. (3.38). This amplitude consists of four terms and we will look at each of them in turn.

The first and second term will be dealt with in Section 3.2.4 and 3.2.4 respectively. For the third term of Eq. (3.38) we need the dressing factor $\mathcal{W}^{(2)}(q_{p1}, \bar{q}_{p2}; q_{q1}, \bar{q}_{q2})$. There are various combinations of interaction terms of the asymptotic Hamiltonian that give rise to non-vanishing contributions to $\mathcal{W}^{(2)}$. These can be found using the diagrammatic rules of Section 3.2.3. We find that there are four contributing diagrams. These four diagrams can be split into two classes, two self-interaction terms and two one-gluon exchange terms.

The Born term

The first term is

$$\int \mathrm{d}\widetilde{q}_1 \mathrm{d}\widetilde{q}_2 \; \mathcal{W}^{(0)}(q_{p1}, \bar{q}_{p2}; q_{q1}, \bar{q}_{q2}) \times \mathcal{A}^{(0)}(q_{q1}, \bar{q}_{q2}; \gamma(P)) \tag{3.45}$$

and is of order g^0. As discussed previously, Eq. (3.33), this term corresponds precisely to the tree-level amplitude.

$$\begin{aligned} \mathcal{A}^{(0)}(\{q_{p1}, \bar{q}_{p2}\}; \gamma(P)) &= (-ie)\, \delta_{ij}\, \langle p_1|\gamma^\alpha|p_2\rangle\, (2\pi)^D \delta^{(D)}(P - p_1 - p_2) \\ &= \mathcal{A}^{(0)}(q_{p1}, \bar{q}_{p2}; \gamma(P)). \end{aligned}$$

We use a notation where $\langle p_i|$ represents the spinor of a massless outgoing fermion with momentum p_i and similarly $|p_j\rangle$ represents the spinor of a massless incoming fermion of momentum p_j. Of course, these spinors depend on the helicity of the fermion, but we suppress this dependence in the notation. The delta function as usual ensures energy-momentum conservation for the process and the δ_{ij} represents the colour flow through the diagram.

The virtual term

In the same way we see that the second term of Eq. (3.38) corresponds to the one-loop amplitude

$$\mathcal{A}^{(2)}(q_{p1}, \bar{q}_{p2}; \gamma(P)) = \tag{3.46}$$

$$C_F\left(\frac{\alpha_s}{2\pi}\right)\left(\frac{\mu^2}{s}\right)^{\epsilon}\left(-\frac{1}{\epsilon^2}-\frac{3}{2\epsilon}-4+\frac{c_R}{2}+\frac{\pi^2}{12}\right)\mathcal{A}^{(0)}(q_{p1},\bar{q}_{p2};\gamma(P))+\mathcal{O}(\epsilon).$$

The infrared singularities appearing in Eq. (3.46) will be cancelled by infrared singularities of the third and fourth term of Eq. (3.38). We should mention that the finite term in Eq. (3.46) depends on the regularisation scheme used. The result in conventional dimensional regularisation is obtained by setting $c_R = 0$ whereas in dimensional reduction we set $c_R = 1$.

The self-interaction terms

The two self-interaction terms are obtained by taking the interacting terms V_1, V_5 and V_4, V_8 of the asymptotic Hamiltonian as given in Eq. (3.42). Since there is a symmetry between these two contributions we only need to calculate one of the pair of diagrams. The self interacting term resulting from the vertices V_1, V_5 is shown in Figure 3.6 and is given by

$$\begin{aligned}
a_{15}^{\{2,0\}} &\equiv \int \mathrm{d}\widetilde{q}_1\mathrm{d}\widetilde{q}_2\; g^2\; \mathcal{W}_{15}^{(2)}(q_{p1},\bar{q}_{p2};q_{q1},\bar{q}_{q2})\times\mathcal{A}^{(0)}(q_{q1},\bar{q}_{q2};\gamma(P)) \qquad (3.47)\\
&= -\frac{(-ie)\,g^2}{2}\int d^{D-1}q_1 d^{D-1}q_2 \frac{d^{D-1}q_3}{(2\pi)^{D-1}}\; T^a_{ik}T^b_{kj}\\
&\quad \frac{\delta^{ab}}{2\omega(\vec{q}_3)}\left(-g^{\mu\nu}+\frac{q_3^{\mu}\,\overline{q}_3^{\nu}+q_3^{\nu}\,\overline{q}_3^{\mu}}{(q_3\overline{q}_3)}\right)\langle p_1|\gamma_\mu\, \not{q}_2\gamma_\nu\, \not{q}_1\gamma^\alpha|p_2\rangle\\
&\quad \frac{\Theta(\Delta-|\omega(\vec{q}_2)+\omega(\vec{q}_3)-\omega(\vec{p}_1)|)\,\Theta(\Delta-|\omega(\vec{q}_2)+\omega(\vec{q}_3)-\omega(\vec{q}_1)|)}{2\omega(\vec{q}_1)\,(\omega(\vec{q}_2)+\omega(\vec{q}_3)-\omega(\vec{p}_1))\;\,2\omega(\vec{q}_2)\,(\omega(\vec{q}_2)+\omega(\vec{q}_3)-\omega(\vec{q}_1))}\\
&\quad \delta^{(D-1)}(\vec{q}_2+\vec{q}_3-\vec{p}_1)\,\delta^{(D-1)}(\vec{q}_2+\vec{q}_3-\vec{q}_1)\,(2\pi)^D\,\delta^{(D)}(P-q_1-p_2).
\end{aligned}$$

Note that this expression contains a D-dimensional delta function coming from $\mathcal{A}^{(0)}$ and two $(D-1)$-dimensional delta functions coming from 3-momentum conservation of the vertices in the dressing factor.

We now proceed to perform the integrals over $\vec{q}_1$ and $\vec{q}_2$, removing the two $(D-1)$ dimensional delta functions. There is an important subtlety here. Since the delta functions are $(D-1)$ dimensional, only the spatial part of the 4-vectors is altered. All 4-vectors in the asymptotic region though must be on-shell and so we are forced to modify the energy component of these 4-vectors to preserve this property. Although these modified 4-vectors are

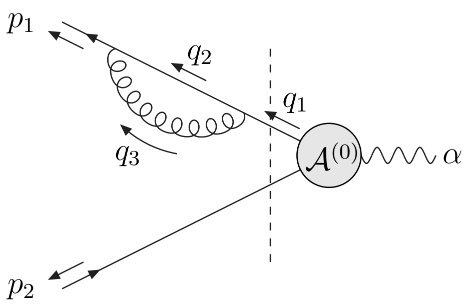

Figure 3.6: Cut diagram for self interaction with 2-particle intermediate state.

4 component objects they no longer transform as tensors. This is simply a manifestation of the breaking of Lorentz invariance that occurs in time-ordered perturbation theory. To denote such objects we place curly brackets of the type { } around them, i.e. we define

$$\{p_1 - q_3\} \equiv (\omega(\vec{p}_1 - \vec{q}_3), \vec{p}_1 - \vec{q}_3) \tag{3.48}$$

We then have

$$\begin{aligned} a_{15}^{\{2,0\}} \quad = \quad & -\frac{(-ie)\, g^2}{2} T^a_{ik} T^a_{kj} \, (2\pi)^D \delta^{(D)}(P - p_1 - p_2) \\ & \int \mathrm{d}\widetilde{q}_3 \left(-g^{\mu\nu} + \frac{q_3^\mu \, \overline{q}_3^\nu + q_3^\nu \, \overline{q}_3^\mu}{(q_3 \overline{q}_3)} \right) \Theta(\Delta - |\rho(\vec{q}_3, \vec{p}_1 - \vec{q}_3)|) \\ & \frac{\langle p_1 | \gamma_\mu \{\not{p}_1 - \not{q}_3\} \gamma_\nu \not{p}_1 \gamma^\alpha | p_2 \rangle}{2\omega(\vec{p}_1) 2\omega(\vec{p}_1 - \vec{q}_3) \rho(\vec{q}_3, \vec{p}_1 - \vec{q}_3)^2} \end{aligned} \tag{3.49}$$

where we defined

$$\rho(\vec{k}_1, \vec{k}_2) \equiv \omega(\vec{k}_1) + \omega(\vec{k}_2) - \omega(\vec{k}_1 + \vec{k}_2) \tag{3.50}$$

This diagram contains infrared singularities coming from the region where q_3 is soft and/or collinear to p_1. We discuss its evaluation in Appendix A. Multiplying by two to take into account both of the self-interaction diagrams we get the final result

$$\begin{aligned} 2\,a_{15}^{\{2,0\}} &= 2\int \mathrm{d}\widetilde{q}_1\mathrm{d}\widetilde{q}_2\; g^2\; \mathcal{W}_{15}^{(2)}(q_{p1},\bar{q}_{p2};q_{q1},\bar{q}_{q2}) \times \mathcal{A}^{(0)}(q_{q1},\bar{q}_{q2};\gamma(P)) \quad (3.51)\\ &= C_F\left(\frac{\alpha_s}{2\pi}\right)\left(\frac{\mu^2}{s}\right)^{\epsilon}\Bigg(-\frac{1}{\epsilon^2}-\frac{5}{2\epsilon}+g_1(\Delta)+\frac{c_R}{2}\\ &\quad+\int \mathrm{d}\widetilde{q}_3\,\Theta(\Delta-|\rho(\vec{q}_3,\vec{p}_1-\vec{q}_3)|)f_1(p_1,p_2,q_3)\Bigg)\mathcal{A}^{(0)}(q_{p1},\bar{q}_{p2};\gamma(P)) \end{aligned}$$

with

$$\begin{aligned} g_1(\Delta) &= -\frac{7}{2}-\frac{5}{2}\left(\frac{\Delta}{2}\right)^2-\frac{7\pi^2}{12}+\left[\frac{7}{2}+\left(\frac{\Delta}{2}\right)+\frac{1}{2}\left(\frac{\Delta}{2}\right)^2\right]\log\left(\frac{\Delta}{2}\right)\\ &+\;\log^2\left(\frac{\Delta}{2}\right)+2\log^2\left(1+\frac{\Delta}{2}\right)+4\,\mathrm{Li}_2\left(\frac{2}{2+\Delta}\right) \quad (3.52) \end{aligned}$$

and where $f_1(p_1,p_2,q_3)$ is a function that is free from singularities when integrated over $\mathrm{d}\widetilde{q}_3$. The explicit form is given in Eq. (A.7). Note that we took care to sum over the physical polarisations of the gluon only and evaluated the diagram in the centre-of-mass frame $\vec{p}_1=-\vec{p}_2$.

The one-gluon exchange terms

We now look at the one-gluon exchange diagrams. There are two such diagrams, one for each time ordering of the two vertices. One diagram is obtained from taking the vertices V_1, V_8 of Eq. (3.42), the other from taking the vertices V_4, V_5. These diagrams are symmetric under exchange of all momenta and so we need only calculate one of them. The diagram shown in Figure 3.7 gives us

$$\begin{aligned} a_{18}^{\{2,0\}} &= \int \mathrm{d}\widetilde{q}_1\mathrm{d}\widetilde{q}_2\; g^2\; \mathcal{W}_{18}^{(2)}(q_{p1},\bar{q}_{p2};q_{q1},\bar{q}_{q2}) \times \mathcal{A}^{(0)}(q_{q1},\bar{q}_{q2};\gamma(P)) \quad (3.53)\\ &= \frac{(-ie)\,g^2}{2}\int d^{D-1}q_1 d^{D-1}q_2\frac{d^{D-1}q_3}{(2\pi)^{D-1}}\;T^a_{ik}T^b_{kj}\\ &\quad\frac{\delta^{ab}}{2\omega(\vec{q}_3)}\left(-g^{\mu\nu}+\frac{q_3^\mu\,\overline{q}_3^\nu+q_3^\nu\,\overline{q}_3^\mu}{(q_3\,\overline{q}_3)}\right)\langle p_1|\gamma_\mu\,\not{q}_1\gamma_\alpha\,\not{q}_2\gamma_\nu|p_2\rangle \end{aligned}$$

$$\frac{\Theta(\Delta - |\omega(\vec{q}_1) + \omega(\vec{q}_3) - \omega(\vec{p}_1)|)\,\Theta(\Delta - |\omega(\vec{p}_2) + \omega(\vec{q}_3) - \omega(\vec{q}_2)|)}{2\omega(\vec{q}_1)\,(\omega(\vec{q}_1) + \omega(\vec{q}_3) - \omega(\vec{p}_1))\;\,2\omega(\vec{q}_2)\,(\omega(\vec{p}_2) + \omega(\vec{q}_3) - \omega(\vec{q}_2))}$$
$$\delta^{(D-1)}(\vec{q}_1 + \vec{q}_3 - \vec{p}_1)\,\delta^{(D-1)}(\vec{p}_2 + \vec{q}_3 - \vec{q}_2)\,(2\pi)^D\,\delta^{(D)}(P - q_1 - q_2).$$

We again integrate over $\vec{q}_1$ and $\vec{q}_3$ with the delta functions and introduce the on-shell momenta $\{\not{p}_1 - \not{q}_3\}$ and $\{\not{p}_2 + \not{q}_3\}$ to obtain

$$\begin{aligned} a_{18}^{\{2,0\}} \;=\; & \frac{(-ie)\,g^2}{2}\,T^a_{ik}T^a_{kj}\int\frac{d^{D-1}q_3}{(2\pi)^{D-1}}\,(2\pi)^D\,\delta^{(D)}(P - \{p_1 - q_3\} - \{p_2 + q_3\}) \\ & \frac{1}{2\omega(\vec{q}_3)}\left(-g^{\mu\nu} + \frac{q_3^\mu\,\overline{q}_3^\nu + q_3^\nu\,\overline{q}_3^\mu}{(q_3\,\overline{q}_3)}\right)\langle p_1|\gamma_\mu\{\not{p}_1 - \not{q}_3\}\gamma_\alpha\{\not{p}_2 + \not{q}_3\}\gamma_\nu|p_2\rangle \\ & \frac{\Theta(\Delta - |\rho(\vec{q}_3, \vec{p}_1 - \vec{q}_3)|)\,\Theta(\Delta - |\rho(\vec{q}_3, \vec{p}_2)|)}{2\omega(\vec{p}_1 - \vec{q}_3)\,\rho(\vec{q}_3, \vec{p}_1 - \vec{q}_3)\,2\omega(\vec{p}_2 + \vec{q}_3)\,\rho(\vec{q}_3, \vec{p}_2)} \end{aligned} \tag{3.54}$$

Looking at the denominator $\rho(\vec{q}_3, \vec{p}_1 - \vec{q}_3)\,\rho(\vec{q}_3, \vec{p}_2)$ it appears that there are collinear singularities for $q_3 \| p_2$, $\;q_3 \| p_1$ and a soft singularity $q_3 \to 0$. However, the denominator

$$\left(-g^{\mu\nu} + \frac{q_3^\mu\,\overline{q}_3^\nu + q_3^\nu\,\overline{q}_3^\mu}{(q_3\,\overline{q}_3)}\right)\langle p_1|\gamma_\mu\{\not{p}_1 - \not{q}_3\}\gamma_\alpha\{\not{p}_2 + \not{q}_3\}\gamma_\nu|p_2\rangle \tag{3.55}$$

vanishes in the collinear regions $q_3 \| p_2$ and $q_3 \| p_1$. Thus, this diagram has only a soft singularity.

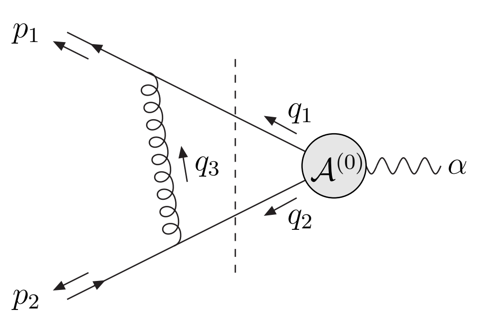

Figure 3.7: Cut diagram for the 2-particle cut diagram with one-gluon exchange in the asymptotic region.

We delegate the explicit evaluation of $a_{18}^{\{2,0\}}$ to Appendix A. Multiplying by two to account for both one-gluon exchange diagrams we have the final result

$$\begin{aligned}
2\,a_{18}^{\{2,0\}} &= 2\int \mathrm{d}\widetilde{q}_1 \mathrm{d}\widetilde{q}_2 \; g^2\, \mathcal{W}_{18}^{(2)}(q_{p1}, \bar{q}_{p2}; q_{q1}, \bar{q}_{q2}) \times \mathcal{A}^{(0)}(q_{q1}, \bar{q}_{q2}; \gamma(P)) \qquad (3.56)\\
&= C_F \left(\frac{\alpha_s}{2\pi}\right)\left(\frac{\mu^2}{s}\right)^{\epsilon} \left(\left(\frac{1}{\epsilon} + g_2(\Delta)\right) \mathcal{A}^{(0)}(q_{p1}, \bar{q}_{p2}; \gamma(P)) \right.\\
&- \; (-ie)\,\delta_{ij}\,\langle p_1|\gamma^{\alpha}|p_2\rangle (2\pi)^{(D-1)} \delta^{(D-1)}(\vec{P} - \vec{p}_1 - \vec{p}_2)\\
&\times \left. \int \mathrm{d}\widetilde{q}_3 \; \Theta(\Delta - |\rho(\vec{q}_3, \vec{p}_1 - \vec{q}_3)|)\Theta(\Delta - |\rho(\vec{q}_3, \vec{p}_2)|) f_2(p_1, p_2, q_3) \right)
\end{aligned}$$

where again we have not performed the finite f_2 integral analytically and

$$g_2(\Delta) = 2\log 2 - 2\log\left(\frac{\Delta}{2}\right). \qquad (3.57)$$

The explicit form of f_2 is given in Eq. (A.9).

3 Particle Cut Diagram

Let us now turn to the fourth part of Eq. (3.38). For this term we need the dressing factor $\mathcal{W}^{(1)}(q_{p1}, \bar{q}_{p2}; q_{q1}, \bar{q}_{q2}, g_{q3})$. Again we use the diagrammatic rules of Section 3.2.3.

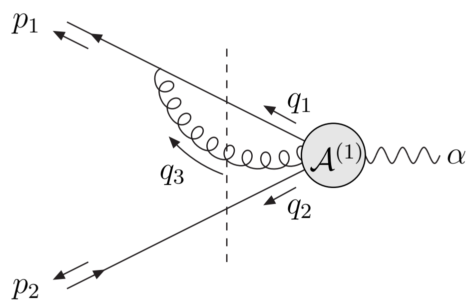

Figure 3.8: Cut diagram for 3-particle intermediate state.

There are two possible diagrams as the gluon can be absorbed either by the quark or antiquark line. The two diagrams are obtained by taking either the vertex V_1 or V_4 and they are symmetric under exchange of momenta. So we need only calculate one of them. For the diagram shown in Figure 3.8 we get

$$\begin{aligned}
a_1^{\{1,1\}} &= \int \mathrm{d}\widetilde{q}_1 \mathrm{d}\widetilde{q}_2 \mathrm{d}\widetilde{q}_3\, g^2\, \mathcal{W}_1^{(1)}(q_{p1}, \bar{q}_{p2}; q_{q1}, \bar{q}_{q2}, g_{q3}) \times \mathcal{A}^{(1)}(q_{q1}, \bar{q}_{q2}, g_{q3}; \gamma(P)) \\
&= (-ie)\, g^2 \int d^{D-1}q_1 d^{D-1}q_2 \frac{d^{D-1}q_3}{(2\pi)^{D-1}} \frac{\delta^{ab}}{2\omega(\vec{q}_3)} T^a_{ik} T^b_{kj} \qquad (3.58) \\
&\left(-g^{\mu\nu} + \frac{q_3^\mu\, \overline{q}_3^\nu + q_3^\nu\, \overline{q}_3^\mu}{(q_3\, \overline{q}_3)}\right) \frac{\Theta(\Delta - |\omega(\vec{q}_1) + \omega(\vec{q}_3) - \omega(\vec{p}_1)|)}{2\omega(\vec{q}_1)\,(\omega(\vec{q}_1) + \omega(\vec{q}_3) - \omega(\vec{p}_1))} \\
&\langle p_1|\gamma_\mu\, \not{q}_1 \left(\frac{\gamma^\nu(\not{q}_1 + \not{q}_3)\gamma^\alpha}{2(q_1 q_3)} - \frac{\gamma^\alpha(\not{q}_2 + \not{q}_3)\gamma^\nu}{2(q_2 q_3)}\right)|p_2\rangle \\
&\delta^{(D-1)}(\vec{q}_1 + \vec{q}_3 - \vec{p}_1)\, \delta^{(D-1)}(\vec{p}_2 - \vec{q}_2)(2\pi)^D\, \delta^{(D)}(P - q_1 - q_2).
\end{aligned}$$

After integration over $\vec{q}_1$ and $\vec{q}_2$ using the delta functions we observe that there are collinear singularities $q_3 \| p_1$ and soft singularities $q_3 \to 0$. There are, however, no collinear singularities $q_3 \| p_2$. This is expected since the amplitude $\mathcal{A}^{(1)}(q_{q1}, \bar{q}_{q2}, g_{q3}; \gamma(P))$ has only an integrable square-root singularity for $q_3 \| q_2$ and the dressing factor $\mathcal{W}_1^{(1)}(q_{p1}, \bar{q}_{p2}; q_{q1}, \bar{q}_{q2}, g_{q3})$ is regular for $q_3 \| q_2$.

As for the other diagrams we have to multiply by two to take into account both pairs of diagrams and we get the final result

$$\begin{aligned}
2\, a_1^{\{1,1\}} &= 2 \int \mathrm{d}\widetilde{q}_1 \mathrm{d}\widetilde{q}_2 \mathrm{d}\widetilde{q}_3\, g^2\, \mathcal{W}_1^{(1)}(q_{p1}, \bar{q}_{p2}; q_{q1}, \bar{q}_{q2}, g_{q3}) \qquad (3.59) \\
&\qquad \times \mathcal{A}^{(1)}(q_{q1}, \bar{q}_{q2}, g_{q3}; \gamma(P)) \\
&= C_F \left(\frac{\alpha_s}{2\pi}\right) \left(\frac{\mu^2}{s}\right)^\epsilon \left(\left(\frac{2}{\epsilon^2} + \frac{3}{\epsilon} + g_3(\Delta) - c_R\right) \mathcal{A}^{(0)}(q_{p1}, \bar{q}_{p2}; \gamma(P)) \right. \\
&+ (-ie)\, \delta_{ij}\, \langle p_1|\gamma^\alpha|p_2\rangle (2\pi)^{(D-1)} \delta^{(D-1)}(\vec{P} - \vec{p}_1 - \vec{p}_2) \\
&\qquad \left. \times \int \mathrm{d}\widetilde{q}_3\; \Theta(\Delta - |\rho(\vec{q}_3, \vec{p}_1 - \vec{q}_3)|) f_3(p_1, p_2, q_3) \right)
\end{aligned}$$

where

$$g_3(\Delta) = 7 + \left(\frac{\Delta}{2}\right)^2 + \frac{7\pi^2}{6} + \left[-3 + 2\left(\frac{\Delta}{2}\right) - \left(\frac{\Delta}{2}\right)^2\right] \log\left(\frac{\Delta}{2}\right)$$

$$- \quad 2\log^2\left(\frac{\Delta}{2}\right) - 4\log^2\left(1+\frac{\Delta}{2}\right) - 8\,\mathrm{Li}_2\left(\frac{2}{2+\Delta}\right). \qquad (3.60)$$

The function f_3 is given in Eq. (A.11) and does not produce any infrared singularity upon integration over $\mathrm{d}\widetilde{q}_3$.

An infrared-finite amplitude

We have now calculated all terms contributing to the amplitude $\mathcal{A}(\{q,\bar{q}\};\gamma)$, Eq. (3.38), at next-to-leading order. Using Eqs. (3.46, 3.51, 3.56) and (3.59) to assemble the amplitude we get

$$\begin{aligned}
&\mathcal{A}(\{q_{p1},\bar{q}_{p2}\};\gamma) = \qquad (3.61)\\
&1 + C_F\left(\frac{\alpha_s}{2\pi}\right)\left(g_1(\Delta)+g_2(\Delta)+g_3(\Delta)-4+\frac{\pi^2}{12}\right)\mathcal{A}^{(0)}(q_{p1},\bar{q}_{p2};\gamma(P))\\
&+(-ie)\,\delta_{ij}\,\langle p_1|\gamma^\alpha|p_2\rangle(2\pi)^{(D-1)}\delta^{(D-1)}(\vec{P}-\vec{p}_1-\vec{p}_2)\\
&\times\int \mathrm{d}\widetilde{q}_3\,\Big(f_1(p_1,p_2,q_3)\Theta(\Delta-|\rho(\vec{q}_3,\vec{p}_1-\vec{q}_3)|)\delta(\sqrt{s}-\omega(\vec{p}_1)-\omega(\vec{p}_2))\\
&\qquad +f_2(p_1,p_2,q_3)\Theta(\Delta-|\rho(\vec{q}_3,\vec{p}_1-\vec{q}_3)|)\Theta(\Delta-|\rho(\vec{q}_3,\vec{p}_2)|)\\
&\qquad +f_3(p_1,p_2,q_3)\Theta(\Delta-|\rho(\vec{q}_3,\vec{p}_1-\vec{q}_3)|)\Big)
\end{aligned}$$

up to order α_s in the coupling. The functions g_1, g_2, g_3 are given in Eqs. (3.52, 3.57) and (3.60) and the functions f_1, f_2 and f_3 are given in Eqs. (A.7, A.9) and (A.11) respectively.

We see that this result is completely free of infrared singularities. We are only left with some finite Δ dependent terms, g_i and some finite terms, f_i which will in general need to be numerically integrated. Even though the amplitude $\mathcal{A}(\{q_{p1},\bar{q}_{p2}\};\gamma)$ depends on Δ this dependence will disappear when we combine the various amplitudes to calculate physical observables.

3.2.5 The amplitude $\mathcal{A}(\{q(p_1),\bar{q}(p_2),g(p_3)\};\gamma)$

We are now going to calculate the amplitude $\mathcal{A}(\{q_{p1},\bar{q}_{p2},g_{p3}\};\gamma)$ given in Eq. (3.39). There are only two terms to calculate for this amplitude and there is no integration over the final state gluon as it is now a real final state particle.

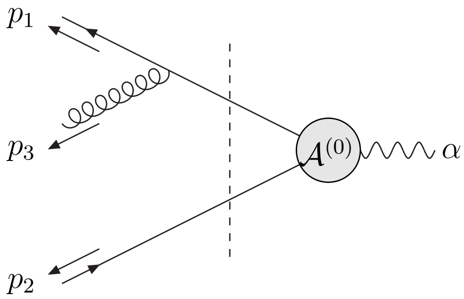

Figure 3.9: Cut diagram for the 3-particle asymptotic region with a 2-particle intermediate state.

Again we calculate these terms using the diagrammatic rules from Section 3.2.3. Let us start with the diagrams where the gluon is emitted in the dressing factor. Figure 3.9 shows one of the two possible diagrams, the other is exactly the same but with all momenta interchanged. So for both diagrams we have

$$\begin{aligned}
&\int \mathrm{d}\widetilde{q}_1 \mathrm{d}\widetilde{q}_2 \; g\,\mathcal{W}_1^{(1)}(q_{p1}, \bar{q}_{p2}, g_{p3}; q_{q1}, \bar{q}_{q2}) \times \mathcal{A}^{(0)}(q_{q1}, \bar{q}_{q2}; \gamma(P)) \\
&= \; (-ie) g\, T^a_{ij}\, (2\pi)^D \delta^{(D-1)}(\vec{P} - \vec{p}_1 - \vec{p}_2 - \vec{p}_3)\, \langle p_1| \qquad (3.62) \\
&\Bigg(- \frac{\not{\epsilon}_{p3} \{\not{p}_1 + \not{p}_3\} \gamma^\alpha}{2\omega(\vec{p}_1 + \vec{p}_3) r_1} \Theta(\Delta - |r_1|) \delta(\sqrt{s} - \omega(\vec{p}_1) - \omega(\vec{p}_2) - \omega(\vec{p}_3) + r_1) \\
&+ \frac{\gamma^\alpha \{\not{p}_2 + \not{p}_3\} \not{\epsilon}_{p3}}{2\omega(\vec{p}_2 + \vec{p}_3) r_2} \Theta(\Delta - |r_2|) \delta(\sqrt{s} - \omega(\vec{p}_1) - \omega(\vec{p}_2) - \omega(\vec{p}_3) + r_2) \Bigg) |p_2\rangle
\end{aligned}$$

where we used the notation

$$\begin{aligned}
r_1 &\equiv \rho(\vec{p}_1, \vec{p}_3) = \omega(\vec{p}_1) + \omega(\vec{p}_3) - \omega(\vec{p}_1 + \vec{p}_3) \qquad (3.63) \\
r_2 &\equiv \rho(\vec{p}_2, \vec{p}_3) = \omega(\vec{p}_2) + \omega(\vec{p}_3) - \omega(\vec{p}_2 + \vec{p}_3),
\end{aligned}$$

with ρ defined in Eq. (3.50).

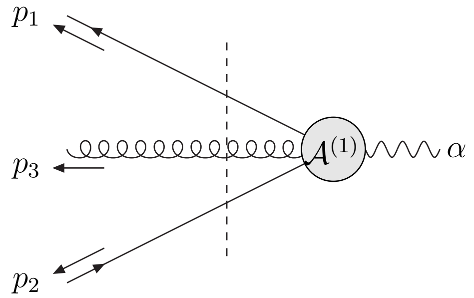

Figure 3.10: Cut diagram for 3-particle asymptotic region with a 3-particle intermediate state.

The second contribution is just the usual $\mathcal{A}^{(1)}(q_{p1}, \bar{q}_{p2}, g_{p3}; \gamma(P))$ amplitude. The three external particles of this amplitude do not interact in the asymptotic region and so we simply have the diagram as shown in Figure 3.10, this gives

$$\begin{aligned}
&\int \mathrm{d}\widetilde{q}_1\,\mathrm{d}\widetilde{q}_2\; g\,\mathcal{W}^{(0)}(q_{p1}, \bar{q}_{p2}, g_{p3}; q_{q1}, \bar{q}_{q2}, g_{q3}) \times \mathcal{A}^{(1)}(q_{q1}, \bar{q}_{q2}, g_{q3}; \gamma(P)) \\
&\quad = (-ie)g\,T^a_{ij}\,\langle p_1|\left(\frac{\not\epsilon_{p3}(\not p_1 + \not p_3)\gamma^\alpha}{2(p_1 p_3)} - \frac{\gamma^\alpha(\not p_2 + \not p_3)\not\epsilon_{p3}}{2(p_2 p_3)}\right)|p_2\rangle \\
&\quad\quad (2\pi)^D \delta^{(D)}(P - p_1 - p_2 - p_3). \qquad (3.64)
\end{aligned}$$

We now assemble Eq. (3.39) to find

$$\begin{aligned}
\mathcal{A}(\{q_{p1}, \bar{q}_{p2}, g_{p3}\}; \gamma) &= (-ie)g\,T^a_{ij}\,\langle p_1|\Bigg(\\
&- \frac{\not\epsilon_{p3}\{\not p_1 + \not p_3\}\gamma^\alpha}{2\omega(\vec{p}_1 + \vec{p}_3) r_1}\Theta(\Delta - |r_1|)\delta(\sqrt{s} - \omega(\vec{p}_1) - \omega(\vec{p}_2) - \omega(\vec{p}_3) + r_1) \\
&+ \frac{\not\epsilon_{p3}(\not p_1 + \not p_3)\gamma^\alpha}{2(p_1 p_3)}\delta(\sqrt{s} - \omega(\vec{p}_1) - \omega(\vec{p}_2) - \omega(\vec{p}_3)) \\
&+ \frac{\gamma^\alpha\{\not p_2 + \not p_3\}\not\epsilon_{p3}}{2\omega(\vec{p}_2 + \vec{p}_3) r_2}\Theta(\Delta - |r_2|)\delta(\sqrt{s} - \omega(\vec{p}_1) - \omega(\vec{p}_2) - \omega(\vec{p}_3) + r_2)
\end{aligned}$$

$$
\left. - \frac{\gamma^\alpha (\not{p}_2 + \not{p}_3)\ \not{\epsilon}_{p3}}{2(p_2 p_3)} \delta(\sqrt{s} - \omega(\vec{p}_1) - \omega(\vec{p}_2) - \omega(\vec{p}_3)) \right) |p_2\rangle
$$
$$
(2\pi)^D \delta^{(D-1)}(\vec{P} - \vec{p}_1 - \vec{p}_2 - \vec{p}_3). \tag{3.65}
$$

This amplitude splits up into two pairs. The first (last) two terms are due to the gluon being emitted from the leg p_1 (p_2). Looking at the first two terms shows that for $r_1 > \Delta$ the contribution from the asymptotic region disappears. We are then left with the normal amplitude, $\mathcal{A}(q_{p1}, \bar{q}_{p2}, g_{p3}; \gamma)$. For $r_1 < \Delta$ the term from the asymptotic region does contribute and will cancel any potential infrared singularities. We can see this by taking the limit $\Delta \to 0$, we have

$$
\begin{aligned}
\omega(\vec{p}_1 + \vec{p}_3) r_1 &\to (p_1 p_3), \\
\{\not{p}_1 + \not{p}_3\} &\to (\not{p}_1 + \not{p}_3), \\
\delta(\sqrt{s} - \omega(\vec{p}_1) - \omega(\vec{p}_2) - \omega(\vec{p}_3) + r_1) &\to \delta(\sqrt{s} - \omega(\vec{p}_1) - \omega(\vec{p}_2) - \omega(\vec{p}_3)).
\end{aligned}
$$

With these we can see that the terms from the asymptotic region approach those of the normal amplitude in the soft and collinear limits, but with the opposite sign. So the two terms will cancel in the $\Delta \to 0$ limit, leaving us with an amplitude that is infrared finite when integrated over the phase space.

3.2.6 Calculation of the total cross section

In the previous sections we computed the two infrared finite amplitudes that contribute to the process $\gamma^*(P) \to 2$ jets at next-to-leading order. In this section we would like to check our results by computing the total cross section, starting from the infrared finite amplitudes, Eqs. (3.61) and (3.65). Of course, we have to recover the well known result, Eq. (1.19).

Let us stress that the idea of our approach is to compute the amplitudes numerically and perform the phase-space integration also numerically. It is for the sole purpose of checking our results and facilitating the comparison with Eq. (1.19) that in this section we compute the total cross section analytically.

Usually a non zero value of Δ would be chosen for a numerical calculation and we would expect all Δ dependence to cancel between the contributions of the two amplitudes (squared) to the cross section. Here though to simplify the analytical calculation we will take the limit $\Delta \to 0$. In this limit even the infrared-finite amplitudes are proportional to a four-dimensional delta function and we can use the standard procedure to obtain the total cross section from the amplitudes. However, since the amplitudes are singular for $\Delta \to 0$ we must be careful in taking this limit and leave it until the end of the calculation. The f_n finite terms of Eq. (3.61) which we would usually have to calculate numerically will all go to zero in this limit. This simplification occurs because the region of integration shrinks to zero as $\Delta \to 0$ and as these terms are finite they can no longer give a contribution.

We now use our infrared finite amplitudes Eq. (3.38) and Eq. (3.39) instead of Eq. (1.8) and Eq. (1.9) and square them in the usual way to obtain

$$\sigma = \sigma_{\{q\overline{q}\}} + \sigma_{\{q\overline{q}g\}}, \tag{3.66}$$

where

$$\sigma_{\{q\overline{q}\}} = \int \mathrm{d}\Phi_2 \left|\mathcal{A}(\{q_{p1}, \overline{q}_{p2}\}; \gamma)\right|^2, \tag{3.67}$$

$$\sigma_{\{q\overline{q}g\}} = \int \mathrm{d}\Phi_3 \left|\mathcal{A}(\{q_{p1}, \overline{q}_{p2}, g_{p3}\}; \gamma)\right|^2. \tag{3.68}$$

Here we integrate Eq. (3.67) over the two particle phase space and Eq. (3.68) over the three particle phase space.

First we rewrite the three-particle final state amplitude, Eq. (3.65), in a more convenient form

$$\begin{aligned}
\mathcal{A}(\{q_{p1}, \bar{q}_{p2}, g_{p3}\}; \gamma) \quad &= \quad (-ie) g\, T^a_{ij} \,\langle p_1| \Bigg(\\
&\left(-\frac{\not{\epsilon}_{p3} \{\not{p}_1 + \not{p}_3\} \gamma^\alpha}{2\omega(\vec{p}_1 + \vec{p}_3) r_1} \delta(E + r_1) + \frac{\not{\epsilon}_{p3} (\not{p}_1 + \not{p}_3) \gamma^\alpha}{2(p_1 p_3)} \delta(E) \right) \Theta(\Delta - |r_1|) \\
&+ \frac{\not{\epsilon}_{p3} (\not{p}_1 + \not{p}_3) \gamma^\alpha}{2(p_1 p_3)} \delta(E) \Theta(|r_1| - \Delta)
\end{aligned}$$

$$+\left(\frac{\gamma^\alpha\{\not{p}_2+\not{p}_3\}\not{\epsilon}_{p_3}}{2\omega(\vec{p}_2+\vec{p}_3)r_2}\delta(E+r_2)-\frac{\gamma^\alpha(\not{p}_2+\not{p}_3)\not{\epsilon}_{p_3}}{2(p_2p_3)}\delta(E)\right)\Theta(\Delta-|r_2|)$$
$$-\frac{\gamma^\alpha(\not{p}_2+\not{p}_3)\not{\epsilon}_{p_3}}{2(p_2p_3)}\delta(E)\Theta(|r_2|-\Delta)\Bigg)|p_2\rangle$$
$$(2\pi)^D\delta^{(D-1)}(\vec{P}-\vec{p}_1-\vec{p}_2-\vec{p}_3), \tag{3.69}$$

where $E=\sqrt{s}-\omega(\vec{p}_1)-\omega(\vec{p}_2)-\omega(\vec{p}_3)$. Taking Eq. (3.69) we then square it in the usual way and sum over the gluon polarisations using

$$\sum\epsilon^\mu_{p_3}\epsilon^\nu_{p_3}=-g^{\mu\nu}+\frac{p_3^\mu\overline{p}_3^\nu+p_3^\nu\overline{p}_3^\mu}{(p_3\overline{p}_3)}$$

where $\overline{p}_3=(\omega(\vec{p}_3),-\vec{p}_3)$. This is because the amplitude is no longer gauge invariant as we are using dressed states. At this point we drop any terms multiplied by $\Theta(\Delta-|r_1|)$ or $\Theta(\Delta-|r_2|)$. These terms are finite and therefore can be shown to go to zero in the $\Delta\to 0$ limit after we have performed the three particle phase space integral in a similar way to the f_n terms.

After integrating one of the phase space integrals using the delta function we are left with

$$|\mathcal{A}(\{q_{p1},\bar{q}_{p2},g_{p3}\};\gamma)|^2=4\,C_F\,(2\pi)^{3-2D}\int\frac{d\Omega_{D-1}}{2^{D-1}}d\Omega_{D-2} \tag{3.70}$$
$$\left(\int_0^{\frac{\Delta}{2}}dy_{13}\int_{1-y_{13}}^0 dy_{23}\frac{2y_{23}-y_{13}\,(y_{13}+y_{23})^2}{y_{13}\,(y_{13}+y_{23})^2}\right.$$
$$-\int_0^{1-\frac{\Delta}{2}}dy_{13}\int_{1-y_{13}}^{\frac{\Delta}{2}}dy_{23}\,\frac{y_{23}^3+y_{13}^2y_{23}+2y_{13}\,(y_{23}-1)^2}{y_{23}\,(y_{13}+y_{23})^2}$$
$$\left.+\int_{\frac{\Delta}{2}}^{1-\frac{\Delta}{2}}dy_{13}\int_{1-y_{13}}^{\frac{\Delta}{2}}dy_{23}\left(2-\frac{2-y_{23}}{y_{13}}-\frac{2-y_{13}}{y_{23}}+\frac{4}{(y_{13}+y_{23})^2}\right)\right)$$

where we defined

$$y_{ij}\equiv\frac{2(p_ip_j)}{\xi_{p_1}^2}. \tag{3.71}$$

We perform the final two integrals and then prematurely take the $\Delta\to 0$ limit everywhere except in the $\log(\Delta)$ terms, as these diverge in this limit.

The $\log(\Delta)$ terms will cancel later in the final result. This then leaves

$$\frac{1}{\sigma_0}\sigma_{\{q\bar{q}g\}} = C_F\left(\frac{\alpha_s}{\pi}\right)\left(\frac{5}{4} - \log 4 + \frac{3}{2}\log\left(\frac{\Delta}{2}\right) + \log^2\left(\frac{\Delta}{2}\right)\right) \tag{3.72}$$

where σ_0 is the total Born cross section as given in Eq. (1.13).

Now we calculate $|\mathcal{A}(\{q_{p1}, \bar{q}_{p2}\}; \gamma)|^2$. Again we take the $\Delta \to 0$ limit early except for the $\log(\Delta)$ pieces of the g_n terms in the finite part of Eq. (3.61). As stated before the $f_n(p_1, p_2, q_3)$ terms go to zero and so we have,

$$\begin{aligned} |\mathcal{A}(\{q_{p1}, \bar{q}_{p2}\}; \gamma)|^2 &= \left|\mathcal{A}^{(0)}(q_{p1}, \bar{q}_{p2}; \gamma(P))\right|^2 \\ \times \; &\left(1 + C_F\left(\frac{\alpha_s}{2\pi}\right)\left(-\frac{1}{2} + \log 4 - \frac{3}{2}\log\left(\frac{\Delta}{2}\right) - \log^2\left(\frac{\Delta}{2}\right)\right)\right)^2 \end{aligned} \tag{3.73}$$

After integrating over the two particle phase space we get

$$\frac{\sigma_{\{q\bar{q}\}}}{\sigma_0} = \left(1 + C_F\frac{\alpha_s}{\pi}\left(-\frac{1}{2} + \log 4 - \frac{3}{2}\log\left(\frac{\Delta}{2}\right) - \log^2\left(\frac{\Delta}{2}\right)\right) + \mathcal{O}(\alpha_s^2)\right) \tag{3.74}$$

Putting Eq. (3.72) and Eq. (3.74) together gives finally

$$\frac{\sigma}{\sigma_0} = \left(1 + \left(\frac{\alpha_s}{\pi}\right)\frac{3}{4}C_F + \mathcal{O}(\alpha_s^2)\right). \tag{3.75}$$

We have recovered the well known result for the total $\gamma \to q\bar{q}$ cross section and all the Δ dependence of the amplitudes has disappeared including the $\log(\Delta)$ terms, justifying our taking of the $\Delta \to 0$ limit early.

3.3 Summary

In this chapter we have presented a method on how to construct infrared finite amplitudes using dressed states and applied it to the case of $e^+e^- \to 2$ jets at next-to-leading order in the strong coupling. The idea is to separate from the Hamiltonian a part that describes the asymptotic dynamics. This asymptotic Hamiltonian is then used to asymptotically evolve the usual states of the Fock space. In this way we construct dressed states, Eqs. (3.16) and

(3.17), such that the transition amplitudes between these states are free from infrared singularities.

Contrary to most of the previous work done in this field we are not so much interested in obtaining all-order re-summed results taking into account soft emission of an arbitrary number of gauge bosons from external partons. Our aim here was to construct dressed states explicitly order-by order in perturbation theory and use them to do explicit calculations. In this chapter we have done this for a particularly simple final state up to next-to-leading order.

The reason that we cannot obtain all-order results is that we include the collinear singularities as well. In non-abelian theories these singularities cannot be avoided. The additional complications due to the collinear singularities make it impossible to obtain exact solutions to the asymptotic dynamics.

As for the standard approach, physical cross sections obtain in general contributions from more than one partonic process. However, in our case all these contributions are separately finite. They depend on a parameter, Δ, that determines the precise split of the Hamiltonian into an asymptotic Hamiltonian and the remainder. The result for any physical quantity is independent of this parameter as long as it is smaller than any experimental resolution. For any finite value of Δ the amplitude contains a part that is not proportional to an energy conserving delta function which represents the spread of the initial wave packet due to the asymptotic evolution.

For any physical cross section at any order in perturbation theory we will get the same answer using the standard cross-section method or infrared-finite amplitudes. Thus, one might wonder what has been gained using this approach. Apart from the conceptional benefit that the S-matrix between dressed states is well defined there are also practical advantages. First of all, the avoidance of infrared singularities facilitates the use of numerical methods. This might not be apparent in the approach we have taken. In fact, using Eq. (3.21) to split the infrared finite amplitudes into separately divergent factors still requires us to use an infrared regulator (dimensional regularisation in our case) and revert to analytical calculations. However, since the final amplitude is infrared finite it is feasible to compute it directly in a numerical way, avoiding the split into separately divergent pieces. Once the amplitudes have been obtained, the integration over the phase space is trivial and no sophisticated method is needed. This also opens up the possibility of combining fixed-order calculations directly with a parton shower approach.

Needless to say that the explicit example we considered, $e^+e^- \to 2$ jets has many simplifying features. To start with, the non-abelian nature of QCD does not really enter. Secondly, we only considered the amplitudes at next-to-leading order. Furthermore, the initial state does not interact strongly.

The last point simply results in the fact that there is no need to dress the initial state. While this is a simplification concerning the amount of computations to be performed, there is no conceptual problem associated with more complicated initial states. If the initial state contains hadrons a physical cross section is obtained by folding the partonic cross section with parton densities. In the conventional approach these parton densities are associated with the probability of finding a certain partonic state within a hadron. In our case, we would have to use modified parton densities that are related to the probability of finding a certain dressed state within a hadron. Thus the global analyses of extracting the parton densities would have to be modified and repeated.

The fact that the non-abelian nature of QCD does not really show up in the explicit example we considered results in a particularly simple asymptotic Hamiltonian. In fact, the asymptotic Hamiltonian we use involves only quark-gluon interactions and is basically the same that was used many times previously [27]. Again, this results in a technical simplification of the computation and facilitates the explicit construction of the asymptotic Hamiltonian. In more complicated examples the full non-abelian structure of the asymptotic Hamiltonian will enter the problem and its construction will be much more involved. However, the only crucial feature is that the asymptotic Hamiltonian reproduces the full asymptotic dynamics, i.e. it has to reproduce the soft and collinear behaviour of the full theory. There are no further requirements and the construction of dressed states presented in this paper can be taken over directly. However, it is clear that the construction used so far is rather cumbersome. In order to exploit the advantage of the infrared finiteness a systematic numerical approach would need to be developed. This will become particularly important if this method is to be extended beyond next-to-leading order. Therefore in the next chapter we will attempt to streamline and extend the methods described here.

Chapter 4

A Covariant Approach

In the previous chapter we demonstrated a practical application of the use of dressed states and showed that amplitudes constructed using them were infrared finite. The formalism suffered from two distinct problems though. The first is that the amplitudes were constructed from separate pieces which were themselves infrared divergent. So although the final amplitude was infrared finite the intermediate steps were not necessarily so, this would mean that a purely numerical approach would be difficult to implement. The second problem was that the pieces once combined were not all multiplied by the same energy delta function. Instead separate pieces of the amplitude were multiplied by different energy delta functions which differed by a soft/collinear energy difference. This means that the calculation of physical observables from these amplitudes becomes difficult due to the need to "square" the different delta functions in the amplitude.

The aim of this chapter is to surmount these problems. We will begin to do this by investigating the techniques required to produce amplitudes which are infrared finite throughout the calculational procedure. This will follow on from the discussions in Sections 2.3 and 2.4. The amplitudes produced in this way will be described using time ordered perturbation theory. The problem with this is that at order n in the perturbation series we will have $n!$ different time ordered diagrams to calculate for what would be each Feynman diagram in covariant perturbation theory. For complex diagrams therefore the amount of computation required will quickly become too difficult to manage. Furthermore we will see that the number of diagrams required will actually be even greater than this, making the situation even more difficult.

To avoid this problem we will therefore attempt to combine these time ordered diagrams to produce a completely covariant amplitude. In the process of this we should massively reduce the number of diagrams which need to be calculated. We will outline the difficulties involved in doing this.

After this there is the second problem of the different delta functions within each amplitude. The root cause of this problem is that dressed states involve the use of the S_A operator on the basis of free states $|\phi_\alpha\rangle$. The S_A operator does not commute with the free field Hamiltonian H_0, and so does not conserve the energy as given by the free Hamiltonian. The obvious solution to this is therefore to attempt to expand S_A on the basis of eigenstates of the asymptotic Hamiltonian H_Δ used to derive S_A.

As stated in Section 2.3 we do not know how to exactly solve for the eigenstates of the asymptotic basis and so we must relate them to the basis of free states in some way. To do this previously we have used the Møller operator $\Omega_\Delta^{(\pm)}$, relating the basis of free states to the basis of asymptotic states, for example in Eq.(2.83). The problem with this operator though is that it contains infrared divergences and therefore is not isometric unless regulated. Unfortunately it can be shown that this Møller operator is the only way of perturbatively relating the asymptotic states to the free states and so proceeding in this way just returns the original infrared singularities. This difficulty will lead us to abandoning the use of the interaction picture entirely and to instead investigate the use of the asymptotic interaction picture.

The asymptotic interaction picture will therefore be the focus of the remainder of the chapter. We will only be able to give a general flavour of how calculations should proceed in this picture, with a more rigorous investigation postponed for future work. Field theory calculations are usually performed in the interaction picture with the evolution of the fields being governed by the free Hamiltonian. Our aim here is to use an asymptotic Hamiltonian instead to describe the evolution of the fields. Feynman diagrams generated in this picture should then be free of infrared singularities. Instead the divergent soft regions are shifted into the propagators. No infrared divergences should appear because the vertices in the Feynman diagram will restrict the momentum flowing through the propagators such that no soft or collinear momentum flows through the propagators.

The first crucial part of working in this picture is being able to define a covariant splitting of the hard from the soft regions. We will then show that any Feynman diagram constructed in the asymptotic interaction picture will be infrared finite. After this we will discuss briefly what we mean by asymptotic states and then give an outline of a derivation of a modified LSZ reduction formula. This relates correlation functions to S_A matrix elements calculated using the S_A operator on the asymptotic states. Finally we show how we can construct the asymptotic field propagators in a perturbative way and derive the form of the fermion propagator in QED.

4.1 The S_A operator in the interaction picture

The form of the Møller operators used for the dressed states in the previous chapter arises from Eq.(2.91). Using this we found that we had to split up the amplitude into infrared divergent pieces, the divergences only cancelled when we summed all the pieces together, e.g. Eq.(3.37). In this section we will instead derive Møller operators from the form for the amplitudes given in Eq.(2.92), which is,

$$\Omega^{(+)} \equiv \Omega_f^{(+)} \Omega_\Delta^{(+)\dagger} \equiv \Omega_A^{(+)} \tag{4.1}$$

Once we have derived forms for $\Omega_A^{(+)}$ and $\Omega_A^{(-)\dagger}$ we can then construct the S_A operator.

4.1.1 The time-independent form

Initially we want to derive the operator $\Omega_A^{(+)}$ in a time independent way. From Eq.(2.35) we have,

$$\Omega_A^{(+)}|\Xi_\alpha(E)\rangle = \left(1 + \frac{1}{E_\alpha - H_f + i\epsilon}h\right)|\Xi_\alpha(E)\rangle \tag{4.2}$$

where $h = H_f - H_\Delta - H_0$ and $|\Xi_\alpha(E)\rangle$ is an eigenstate of H_Δ. Here H_f is the Hamiltonian of the full theory. In the interaction picture the particles evolve with the free Hamiltonian H_0. The denominators of Eq.(2.35) give rise to this evolution. Therefore we must expand $1/(E_\alpha - H_f + i\epsilon)$ using Eq.(2.37) and $K = H_0$. This gives,

$$\begin{aligned}\Omega_A^{(+)}|\Xi_\alpha(E)\rangle &= \Bigg(1 + \frac{1}{E_\alpha - H_0 + i\epsilon}h \\ &\quad + \frac{1}{E_\alpha - H_0 + i\epsilon}H_{int}\frac{1}{E_\alpha - H_0 + i\epsilon}h \\ &\quad + ...\Bigg)|\Xi_\alpha(E)\rangle \end{aligned} \tag{4.3}$$

where $H_{int} = H_f - H_0$. From this we then associate $\Omega_A^{(+)}$ in the interaction picture with the term multiplying the state $|\Xi_\alpha(E)\rangle$.

We know that in the usual interaction picture the Møller operator on the basis of free states $|\phi_\alpha\rangle$ is given by,

$$\begin{aligned}\Omega^{(+)}|\phi_\alpha\rangle &= \left(1 + \frac{1}{E_\alpha - H_f + i\epsilon}H_{int}\right)|\phi_\alpha\rangle \\ &= \Bigg(1 + \frac{1}{E_\alpha - H_0 + i\epsilon}H_{int} \\ &\quad + \frac{1}{E_\alpha - H_0 + i\epsilon}H_{int}\frac{1}{E_\alpha - H_0 + i\epsilon}H_{int} + ...\Bigg)|\phi_\alpha\rangle \end{aligned} \tag{4.4}$$

Our result from Eq.(4.3) can be checked using the following relation between these two Møller operators,

$$\Omega^{(+)}|\phi_\alpha\rangle = \Omega_A^{(+)}\Omega_\Delta^{(+)}|\phi_\alpha\rangle$$

$$\begin{aligned}
&= \Big(1 + \frac{1}{E_\alpha - H_0 + i\epsilon} h + \frac{1}{E_\alpha - H_0 + i\epsilon} H_{int} \frac{1}{E_\alpha - H_0 + i\epsilon} h \\
&\quad +...\Big) \times \Big(1 + \frac{1}{E_\alpha - H_0 + i\epsilon} H_\Delta \\
&\quad + \frac{1}{E_\alpha - H_0 + i\epsilon} H_\Delta \frac{1}{E_\alpha - H_0 + i\epsilon} H_\Delta + ...\Big)|\phi_\alpha\rangle \\
&= \Big(1 + \frac{1}{E_\alpha - H_0 + i\epsilon} H_{int} \\
&\quad + \frac{1}{E_\alpha - H_0 + i\epsilon} H_{int} \frac{1}{E_\alpha - H_0 + i\epsilon} H_{int} + ...\Big)|\phi_\alpha\rangle
\end{aligned} \tag{4.5}$$

Thus confirming our result in Eq.(4.3). Here we have used the standard Møller operator form of $\Omega_\Delta^{(+)}$ which is given by Eq.(2.38) with $H_f = H_\Delta + H_0$ and $H_{asym} = H_0$. We can construct $\Omega_A^{(-)\dagger}$ in a similar fashion to Eq.(4.3).

4.1.2 The time-dependent form

Now that we have time independent forms for $\Omega_A^{(+)}$ and $\Omega_A^{(-)\dagger}$ we will want to derive time dependent forms as these will be easier to work with later on. We begin by deriving a form for $\Omega_A^{(+)}$ starting with,

$$\begin{aligned}
\Omega_A^{(+)} &= \Omega^{(+)}\Omega_\Delta^{(+)\dagger} \\
&= \left(1 + ... + (-i)^m \int dt_1...dt_m \theta_{01}\theta_{12}...\theta_{(m-1)m} H_1...H_m\right) \\
&\quad \times \left(1 + ... + (+i)^p \int dt_1...dt_p \theta_{0p}\theta_{p(p-1)}...\theta_{21} s_1...s_p\right)
\end{aligned} \tag{4.6}$$

where $\theta_{ij} = \theta(t_i - t_j)$ and $H_i = H_{int}(t_i)$, $s_i = H_\Delta(t_i)$ and $h_i = H_{int}(t_i) - H_\Delta(t_i)$. The time evolution of these Hamiltonians is given in the interaction picture by,

$$H(t_i) = e^{iH_0 t_i} H e^{-iH_0 t_i} \tag{4.7}$$

We now need to multiply the two time ordered operators together, doing this requires great care. When multiplying two time ordered operators together the time of the Hamiltonians in each operator must be time ordered. So that the time of all Hamiltonians in the operator to the left must be after the times of the Hamiltonians in the operator to the right, if the Hamiltonians involved are different. If the Hamiltonians are the same then we just have a direct product of the two operators. So for example we would have,

$$(-i)\int_{-\infty}^{\infty} dt_1\theta_{10}s_1 \times (-i)\int_{-\infty}^{\infty} dt_1\theta_{10}h_1 \rightarrow (-i)^2\int_{-\infty}^{\infty} dt_1 dt_2\theta_{12}\theta_{20}s_1 h_2 \quad (4.8)$$

This can be seen more clearly when we have blocks of soft and hard vertices, for example,

$$\int dt_1 dt_2 h_1 s_2\theta_{01}\theta_{12} \times \int dt_3 s_3\theta_{03} \rightarrow \int dt_1 dt_2 dt_3 h_1 s_2 s_3\theta_{01}\theta_{12}\theta_{13} \quad (4.9)$$

So when we expand out the operator in eq.(4.6) we should get for a term at order n,

$$\Omega_A^{(+)}\Big|_n = (-i)^n\int dt_1...dt_n\theta_{01}\theta_{12}...\theta_{(n-1)n}(h+s)_1...(h+s)_{n-1}h_n \quad (4.10)$$

A similar result for $\Omega_A^{(-)\dagger}$ at order n can also be derived,

$$\Omega_A^{(-)\dagger}\Big|_n = (-i)^n\int dt_1...dt_n\theta_{12}...\theta_{(n-1)n}\theta_{n0}h_1(h+s)_1...(h+s)_n \quad (4.11)$$

If we were now to perform the time integrals of Eq.(4.10) and Eq.(4.11) we will get the same result as in Eq.(4.3), after we have inserted complete sets of free Hamiltonian eigenstates between all the Hamiltonians. This then confirms these time dependent forms for the Møller operator.

This result differs from the result given in [34] for the same operator. Our result here does not contain any s terms after the last hard vertex. If we perform the time integrals of the form of the Møller operator given in [34] we will get,

$$\begin{aligned}\Omega_A^{(+)}|\Xi_\alpha\rangle &= \bigg(1+(-i)\int_{-\infty}^{0} dt_1 h_1 + (-i)^2\int_{-\infty}^{0} dt_1 dt_2\theta_{12}\left(h_1h_2+[s_1,h_2]\right)\\ &\quad +...\bigg)|\Xi_\alpha\rangle\end{aligned}$$

$$\begin{aligned}
&\equiv \Big(1+\frac{1}{E_\alpha-H_0+i\epsilon}h+\frac{1}{E_\alpha-H_0+i\epsilon}H_{int}\frac{1}{E_\alpha-H_0+i\epsilon}h \\
&\quad -\frac{1}{E_\alpha-H_0+i\epsilon}h\frac{1}{E_\alpha-H_0+i\epsilon}H_\Delta+...\Big)|\Xi_\alpha\rangle
\end{aligned} \tag{4.12}$$

To check this form of the Møller operator we will repeat the calculation of Eq.(4.5), using this form of $\Omega_A^{(+)}$ and attempt to get $\Omega^{(+)}$ given in Eq.(4.4). So we have,

$$\begin{aligned}
\Omega^{(+)}|\phi_\alpha\rangle &= \Omega_A^{(+)}\Omega_\Delta^{(+)}|\phi_\alpha\rangle \\
&= \Big(1+\frac{1}{E_\alpha-H_0+i\epsilon}h+\frac{1}{E_\alpha-H_0+i\epsilon}H_{int}\frac{1}{E_\alpha-H_0+i\epsilon}h \\
&\quad -\frac{1}{E_\alpha-H_0+i\epsilon}h\frac{1}{E_\alpha-H_0+i\epsilon}H_\Delta...\Big)\times\Big(1+\frac{1}{E_\alpha-H_0+i\epsilon}H_\Delta \\
&\quad +\frac{1}{E_\alpha-H_0+i\epsilon}H_\Delta\frac{1}{E_\alpha-H_0+i\epsilon}H_\Delta+...\Big)|\phi_\alpha\rangle \\
&= \Big(1+\frac{1}{E_\alpha-H_0+i\epsilon}H_{int}+\frac{1}{E_\alpha-H_0+i\epsilon}H_{int}\frac{1}{E_\alpha-H_0+i\epsilon}h \\
&\quad +\frac{1}{E_\alpha-H_0+i\epsilon}H_\Delta\frac{1}{E_\alpha-H_0+i\epsilon}H_\Delta+...\Big)|\phi_\alpha\rangle
\end{aligned} \tag{4.13}$$

The expected result is not returned suggesting that this form of the Møller operator $\Omega_A^{(+)}$ from [34] is incorrect.

4.1.3 The S_A operator

Now that we have a time dependent form for the Møller operators $\Omega_A^{(+)}$ and $\Omega_A^{(-)\dagger}$ in the interaction picture then we can construct the S_A operator in the interaction picture. We do this using Eq.(2.62), a general term of the S_A operator is then given at order n by,

$$\begin{aligned}
S_A\Big|_n &= \Omega_A^{(-)\dagger}\Omega_A^{(+)}\Big|_n \\
&= (-i)^n\int dt_1...dt_n\Big(\theta_{12}...\theta_{(n-1)n}\theta_{n0}h_1(h+s)_2...(h+s)_n \\
&\quad +\theta_{12}...\theta_{(n-2)(n-1)}\theta_{(n-1)0}\theta_{0n}h_1(h+s)_2...(h+s)_{n-1}h_n \\
&\quad +\theta_{12}...\theta_{(n-3)(n-2)}\theta_{(n-2)0}\theta_{0(n-1)}\theta_{(n-1)n}h_1(h+s)_2...(h+s)_{n-1}h_n \\
&\quad +...
\end{aligned}$$

$$
\begin{aligned}
&+\theta_{10}\theta_{02}\theta_{23}...\theta_{(n-1)n}h_1(h+s)_2...(h+s)_{n-1}h_n \\
&+\theta_{01}\theta_{23}...\theta_{(n-1)n}(h+s)_1(h+s)_2...(h+s)_{n-1}h_n\Big) \\
= \; & (-i)^n\int dt_1...dt_n\Big(\theta_{12}\theta_{23}...\theta_{(n-1)n}h_1(h+s)_2...(h+s)_{n-1}h_n \\
&+\theta_{12}...\theta_{(n-1)n}\theta_{n0}h_1(h+s)_2...(h+s)_{n-1}s_n \\
&+\theta_{01}\theta_{12}...\theta_{(n-1)n}s_1(h+s)_2...(h+s)_{n-1}h_n\Big)
\end{aligned} \tag{4.14}
$$

As each operator is time ordered entirely above t_0 or below t_0 then we can just multiply these operators together directly. If we were then to perform the time integrals of this result we get,

$$
\begin{aligned}
S_A\Big|_n \; = \; & \frac{\langle\phi_\beta|h_1r_2...r_{n-1}h_n|\phi_\alpha\rangle}{(\omega_n+i\epsilon)(\omega_n+\omega_{n-1}+i\epsilon)...(\omega_n+...+\omega_2+i\epsilon)}\delta(\omega_1+...+\omega_n) \\
&+(-1)^n\frac{\langle\phi_\beta|h_1r_2...r_{n-1}s_n|\phi_\alpha\rangle}{(\omega_1-i\epsilon)(\omega_1+\omega_2-i\epsilon)...(\omega_1+...+\omega_n-i\epsilon)} \\
&+\frac{\langle\phi_\beta|s_1r_2...r_{n-1}h_n|\phi_\alpha\rangle}{(\omega_n+i\epsilon)(\omega_n+\omega_{n-1}+i\epsilon)...(\omega_n+...+\omega_1+i\epsilon)}
\end{aligned} \tag{4.15}
$$

where r_i is either s_i or h_i. We see from this that we have terms which are not multiplied by any delta function at all, a worrying result.

4.1.4 The unitarity of $\Omega_A^{(+)}$ in the interaction picture

The result for the S_A operator in the previous subsection did not appear to be unitary. This is clearly a problem and so we need to check the unitary of our form of the $\Omega_A^{(+)}$ operator. We can do this in the standard way by performing the following calculation,

$$
\begin{aligned}
&\Omega_A^{(+)\dagger}\Omega_A^{(+)} \\
= \; & \left(1+(i)\int_{-\infty}^{\infty}dt_1\theta_{01}h_1+(i)^2\int_{-\infty}^{\infty}dt_1dt_2\theta_{02}\theta_{21}h_1(h+s)_2+...\right) \\
&\times\left(1+(-i)\int_{-\infty}^{\infty}dt_1\theta_{01}h_1+(-i)^2\int_{-\infty}^{\infty}dt_1dt_2\theta_{01}\theta_{12}h_1(h+s)_2+...\right) \\
= \; & 1+(-i)^2\int_{-\infty}^{\infty}dt_1dt_2(\theta_{02}\theta_{21}+\theta_{01}\theta_{12}-\theta_{01}\theta_{02})h_1h_2
\end{aligned}
$$

$$
\begin{aligned}
& +(-i)^2\int_{-\infty}^{\infty} dt_1 dt_2 \theta_{02}\theta_{21} h_1 s_2 + (i)^2\int_{-\infty}^{\infty} dt_1 dt_2 \theta_{01}\theta_{12} s_1 h_2 + ... \\
= \;& 1 + (-i)^2\int_{-\infty}^{\infty} dt_1 dt_2 \left(\theta_{02}\theta_{21} h_1 s_2 + \theta_{01}\theta_{12} s_1 h_2\right) + ... \qquad (4.16)
\end{aligned}
$$

We see that not all the terms proportional to g cancel. So apparently some extra non-unitary terms appear when we try to calculate this result in the interaction picture.

Initially we started with a unitary operator Eq.(4.2) and we only developed problems after perturbatively expanding the energy denominators. So from this we can quickly deduce that the operator,

$$
\left(1 + \frac{1}{E_\alpha - H_A \pm i\epsilon}\right)|\phi_\alpha\rangle = \Omega_A^{(+)}|\phi_\alpha\rangle \qquad (4.17)
$$

where $H_A = H_\Delta + H_0$, is not well defined. The dependence upon g in the energy eigenvalues E_α of the energy denominators of Eq.(4.3) has not been correctly taken into account. These energy eigenvalues are eigenstates of H_Δ and not H_0, because the Møller operators are always related to a particular basis of states, in this case the true asymptotic states are $\Omega_A^{(+)}|\Xi_\alpha\rangle$. So we encounter problems when relating this to $\Omega_A^{(+)}|\phi_\alpha\rangle$.

We can see how this occurs by comparing the perturbative expansion of,

$$
\frac{1}{E_\alpha - H + i\epsilon} h \qquad (4.18)
$$

for both the asymptotic interaction picture and the interaction picture. The asymptotic interaction picture is derived by using $K = H_\Delta$ in Eq.(2.37), this is a formalism we will investigate in greater detail in Section 4.3. The interaction picture is defined as usual. In the asymptotic interaction picture we have,

$$
\frac{1}{E_\alpha - H_A + i\epsilon} h + \frac{1}{E_\alpha - H_A + i\epsilon} h \frac{1}{E_\alpha - H_A + i\epsilon} h + ... \qquad (4.19)
$$

and in the interaction picture,

$$\frac{1}{E_\alpha - H_0 + i\epsilon}h + \frac{1}{E_\alpha - H_0 + i\epsilon}H_{int}\frac{1}{E_\alpha - H_A + i\epsilon}h + ... \tag{4.20}$$

We see that the extra terms at second order are,

$$\frac{1}{E_\alpha - H_0 + i\epsilon}H_\Delta\frac{1}{E_\alpha - H_A + i\epsilon}h \tag{4.21}$$

which corresponds to expanding to first order,

$$\begin{aligned}\frac{1}{E_\alpha - H_A + i\epsilon}h &= \frac{1}{E_\alpha - H_0 + i\epsilon}h + \frac{1}{E_\alpha - H_0 + i\epsilon}H_\Delta\frac{1}{E_\alpha - H_0 + i\epsilon}h + ... \\ &= \left(1 + \frac{1}{E_\alpha - H_0 + i\epsilon}H_\Delta + ...\right)\frac{1}{E_\alpha - H_0 + i\epsilon}h \end{aligned} \tag{4.22}$$

So the asymptotic interaction picture re-sums all these soft terms and the Møller operator in this picture is well defined. These extra terms though are not re-summed in the interaction picture and appear as the extra terms in Eq.(4.16) after the time integrals have been performed.

4.2 Producing covariant amplitudes

Ignoring the difficulty of expanding S_A in the interaction picture for now we would want to calculate scattering amplitudes using the S_A operator on the free states,

$$\mathcal{A} = \langle\phi_\beta|S_A|\phi_\alpha\rangle \tag{4.23}$$

Such amplitudes are then free of infrared singularities at all stages of the calculation.

The problem we have now is that the S_A operator is defined in time ordered perturbation theory. This means that at order n in the perturbative expansion we will have $n!$ different time ordered diagrams to consider for each different topology. We have also split the interaction Hamiltonian H_{int}, into two pieces s_i and h_i. This means that we must also consider all the different permutations of these s_i and h_i vertices in the amplitude, except for the first and last vertices which are always h_i's. This leads to an extra 2^{n-2} diagrams for each time ordered diagram. So using this method we would have $2^{n-2}n!$ diagrams to compute. As we increase the complexity of the processes we wish to calculate, by going to higher orders in perturbation theory, we quickly get to a point where there are too many diagrams to realistically calculate.

We therefore need to reduce the large number of diagrams generated. We know from the standard field theory approach in the interaction picture that we can combine the $n!$ different time ordered diagrams into a single time independent Feynman diagram. Clearly a similar approach is required here.

4.2.1 The asymptotic Hamiltonian

In Chapter 3 we split up the interaction vertex into eight pieces, see Section 3.2.2. Then using a theta function we divided up each of these eight terms into a soft and hard piece depending on whether it contributed infrared singularities to the amplitude. Each term had a different theta function which depended only on the energy and the direction of the particles entering the vertex. The advantage of this form of the asymptotic Hamiltonian was that as we were only calculating the dressing factors in time ordered perturbation theory we were minimising the number of dressing factor diagrams to calculate by reducing the number of possible vertices.

If we are now to relate the time ordered diagrams generated in Eq.(4.15) to a covariant diagram we will need a covariant division between the soft and hard parts of the interaction Hamiltonian. As stated in Section 3.2.2 the soft Hamiltonian must include all the infrared divergent regions but can contain as much of the hard part as we want[1]. The hard Hamiltonian will then contain everything else.

We will define the arbitrary function which performs this split for the

[1]We should note that strictly the asymptotic Hamiltonian is given by $H_{asym} = \lim_{t\to\pm\infty} H_f$, our H_Δ will only differ from this by a finite amount, unlike in the usual case with H_0.

three point vertex as $f_s(\vec{p}_1, \vec{p}_2, \vec{p}_3; \Delta)$. We place this in the interaction vertex,

$$H_{int}(t) = \int d^3x \overline{\Psi}(x)\gamma^\mu \Psi(x) A_\mu(x) \tag{4.24}$$

as follows,

$$\begin{aligned} H_\Delta \;=\; & \int d^3x \frac{d^3p_1}{(2\pi)^3 2\omega p_1} \cdots \frac{d^3p_3}{(2\pi)^3 2\omega p_3} \left(\overline{u}_\alpha(\vec{p}_1) b^\dagger_{p_1} e^{-ip_1x} + \overline{v}_\alpha(\vec{p}_1) d_{p_1} e^{ip_1x}\right) \\ & \times \gamma^\mu \left(u_\alpha(\vec{p}_3) b_{p_3} e^{ip_3x} + v_\alpha(\vec{p}_3) d^\dagger_{p_3} e^{-ip_3x}\right) \\ & \times \left(\epsilon_\mu(\vec{p}_2) a_{\vec{p}_2} e^{-ip_2x} + \epsilon^*_\mu(\vec{p}_2) a^\dagger_{\vec{p}_2} e^{ip_2x}\right) f_s(\vec{p}_1, \vec{p}_2, \vec{p}_3; \Delta) \end{aligned} \tag{4.25}$$

So the momenta $\vec{p}_i$ are associated with the legs of the vertex and the parameter Δ controls how much of the hard region we include in H_Δ. We now require that this function f_s satisfies the following requirements so that it correctly encapsulates the soft region. First we require that no leg of the vertex is "special" so,

$$f_s(\vec{p}_1, \vec{p}_2, \vec{p}_3; \Delta) \;=\; f_s(\vec{p}_2, \vec{p}_1, \vec{p}_3; \Delta) = f_s(\vec{p}_2, \vec{p}_3, \vec{p}_1; \Delta) = \ldots \tag{4.26}$$

Next we need to separate the infrared region from the hard region correctly,

$$\begin{aligned} f_s(0, \vec{p}_2, \vec{p}_3; \Delta) &= f_s(\vec{p}_1, 0, \vec{p}_3; \Delta) = f_s(\vec{p}_1, \vec{p}_2, 0; \Delta) = 1 \\ f_s(\vec{p}_1, \lambda\vec{p}_1, \vec{p}_3; \Delta) &= f_s(\vec{p}_1, \lambda\vec{p}_3, \vec{p}_3; \Delta) = f_s(\vec{p}_1, \vec{p}_2, \lambda\vec{p}_1; \Delta) \\ &= f_s(\vec{p}_1, \vec{p}_2, \lambda\vec{p}_2; \Delta) = f_s(\lambda\vec{p}_2, \vec{p}_2, \vec{p}_3; \Delta) \\ &= f_s(\lambda\vec{p}_3, \vec{p}_2, \vec{p}_3; \Delta) = 1 \end{aligned} \tag{4.27}$$

Finally we require the UV regions to be in the hard Hamiltonian so we have,

$$f_s(\pm\infty, \vec{p}_2, \vec{p}_3; \Delta) = f_s(\vec{p}_1, \pm\infty, \vec{p}_3; \Delta) = f_s(\vec{p}_1, \vec{p}_3, \pm\infty; \Delta) = 0 \tag{4.28}$$

Now that we have defined f_s it is simple to define the function that gives the hard region as,

$$f_h(\vec{p}_1, \vec{p}_2, \vec{p}_3; \Delta) = 1 - f_s(\vec{p}_1, \vec{p}_2, \vec{p}_3; \Delta) \tag{4.29}$$

These splitting functions for the hard and soft regions still depend upon the momentum three-vector $\vec{p}_i$. They will therefore not be covariant in their current form.

4.2.2 Removing the time order dependence

If we are going to produce covariant diagrams from the time ordered diagrams we will need to replace the explicit dependence of the time ordered diagrams on the time ordering theta functions $\theta(t_i - t_j)$. We would also like to remove the three-momentum dependence of the soft-hard splitting functions $f_{s/h}$ and replace it with a covariant four-momentum dependence. In the standard field theory approach there are multiple methods for taking the time ordered diagrams and removing the time ordering dependence.

To explore how these would work in our situation we will consider the simplest type of diagram. We will attempt to combine the two time ordered diagrams shown in Figure 4.1 into a single covariant diagram. These diagrams

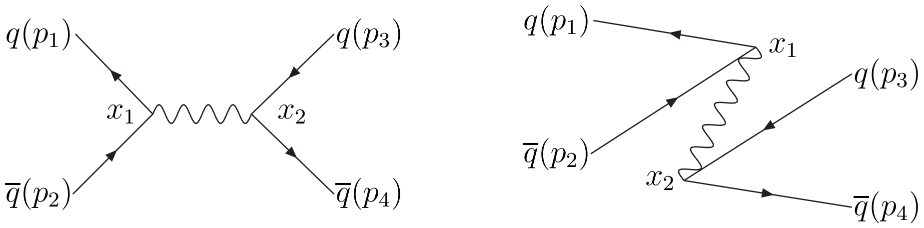

Figure 4.1: The two time ordered diagrams for a single propagator.

contain a single propagator and by attempting to derive a covariant infrared finite amplitude from them we will be able to highlight all the issues involved in “covariantising” the amplitudes. The vertices labelled x_i can be either hard or soft, we will initially consider both vertices as being hard. This corresponds to calculating the first line of Eq.(4.15).

The contour integral approach

Our first approach will be that of using contour integration to remove the dependence on the time order. When combined, the two time ordered diagrams from Figure 4.1 will give us,

$$\int_{-\infty}^{\infty} d^4x_1 \int_{-\infty}^{\infty} d^4x_2 \int_{-\infty}^{\infty} \frac{d^3p}{(2\pi)^3 2\omega_p} \left(\theta_{12} e^{-ip(x_1-x_2)} + \theta_{21} e^{-ip(x_2-x_1)}\right) e^{ix_1p_1} e^{ix_1p_2}$$
$$\times e^{-ix_2p_3} e^{-ix_2p_4} f_h(\vec{p},\vec{p}_1,\vec{p}_2;\Delta) f_h(\vec{p},\vec{p}_3,\vec{p}_4;\Delta) \langle q(p_1)\overline{q}(p_2)|hh|q(p_3)\overline{q}(p_4)\rangle \tag{4.30}$$

where $p = (\omega_p, \vec{p})$ with $\omega_p = |\vec{p}|$, i.e. all four-momenta are on-shell and we also have $x_i^0 = t_i$. We now want to use the following identities which come from contour integration, to simplify Eq.(4.30),

$$\begin{aligned}
& i\int \frac{dk_0}{2\pi} \frac{e^{-ik_0(t_1-t_2)}}{k^2+i\epsilon} F(k_0)\theta_{12} - \int_0^{\pi} d\theta R e^{i\theta} \frac{e^{-iRe^{i\theta}(t_1-t_2)}}{R^2 e^{2i\theta} - \vec{k}^2 + i\epsilon} F(Re^{i\theta})\theta_{12} \\
= & \ \frac{1}{2\omega_k} e^{-i\omega_k(t_1-t_2)} F(\omega_k)\theta_{12} \\
& i\int \frac{dk_0}{2\pi} \frac{e^{-ik_0(t_1-t_2)}}{k^2+i\epsilon} F(k_0)\theta_{21} - \int_0^{-\pi} d\theta R e^{i\theta} \frac{e^{-iRe^{i\theta}(t_1-t_2)}}{R^2 e^{2i\theta} - \vec{k}^2 + i\epsilon} F(Re^{i\theta})\theta_{21} \\
= & \ \frac{1}{2\omega_k} e^{i\omega_k(t_1-t_2)} F(-\omega_k)\theta_{21}
\end{aligned} \tag{4.31}$$

For these relations to hold we require that $F(k_0)$ be analytic in k_0 and also that $F(k_0)$ vanishes sufficiently quickly as $k_0 \to \infty$ in the complex plane. If these conditions are satisfied then the second terms on the left hand sides of Eq.(4.31) will vanish when we apply Jordan's Lemma with the $e^{ik_0(t_1-t_2)}$ term. These terms correspond to the semicircle in either the upper or lower half of the complex plane used to close the contour of integration.

The key now would be to find forms of $f_{s/h}$ which satisfied these requirements on $F(k_0)$ as well as those of Section 4.2.1. Unfortunately we can quickly see that the only function that satisfies the requirements on $F(k_0)$ is a constant and this does not separate the soft and hard regions. Therefore we cannot use this formalism to produce covariant amplitudes.

The θ function replacement procedure

In the previous subsection we saw that we could not find an f_s function such that the semi-circle used to close the contour in the complex plane would vanish. So we will now consider an alternative approach.

Again we start from Eq.(4.30), but we now replace the theta functions with,

$$\theta(t) = \lim_{\epsilon \to +0} \int_{-\infty}^{\infty} \frac{d\omega}{2\pi i} \frac{e^{i\omega t}}{\omega - i\epsilon} \tag{4.32}$$

So Eq.(4.30) becomes,

$$\begin{aligned}
&\int_{-\infty}^{\infty} d^4x_1 \int_{-\infty}^{\infty} d^4x_2 \int_{-\infty}^{\infty} \frac{d^3p}{(2\pi)^3 2\omega_p} \int_{-\infty}^{\infty} \frac{d\omega}{2\pi i} e^{ix_1p_1} e^{ix_1p_2} e^{-ix_2p_3} e^{-ix_2p_4} \\
&\quad \times \left(\frac{e^{i\omega(t_1-t_2)} e^{-ip(x_1-x_2)}}{\omega - i\epsilon} + \frac{e^{-i\omega(t_1-t_2)} e^{ip(x_1-x_2)}}{\omega - i\epsilon} \right) \\
&\quad \times f_h(\vec{p}, \vec{p}_1, \vec{p}_2; \Delta) f_h(\vec{p}, \vec{p}_3, \vec{p}_4; \Delta) \langle q(p_1)\overline{q}(p_2)|hh|q(p_3)\overline{q}(p_4)\rangle
\end{aligned} \tag{4.33}$$

If we then shift $\omega \longrightarrow \omega_p - p_0$ and $\vec{p} \longrightarrow \vec{p}$ in the first term above and $\omega \longrightarrow \omega_p + k_0$ and $\vec{p} \rightarrow -\vec{p}$ in the second term then we get,

$$\begin{aligned}
&(-i) \int_{-\infty}^{\infty} d^4x_1 \int_{-\infty}^{\infty} d^4x_2 \int_{-\infty}^{\infty} \frac{d^4p}{(2\pi)^4 2\omega_p} e^{ix_1p_1} e^{ix_1p_2} e^{-ix_2p_3} e^{-ix_2p_4} \\
&\quad \times \left(\frac{e^{-ip(x_1-x_2)}}{\omega_p - p_0 - i\epsilon} f_h(\vec{p}, \vec{p}_1, \vec{p}_2; \Delta) f_h(\vec{p}, \vec{p}_3, \vec{p}_4; \Delta) \right. \\
&\quad \left. + \frac{e^{-ip(x_1-x_2)}}{\omega_p + p_0 - i\epsilon} f_h(-\vec{p}, \vec{p}_1, \vec{p}_2; \Delta) f_h(-\vec{p}, \vec{p}_3, \vec{p}_4; \Delta) \right) \\
&\quad \times \langle q(p_1)\overline{q}(p_2)|hh|q(p_3)\overline{q}(p_4)\rangle
\end{aligned} \tag{4.34}$$

where p is now an off-shell four-vector $p = (p_0, \vec{p})$. Now we require a form of $f_h(\vec{q}_1, \vec{q}_2, \vec{q}_3)$ such that,

$$f_h(-\vec{q}_1, \vec{q}_2, \vec{q}_3) = f_h(\vec{q}_1, \vec{q}_2, \vec{q}_3) \tag{4.35}$$

If this is the case then we get,

$$\begin{aligned}
&(-i)(2\pi)^4 \frac{\langle q(p_1)\overline{q}(p_2)|hh|q(p_3)\overline{q}(p_4)\rangle}{(p_1+p_2)^2 + i\epsilon} f_h(\vec{p}_1 + \vec{p}_2, \vec{p}_1, \vec{p}_2; \Delta) \\
&\quad \times f_h(\vec{p}_1 + \vec{p}_2, \vec{p}_3, \vec{p}_4; \Delta) \delta^{(4)}(p_1 + p_2 - p_3 - p_4)
\end{aligned} \tag{4.36}$$

We have removed the time ordering dependence from the amplitude but this result is not covariant because it depends upon the three-vectors $\vec{p}_i$ in f_h.

If we do not have a form for f_s that satisfies the requirement Eq.(4.35) then we must define the propagator as,

$$\begin{aligned}
&(-i)\int_{-\infty}^{\infty} d^4x_1 \int_{-\infty}^{\infty} d^4x_2 \int_{-\infty}^{\infty} \frac{d^4p}{(2\pi)^4 2\omega_p} e^{ix_1p_1} e^{ix_1p_2} e^{-ix_2p_3} e^{-ix_2p_4} \frac{e^{-ip(x_1-x_2)}}{p^2+i\epsilon} \\
&\times\Bigg((\omega_p - i\epsilon)\Big(f_h(\vec{p},\vec{p}_1,\vec{p}_2;\Delta)f_h(\vec{p},\vec{p}_3,\vec{p}_4;\Delta) \\
&+f_h(-\vec{p},\vec{p}_1,\vec{p}_2;\Delta)f_h(-\vec{p},\vec{p}_3,\vec{p}_4;\Delta)\Big) \\
&+p_0\Big(f_h(\vec{p},\vec{p}_1,\vec{p}_2;\Delta)f_h(\vec{p},\vec{p}_3,\vec{p}_4;\Delta) \\
&-f_h(-\vec{p},\vec{p}_1,\vec{p}_2;\Delta)f_h(-\vec{p},\vec{p}_3,\vec{p}_4;\Delta)\Big)\Bigg)\langle q(p_1)\overline{q}(p_2)|hh|q(p_3)\overline{q}(p_4)\rangle \qquad (4.37)
\end{aligned}$$

Although complicated this also contains no dependence upon the time order of the vertices.

We can therefore remove the time dependence from the propagator terms but not in a covariant way. So although we have reduced the number of diagrams to be calculated we are still in a frame dependant formalism. Furthermore the requirements that $f_{s/h}$ are independent of the direction of the momentum entering the vertices means that we will alter the UV region of the theory as we will be forced to include anti-collinear regions entirely in the infrared region when they should be in the hard region.

4.3 The asymptotic interaction picture

In the preceding part of this chapter we have seen all the difficulties of calculating infrared finite scattering amplitudes in the usual interaction picture. All of these difficulties suggest that a better approach would be to drop the use of the interaction picture entirely. The most obvious choice then would be to work directly in the asymptotic interaction picture. For similar reasons as before we would also like to work in a covariant formalism. We have previously used the Hamiltonian as the foundation of our approach because it most clearly shows up the causes and potential solutions to the infrared singularity problem. For the rest of this chapter though we will pursue a different direction for the basis of our formalism. It will be an approach closer to the usual field theory methods described in Chapter 1.

The n-point correlations functions will now be the starting point of our calculations. These will be related to physical S_A-Matrix elements which come from the S_A operator acting upon a basis of asymptotic states and not a basis of free fields states as before. We will then give a heuristic derivation of a modified form of the LSZ theorem which can perform this relation. The correlation functions will then be related to fields in the asymptotic interaction picture using evolution operators. Modifications to the usual Feynman rules for the propagators and vertices in this new picture will be given. We will also prove that amplitudes defined in this asymptotic interaction picture will be entirely free of infrared singularities. We should note that the discussion of these topics in the remainder of this chapter gives just an overview of this area and is only intended as a guide of how such calculations could proceed.

4.3.1 Calculations in the asymptotic interaction picture

We begin from a Lagrangian describing any theory with a three-point interaction. We split this Lagrangian into two parts,

$$\mathcal{L} = \mathcal{L}_{asym} + \mathcal{L}_{hard} = \mathcal{L}_0 + \mathcal{L}_{IR} + \mathcal{L}_{hard} \tag{4.38}$$

$\mathcal{L}_0$ is the usual free field Lagrangian and $\mathcal{L}_{IR}$ contains the parts of the interaction that give rise to soft or collinear momenta flowing through a three-point vertex. Together these two Lagrangian's form the asymptotic Lagrangian, which describes the asymptotic evolution of the fields of the theory. $\mathcal{L}_{hard}$ then contains the remainder of the interaction terms and any renormalisation counter-terms in a renormalised theory.

The fields contained in the Lagrangian, for example Eq.(1.2), can then be used in the calculation of time ordered correlation functions of the form,

$$\langle\Omega|T\{\psi(x_1)...\psi(x_n)\}|\Omega\rangle \tag{4.39}$$

These are then related to physical S-Matrix elements using the LSZ theorem. The usual approach is to take the fields that are a solution to $\mathcal{L}_0$ as the asymptotic fields. Instead we will want to relate the correlation functions to S_A-Matrix elements calculated on asymptotic fields and so we will choose fields that are a solution to $\mathcal{L}_{asym}$ as our asymptotic fields. This will require us to modify the usual LSZ derivation which will be discussed in Section 4.3.4.

The calculation of these correlation functions in the usual interaction picture approach leads to infrared singularities as described in Chapter 1. The asymptotic interaction picture avoids this problem and is derived in the following way. Evolution operators for the asymptotic interaction picture are generated using Eq.(2.52) where H_{asym} is now the asymptotic Hamiltonian derived from the Lagrangian $\mathcal{L}_{asym}$. These evolution operators can be written as,

$$U_A(t,t_0) = T\left\{\exp\left(-i\int_{t_0}^{t} dt_1 H_{A,int}(t_1)\right)\right\} \tag{4.40}$$

where $H_{A,int} = H_f - H_{asym}$. The correlation functions are then placed in the asymptotic interaction picture in the same way as we would place it in the interaction picture, by relating the full fields ψ to the asymptotic fields Ξ using,

$$\psi(t,\vec{x}) = U_A^\dagger(t,t_0)\Xi(t,\vec{x})U_A(t,t_0) \tag{4.41}$$

The correlation functions then become,

$$\begin{aligned}
&\langle\Omega|T\{\psi(x_1)...\psi(x_n)\}|\Omega\rangle \\
&= \langle\Omega|T\{U_A^\dagger(x_1,t_0)\Xi(x_1)U_A(x_1,t_0)...U_A^\dagger(x_n,t_0)\Xi(x_n)U_A(x_n,t_0)\}|\Omega\rangle \\
&= \frac{\langle\Omega'|T\{U_A(T,x_1)\Xi(x_1)U_A(x_1,x_2)...U_A(x_{n-1},x_n)\Xi(x_n)U_A(x_n,-T)\}|\Omega'\rangle}{\langle\Omega'|T\{U_A(T,t_0)U_A^\dagger(-T,t_0)\}|\Omega'\rangle}
\end{aligned}$$

$$= \frac{\langle \Omega' | T\{\Xi(x_1)...\Xi(x_n)U_A(T,-T)\}|\Omega'\rangle}{\langle \Omega' | T\{U_A(T,-T)\}|\Omega'\rangle} \tag{4.42}$$

where $|\Omega\rangle$ and $|\Omega'\rangle$ are the vacuums of the full and asymptotic fields respectively. If we now take $T \to \infty$ then we get,

$$\langle \Omega | T\{\psi(x_1)...\psi(x_n)\}|\Omega\rangle = \frac{\langle \Omega' | T\{\Xi(x_1)...\Xi(x_n)\exp\left(-i\int_{-\infty}^{\infty} d^4x \mathcal{L}_{hard}\right)\}|\Omega'\rangle}{\langle \Omega' | T\{\exp\left(-i\int_{-\infty}^{\infty} d^4x \mathcal{L}_{hard}\right)\}|\Omega'\rangle} \tag{4.43}$$

The fields in $\mathcal{L}_{hard}$ are now all asymptotic fields Ξ. The amplitudes generated from this will consist entirely of hard vertices, the infrared pieces of $\mathcal{L}$ are now contained entirely in the propagators of the Ξ fields.

Before we can proceed further we will need to define a completely covariant split between the hard and the soft momentum regions of the theory. We can then define forms for $\mathcal{L}_{hard}$ and $\mathcal{L}_{IR}$. To do this we will need to pinpoint the locations of all possible infrared singularities that can appear in a covariant perturbation theory amplitude.

4.3.2 Infrared divergences in covariant perturbation theory

The Landau equations

We wish to examine the general structure of infrared singularities of massless scattering amplitudes. This can be done by considering the general form of the massless Greens function $G(\{p_e\})$ with external momenta $\{p_e\}$ given after Feynman parameterisation has been used to combine the propagators into a single denominator,

$$\begin{aligned} G(\{p_e\}) &= \left(\prod_i \int_0^1 d\alpha_i\right) \delta\left(\sum_i \alpha_i - 1\right) \left(\prod_r \int d^d k_r\right) \\ &\times \frac{F(\alpha_i, k_r, p_e)}{\sum_j \alpha_j l_j^2(p,k) + i\epsilon} \end{aligned} \tag{4.44}$$

where there are i lines in the diagram and k loops. $F(\alpha_i, k_r, p_e)$ contains all the numerator factors of the diagram and,

$$l_j^\mu(p_e, k_r) = \sum_n b_{j,n} k_n^\mu + \sum_n c_{j,n} p_n^\mu \tag{4.45}$$

where b and c are just c-numbers and are zero whenever k_n is not contained in the propagator denoted by l_j^μ.

We now concern ourselves with the type of singularities this general amplitude can have. We want to analytically continue the arguments of $G(\{p_e\})$ onto the complex plane so that the integrals involved become contour integrals in the complex plane. This would then allow us to avoid any poles along the real axis. In doing this though we find that there are two possible classes of singularity in the complex plane where this cannot be done and hence the integral contour cannot be deformed.

We will first examine the possible singularities in the single variable case and then extend this discussion to the multi-variable case. The first class of singularity is the *end-point* singularity, these occur when the integrand contains a pole at one of the fixed end points of the integration contour. The contour can then not be deformed around this singular point and it is therefore a real singularity of the amplitude. The second class of singularity is the *pinch* singularity. Such a singularity is a result of the integration contour being trapped between two poles, the contour is then pinched between these two poles and the singularity cannot be avoided, see Figure 4.2. In the multi-

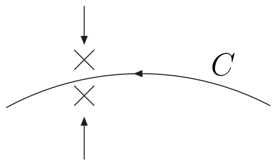

Figure 4.2: A pinch singularity where the contour C is trapped between the two poles indicated by arrows in the complex plane.

variable case these pinch points become surfaces in the space of the complex variables $\{k_i, \alpha_j\}$, if at each possible pinch point of a particular variable in $\{k_i, \alpha_j\}$ the variable is trapped whilst we keep the remaining variables fixed. These are known as *pinch surfaces.*

Here we will only be interested in pinch surfaces as the momentum integrals before Feynman parametrisation were unbounded and so we have no end-point singularities. It is only when the internal variables $\{k_i, \alpha_j\}$, of $G(\{p_e\})$ are on a pinch surfaces that an infrared singularity can appear. To find all the possible pinch surfaces and hence all the possible regions of infrared singularities we will need to use the Landau equations [1, 44]. We can derive these as follows. Singularities appear when,

$$\sum_j \alpha_j l_j^2(p,k) + i\epsilon = 0 \tag{4.46}$$

This is quadratic in k^μ and so we expect there to be two solutions to this equation. These will give a pinch singularity only when the derivative of this equation is zero at these solutions. This would mean that,

$$\frac{\partial}{\partial k_j^\mu}\left(\sum_j \alpha_j l_j^2(p,k) + i\epsilon\right) = 2\sum_j b_{ij}(\alpha_i l_i^\mu) = 0 \tag{4.47}$$

Values of $\{k_i, \alpha_j\}$ that satisfy Eq.(4.46) and Eq.(4.47) are then our required pinch surfaces. The possible solutions are then given by either,

$$l_i^2 = 0 \text{ and } \sum_i b_{ij}\alpha_i l_i^\mu = 0 \tag{4.48}$$

for every loop j that includes the line i, or by,

$$l_i^2 \neq 0 \text{ and } \alpha_i = 0 \tag{4.49}$$

A pinch surface solution to the Landau equations does not guarantee an infrared singularity but it is a necessary condition for the existence of one. To determine whether infrared singularities exist on these surfaces we must investigate the behaviour of the amplitude further at these points.

Reduced diagrams

To investigate the singularity structure closer we will use a diagrammatic method to visualise the pinch surface solutions to the Landau equations. These diagrams are known as *reduced diagrams* [44, 46] and are constructed in the following way. We start from the normal Feynman diagram for the amplitude we wish to calculate. Next we take any off-shell line and reduce it to a point connecting the vertices on either end together to produce a composite vertex. This occurs because the only way for off-shell lines to satisfy the Landau equations is for $\alpha = 0$ which corresponds to a vanishing contribution to the denominator of Eq.(4.44). Any on-shell lines are kept as these satisfy the Landau equations for any α.

The reduced diagrams produced in this way are not necessarily all pinch surfaces. As well as satisfying the Landau equations the diagrams must also satisfy the constraints on the momenta given by four-momentum conservation at each vertex of the diagram and also any restrictions on the external momenta.

We will only be considering nonexceptional reduced diagrams. These are diagrams such that for every proper subset Q of the set of external momenta $\{p_i\}$ of a reduced diagram $G(\{p_i\})$ we have,

$$\left(\sum_{i\in Q} p_i^\mu\right)^2 \neq 0 \tag{4.50}$$

This then removes any reduced diagrams where the external momentum become collinear or soft. In the strictest sense it also means that all of the external momenta are off-shell. So we will relax this requirement slightly and allow the external lines to be on-shell.

To demonstrate how this works we will consider the following example for the vertex correction diagram given in Figure 1.1. If every line is on-shell then the corresponding reduced diagram is given in Figure 4.3. This corresponds to a pinch surface when l_3^μ is soft and leads to a soft singularity. If we now take l_2 off-shell then we get Figure 4.4 which corresponds to a pinch surface giving a collinear singularity. Finally consider taking the propagator

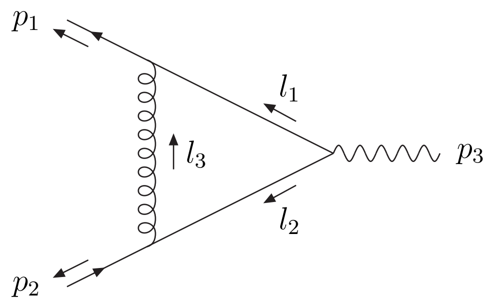

Figure 4.3: The vertex correction reduced diagram with all propagators on-shell.

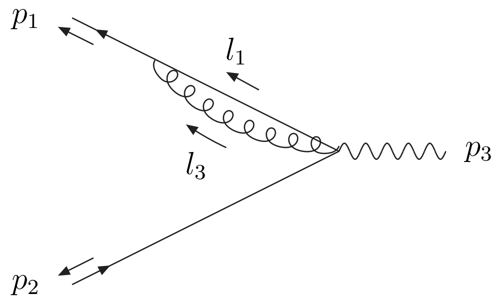

Figure 4.4: The vertex correction reduced diagram where $l_2^2 \neq 0$ and all other propagators are on-shell.

l_3 off-shell this would give the reduced diagram in Figure 4.5 this does not correspond to a pinch surface as this would then require l_1^μ and l_2^μ to be collinear to each other.

The massless limit

For massless theories such as those being discussed here there are only two possible ways for an internal line of a diagram to be on-shell, it must be collinear to some light like momentum, or it must be soft. We can classify these two types of solution in the following way. A *jet* is defined to be a set of connected massless on-shell lines i, with momentum $\{q_i^\mu\}$, which are all collinear to each other and to a light like momentum p^μ. Similarly a *soft*

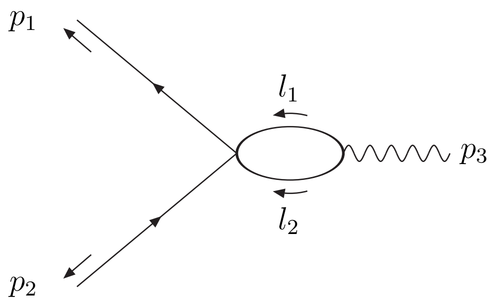

Figure 4.5: The vertex correction reduced diagram where $l_3^2 \neq 0$ and all other propagators are on-shell.

line is one whose momentum $q^\mu = 0$. A set of such lines is known as a *soft sub-diagram*, such sub-diagrams do not have to be self-connected.

Infrared power counting

Not all pinch surfaces give rise to infrared singularities, to investigate whether a particular type of pinch surface is infrared divergent we need to use power counting techniques. To do this we must first consider how the pinch surfaces of a diagram $G(\{p_e\})$ given by Eq.(4.44) behaves depending upon the momenta $\{k_i, \alpha_j\}$ internal to $G(\{p_e\})$. The pinch surfaces of G arise whenever the momenta of a line goes on-shell and is therefore either soft or collinear. This set of requirements upon the momenta of G that lead to pinch surfaces therefore forms a surface σ, in the space of all the momenta variables. We can then split the momenta on this surface into two groups. In the first group we have momenta variables that when arbitrarily altered keep G on the pinch surface. These are therefore internal variables to the momentum surface σ. The second group of momenta variables are those that when altered by even small amounts take G away from the pinch surface. These variables are therefore normal to the momentum variable surface σ. By examining how the pinch surface of G behaves when we alter the normal variables of σ close to it we can examine the behaviour of the diagram near the pinch surface. This can be done by calculating the superficial degree of infrared divergence of the *Homogeneous integral* [44, 46].

To define the Homogeneous integral we start with the general form of an amplitude G, given in Eq.(4.44). We can rewrite this as,

$$G(\{p_e\}) = \int \prod_j dl_j \int_0 \prod_i dk_i I_\sigma(k_i, l_j, p_e) \tag{4.51}$$

The l_i are the internal variables of σ and the k_i are the normal variables of σ. The 0 on the integral of k_i is to indicate we are investigating the k_i variables close to their mass-shell limit and hence to the pinch surface of G. The term I_σ contains numerators and denominators which are polynomials in the normal variables k_i. The Homogeneous integral $\overline{I}_\sigma$ is given as the limit of I_σ as the k_i go on-shell. So for example in the case of a soft limit we would take the internal loop momenta k_i as our normal variables. We would then construct the Homogeneous integral by keeping only the lowest order terms of k_i in the denominator and set powers of k_i in the numerator to zero. So a numerator factor such as $(p+k)^\mu$ would become p^μ and a denominator factor such as $(p+k)^2$ would become $p^2 + 2(pk)$.

We can then examine how G approaches its pinch surfaces by examining how the Homogeneous integral behaves when we scale k_i. So we rewrite the Homogeneous integral as [44],

$$\begin{aligned}
\overline{G}(\{p_e\}) &= \int \prod_j dl_j \int_0 \prod_i dk_i \overline{I}_\sigma(k_i, l_j, p_e) \\
&= \int \prod_j dl_j \int_0^\infty d\lambda^2 \int_0 \prod_i dk_i \delta\left(\lambda^2 - \sum_i |k_i|^2\right) \overline{I}_\sigma(k_i, l_j, p_e) \\
&= 2\int \prod_j dl_j \int_0^\infty d\lambda \lambda^{\mu(\sigma)-1} \int_0 \prod_i dk'_i \delta\left(1 - \sum_i |k'_i|^2\right) \overline{I}_\sigma(k'_i, l_j, p_e)
\end{aligned} \tag{4.52}$$

Where $\mu(\sigma)$ is known as the superficial degree of infrared divergence and $k'_i = k_i/\lambda$. If $\mu(\sigma) > 0$ then we expect the amplitude to be infrared finite. The form of $\mu(\sigma)$ can be derived using power-counting techniques similar to those used for UV divergences [44]. For a diagram to be infrared finite we then assume that we need only show that at each possible pinch surface the superficial degree of divergence calculated using powercounting techniques is greater than zero.

4.3.3 The asymptotic Lagrangian

The soft-hard splitting requirements

Before we go further we need to define how we split the soft and hard regions up between $\mathcal{L}_{IR}$ and $\mathcal{L}_{hard}$. To do this we will use the knowledge derived in the last section from the use of the Landau equations to examine the soft and collinear regions in covariant diagrams. We will want to define two functions $f_s(\{p_i\};\Delta)$ and $f_h(\{p_i\};\Delta)$ connected via,

$$f_h(\{p_i\};\Delta) = 1 - f_s(\{p_i\};\Delta) \tag{4.53}$$

where $\{p_i\}$ are the momenta of the legs attached to the vertex. The requirements we will want are the same as those given in Section 4.2.1 except that all the three-momenta in the $f_{s/h}$ are replaced with four-momenta so that they are completely covariant. Again we will also only consider three-point vertices.

Defining the form of f_s and f_h

The simplest form for f_s that satisfies all the above requirements is given by,

$$f_s(p_1,p_2,p_3;\Delta) = \exp\left(-\frac{1}{\Delta}\left(p_1^2+p_2^2+p_3^2\right)\right) \tag{4.54}$$

this is defined with all the four-momenta p_i in Euclidean space.

We now proceed to confirm that this form for f_s successfully satisfies all the requirements of Section 4.2.1. Firstly it is symmetric and even in all of its arguments. We can only get soft or collinear singularities when all the lines entering a vertex are on-shell (see the next subsection). Immediately we can see from the definition in Eq.(4.54) that when all of the p_i go on-shell that f_s gives one, as expected.

Now we need only check the UV limits. Taking the limit $p_1 \to \pm\infty$ we get,

$$0 \times \exp\left(-\frac{1}{\Delta}\left(p_2^2 + p_3^2\right)\right) \tag{4.55}$$

and immediately see that f_s vanishes. This form for f_s therefore correctly satisfactorily separates the soft and hard regions.

Checking the infrared finiteness of the completely hard amplitude

From the definitions of f_h and f_s above we can now define a *hard* vertex to be a vertex such that at least one of its attached legs is off-shell. A *soft* vertex is then defined to be a vertex where all the attached legs are on-shell. In the asymptotic interaction picture, amplitudes will be calculated from Feynman diagrams which consist entirely of hard vertices, Eq.(4.43). With our definitions of hard vertices we want to guarantee that such a diagram is in fact free of any infrared singularities. We can prove this is true in the following way.

We will consider any field theory which contains scalar, boson or fermion lines and also contains a three-point vertex, for example ϕ^3 scalar theory or QCD. We will only consider the possible infrared divergences coming from the three-point vertex, it should be possible to treat four-point vertices in the same way. Each hard vertex consists of a normal vertex factor from the interaction Lagrangian multiplied by an f_h factor as defined in Eq.(4.53). We will begin by consider an arbitrary graph with n vertices and we will place all of its internal lines on-shell. Such a diagram can only give infrared singularities if it corresponds to a pinch surface. If it is a pinch surface the amplitude will still be finite because each vertex is a hard vertex and therefore the properties of f_h mean that such a diagram will be zero. We will now consider taking the lines of this diagram off-shell one by one. We are therefore considering all the possible reduced diagrams of the original Feynman diagram.

Any hard vertex factors multiplying the vertices attached to an off-shell line can no longer set the graph to zero as they contain an off-shell momenta. If this reduced diagram corresponds to a pinch surface then there is a possibility that this diagram is infrared divergent. All the remaining hard three-point vertices factors in the reduced diagram though will still be enough to keep the resulting reduced diagram infrared finite. We now proceed to take one line connected to each hard vertex off-shell. The resulting reduced diagram no longer contains any hard vertices and so if it corresponds to a pinch surface it could be infrared divergent as there are no f_h factors to set it to zero. This should represent the worst case for the appearance of infrared divergences. If we were to take any further lines off-shell we should be reducing the possible infra-red divergences.

When we take a line off-shell we combine two vertices together in the corresponding reduced diagram. Each vertex started off with a hard vertex factor attached which will now have been removed. In this reduced diagram therefore we have contracted one of the lines connected to each vertex so that we are left with just four-point and higher vertices. This also means that those vertices which were originally connected to an external line can now be connected to two or more external lines. At each vertex we have four-momentum conservation. Therefore when we have l external momenta p_i attached to the vertex and m internal momenta k_j attached to the vertex we will have,

$$\delta^{(4)}\left(\sum_i p_i + \sum_j k_j\right) \Rightarrow \sum_i p_i + \sum_j k_j = 0 \tag{4.56}$$

The internal lines of reduced diagrams can only be on-shell and therefore must be either jets or soft subdiagrams.

In the case when all the internal lines connected to the vertex are soft then $\sum_j k_j = 0$, and so we will require $\sum_i p_i = 0$ at the vertex. Now none of the external lines are soft and so this could only be true for $i \geq 2$ but we are only considering nonexceptional diagrams so we have,

$$\left(\sum_i p_i\right)^2 \neq 0 \tag{4.57}$$

Therefore we cannot conserve four-momentum at this vertex and hence any such diagram will not be a pinch surface. The only exception to this is in the case when all the external lines are connected to a single vertex in the reduced diagram. In this case $\sum_l p_l = 0$ is true and the reduced diagram will be a pinch surface. If all the four-momenta are Euclidean then this will be the only pinch surface we need to consider. The general form of such a reduced diagram is shown in Figure 4.6. The proof that such a general

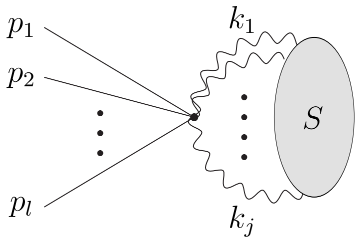

Figure 4.6: The general reduced diagram when we have Euclidean four-momenta after all the hard vertex factors have been removed. We are left with only a soft subdiagram S connected by the soft k_j lines to the external lines at a single vertex.

reduced diagram is infrared finite is the same as that given in [44] for the specific case of four-point and higher vertices only.

More generally we can consider four-vectors in Minkowski space, we will then have reduced diagrams with internal jets. Taking this into account we will now consider what type of vertices we can have external lines connected to. If all the external lines are connected to the same vertex then we can clearly have no internal jets as the only lines that could be connected to this vertex and make it a pinch surface would be a soft loop subdiagram, which we have already considered above. Next we have vertices with more than one external line but not all external lines connected to them. There must be at least two internal jets connected to each such vertex because four-momentum conservation means that $\sum_j k_j = -\sum_i p_i$ but in this case,

$$\left(\sum_i p_i\right)^2 \neq 0 \tag{4.58}$$

therefore,

$$\left(\sum_j k_j\right)^2 \neq 0 \tag{4.59}$$

and so we cannot have a single jet. We can also have as many soft lines connected to these vertices as we want but there must always be at least two internal jets. The only other case is when only a single external line connects to the vertex. Here we must have at least one jet attached to the vertex and we can have as many soft lines as we want.

In general therefore we will get reduced diagrams in which every internal vertex must be connected to at least two jets. We will get soft loops formed whenever a loop exists in the diagram with at least one soft line. Finally different jets can only be connected to each other by vertices that have at least three jets connected and we can have no disconnected internal jets.

Powercounting including jets

We will be considering a theory that contains no numerator factors as this would increase the superficial degree of divergence of the reduced diagram. Therefore we are considering the worst possible case for the appearance of infrared singularities. The contributions to the superficial degree of divergence of the general reduced diagram will come from the L_i soft loops which will contribute $+4$, the L_j collinear loops which will contribute $+2$, the I_i internal soft lines which contribute -2 and the I_j collinear lines in each jet loop which contribute -1. Soft loops contribute $+4$ to the superficial degree of divergence because all four components of each loop momentum are normal coordinates to the pinch surface. For the case of collinear loops though only two of the loop momenta are normal coordinates to the pinch surface and so only contribute +2 to the superficial degree of divergence. We will consider the general reduced diagrams generated by contracting all the hard vertices, these are not necessarily pinch surfaces but we need only prove that all such reduced diagrams have a positive degree of superficial divergence.

Initially we will consider the case where we have a reduced diagram made up of only four-point composite vertices as this should represent the worst case we will encounter. In general we could also have five-point and higher vertices in the reduced diagram. When we take more than one line attached to each hard vertex off-shell there will also be the possibility of three-point vertices. In these cases though we would have needed to take further lines off-shell from a reduced diagram which already consists of four-point or higher composite vertices and so diagrams containing such vertices should contain fewer infrared divergences. With this restriction we see that vertices connected to three external lines cannot exist. We must have two jets attached to any vertex connected to two external lines, as shown in Figure 4.7(a). Vertices connected to only a single external line must have either one internal jet or three internal jets attached to the vertex. This is because we require,

$$p^2 = (k_1 + k_2 + k_3)^2 = 0 \Rightarrow k_1 k_2 + k_1 k_3 + k_2 k_3 = 0 \qquad (4.60)$$

If k_1 is a soft momenta then this becomes $k_2 k_3 = 0$ and so one of the other momenta must be soft or the two must be collinear. In either case we are left with just a single jet. The four different types of vertex coming from this are shown in Figure 4.7(b)-(e).

We will now consider the different types of vertices that can appear inside the reduced diagrams. These consist of three groups, the first are vertices where every line attached is part of a separate jet or is soft, these will have the same form as the external vertices in Figure 4.7(a),(c) and (e). The second type is when two of the lines form a jet and the other two lines either form a second jet or one of the remaining lines is soft and the other is a jet, this has the same form as Figure 4.7(b). Finally the third kind of vertex is when three lines form a jet, the remaining line must then also be a jet, this has the same form as Figure 4.7(d). This third kind of vertex will only appear

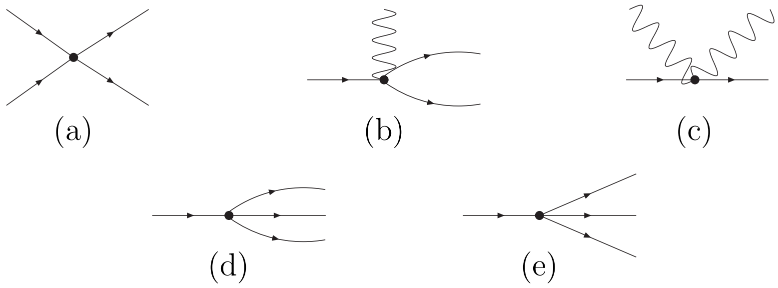

Figure 4.7: The different types of external vertex, the external lines are on the LHS of the vertex and the internal lines of the RHS. The internal lines of (b) and (d) form a single jet whilst the three internal lines of (e) form three separate jets.

inside jets whereas the first two kinds can form soft loops as well.

For reduced diagrams of this type we have the following powercounting,

$$\mu = \mu(S) + \mu(C) = 4L_i - 2I_i + 2L_j - N_j - N_i \tag{4.61}$$

where N_j is the number of internal lines inside collinear loops and N_i is the number of internal collinear lines that are part of soft loops. We can separate the contribution of the soft subdiagram from the collinear loops and calculate its powercounting separately.

We have $L_i = I_i + N_i - (V_1 + V_2 - 1)$, where V_1 is the number of vertices inside the soft subdiagram and V_2 is the number of vertices connected to both soft and collinear lines. Using this gives,

$$\mu(S) = 4L_i - 2I_i = 4 + 4N_i + 2I_i - 4(V_1 + V_2) \tag{4.62}$$

Now the number of vertices internal to the soft subdiagram is given by $4V_1 = 2I + b_i$, where I is the number of soft lines internal to the soft subdiagram, b_i is the number of soft lines connecting the soft subdiagram to the jets and $I + b_i = I_i$. So this then leads to,

$$\mu(S) = 4(1 + N_i - V_2) + 2(I + b_i) - 2I - b_i = 4L_2 + b_i = b_i \tag{4.63}$$

Here $L_2 = N_i - (V_2 - 1) = 0$ as there are no collinear loops in the soft subdiagram.

The total powercounting for the reduced diagram now becomes,

$$\mu = 2L_j - N_j - N_i + b_i = 2L_j - I_j + b_i \tag{4.64}$$

where I_j is the total number of collinear lines inside loops in the diagram. Now again $L_j = I_j + N - (V - 1)$, where N is the number of internal collinear lines that were not part of any soft or collinear loops and V is the number of vertices in the remainder of the diagram once we have removed the soft subdiagram. This then gives us,

$$\mu = 2 + I_j + 2N - 2V + b_i \tag{4.65}$$

The number of vertices in the diagram is related to the number of lines via $4nV = 2I_j + 2N + e + b_i$, where e is the number of external lines attached to the reduced diagram and $n = 1$ in the case of just four-point vertices. Using this we now have,

$$\begin{aligned} \mu &= 2 + \left(1 - \frac{1}{n}\right) I_j + \left(2 - \frac{1}{n}\right) N + \left(1 - \frac{1}{2n}\right) b_i - \frac{e}{2n} \\ &= 2 + N + \frac{b_i}{2} - \frac{e}{2} \end{aligned} \tag{4.66}$$

Here we have set $n = 1$ in the last step.

For this to be less than or equal to zero we will need $N = 0$ and $(e/2) \geq (b_i/2) + 2$. Now there are only five different types of vertex that are connected to external lines, these are shown in Figure 4.7. Of these (b) and (c) will always have at least as many soft lines attached as external lines and so $b_i \geq e_b + e_c$, where the e_i are the number of external lines attached to vertices of type (i).

For the vertex (a) to be part of a divergent reduced diagram it must be attached to some internal loops. Therefore both internal legs must be connected to either an internal vertex which is attached to collinear loops only or to vertices which have soft lines attached. If the vertices which have soft lines attached in the second case are internal vertices then we will have $b_i \geq e_a$. If instead they are both external vertices then the worst case is when both of these external vertices are of type (b). For this to be the case though we must have at least two other internal vertices which are connected to soft lines and therefore in this case $b_i \geq e_a$ also.

If the internal lines of vertex (a) are attached to collinear loops then we see that this means that the only internal vertex it can attach to without a soft line being present is when we have three collinear lines coming out of the internal vertex in either a single jet or as three separate jets. In the case of a single jet though we cannot form any soft loops and so the line connecting vertex (a) to this internal vertex must contribute +1 as $N = 1$. Therefore $\mu > 0$ in this case also. If we get three separate jets then at least two of these must connect to internal vertices as we have no external vertex connected to three external lines. Therefore these must either connect to vertices with soft lines attached in which case we will get $b_i \geq e_a$ or they only attach to collinear vertices in which case there are no soft loops and $N \geq 1$. So again $\mu > 0$.

If we have external vertices of type (e) then the discussion above again applies. Except in this case there is only a single external line attached, therefore it is quicker to see that diagrams containing it will have $2N+b_i \geq e$.

Finally if we have external vertices of type (d) then we see that jets formed from these vertices can only be attached to other jets via a single line. So if no soft vertices are emitted the last vertex in the jet must have three lines collinear to each other entering the vertex and one line exiting. Otherwise we must attach soft lines to the jet in which case $b_i \geq e_d$. If no soft lines are attached then we can see that we will get a diagram of the form shown in Figure 4.8. Now the only way to produce such a reduced diagram is if the original diagram was not an amputated diagram. We are only interested in amputated diagrams so we can never get such a reduced diagram.

From this discussion we see that we will always have $2N + b_i \geq e$ and therefore any pinch surfaces coming from these reduced diagrams will be infrared finite. Initially we only consider the case with four-point composite vertices. In general though we will have five and higher point vertices. In

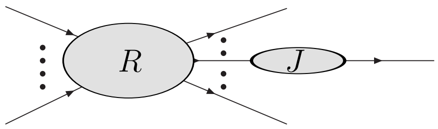

Figure 4.8: A non-amputated reduced diagram, where R represents the reduced diagram and J represents the collinear loops inside the non-amputated jet.

this case n in Eq.(4.66) will be greater than one and so Eq.(4.66) will be more positive as we get a $1-(1/n)$ contribution from each internal line and hence $\mu > 0$ for any number of external lines.

We only have the general reduced diagrams of the types discussed here to consider and so we have proved that $\mu > 0$ for all the possible pinch surfaces of the reduced diagrams generated from taking propagators off-shell in the amplitudes given by Eq.(4.53). As these were the only reduced diagrams which could give pinch surfaces we have therefore proved that Feynman diagrams of any quantum field theory with a three point vertex and made up entirely of hard vertices as defined by f_h in Eq.(4.53) are always infrared finite.

4.3.4 The asymptotic fields

We will now consider the calculation of the physical S_A-Matrix elements on the asymptotic fields. To do this we will produce a heuristic derivation of a modified LSZ reduction formula. For simplicity we will do this for a scalar theory but the extension to fermions and vectors should proceed as in the usual derivation.

The asymptotic condition

The adiabatic assumption asserts that as $t \to \pm\infty$ we have the following weak operator limit result,

$$\psi(x) \to Z_{asym}^{1/2} \phi_{asym}(x) \tag{4.67}$$

where $Z_{asym}^{1/2}$ relates the fields of the full theory ψ to the asymptotic fields $\phi_{asym}(x)$, defined by $\mathcal{L}_{asym}$. Now it is usual to take the asymptotic field ϕ_{asym} to be the free field $\phi(x)$, when this is done though we will usually get infrared divergences in the associated renormalisation factor $Z_0^{1/2}$. We also known that amplitudes calculated on the asymptotic states in the asymptotic interaction picture should be free of such divergences and are also equivalent (after we have regularised the IR divergences) to amplitudes calculated on the free fields in the interaction picture. We therefore assume that we can relate the free fields ϕ to our asymptotic fields Ξ in a weak limit at asymptotic times via a factor Y,

$$\psi(x) \to Z_0^{1/2}\phi(x) \equiv Z_{asym}^{1/2}\Xi(x) \equiv Z_{asym}^{1/2}Y^{1/2}\phi(x) \tag{4.68}$$

Hence we assume that at asymptotic times,

$$\Xi(x) \equiv Y^{1/2}\phi(x) \tag{4.69}$$

This factor Y must contain all the dependence on the infrared region of the theory and therefore any potential IR divergences making it ill-defined.

Defining the asymptotic fields

First we must define the asymptotic field operator, this is given in general by,

$$\begin{aligned}\Xi(t,\vec{x}) &= U_\Delta^\dagger(t,t_0)\phi(t,\vec{x})U_\Delta(t,t_0) \\ &= \int \frac{d^3k}{(2\pi)^3 2\omega_k}\Big(U_\Delta^\dagger(t,t_0)a(t,\vec{k})U_\Delta(t,t_0)e^{i\vec{k}\vec{x}} \\ &\quad +U_\Delta^\dagger(t,t_0)a^\dagger(t,\vec{k})U_\Delta(t,t_0)e^{-i\vec{k}\vec{x}}\Big)\end{aligned} \tag{4.70}$$

where,

$$U_\Delta(t,t_0) = e^{iH_0(t-t_0)}e^{-iH_\Delta(t-t_0)} \tag{4.71}$$

The conjugate momentum is then given by,

$$\begin{aligned}\pi_\Xi(t,\vec{x}) = \partial_0\Xi(t,\vec{x}) &= \partial_0\left(U_\Delta^\dagger(t,t_0)\phi(t,\vec{x})U_\Delta(t,t_0)\right)\\ &= \int\frac{d^3k}{(2\pi)^3 2\omega_k}\partial_0\Big(U_\Delta^\dagger(t,t_0)a(t,\vec{k})U_\Delta(t,t_0)e^{i\vec{k}\vec{x}}\\ &\quad +U_\Delta^\dagger(t,t_0)a^\dagger(t,\vec{k})U_\Delta(t,t_0)e^{-i\vec{k}\vec{x}}\Big) \qquad (4.72)\end{aligned}$$

The field operator Eq.(4.70) and Eq.(4.72) satisfy the usual equal time commutation relations,

$$[\Xi(t,\vec{x}),\pi_\Xi(t,\vec{y})] = i\delta(\vec{x}-\vec{y}) \qquad (4.73)$$

Next we define $a_a^\dagger(t,\vec{k})$ and $a_a(t,\vec{k})$ as asymptotic creation and destruction operators respectively and E_k as the asymptotic field energy. The destruction operators are defined such that they give zero when acting on the vacuum at asymptotic times,

$$\lim_{t\to\infty}\langle\Omega'|a_a^\dagger(t,\vec{k}) = 0 \text{ and } \lim_{t\to-\infty}a_a(t,\vec{k})|\Omega'\rangle = 0 \qquad (4.74)$$

where $|\Omega'\rangle$ is the asymptotic vacuum. Also when the creation operator acts on the vacuum at asymptotic times it creates a "one-particle" asymptotic state,

$$\lim_{t\to-\infty}a_a^\dagger(t,\vec{k})|\Omega'\rangle = \lim_{t\to-\infty}|\Xi(t,\vec{k})\rangle = |\Xi_{in}(\vec{k})\rangle \qquad (4.75)$$

They satisfy the following equal time commutation relations,

$$\begin{gathered}\left[a_a(t,\vec{k}),a_a^\dagger(t,\vec{k}')\right] = 2E_k(2\pi)^3\delta(\vec{k}-\vec{k}')\\ \left[a_a(t,\vec{k}),a_a(t,\vec{k}')\right] = 0\ ,\quad \left[a_a^\dagger(t,\vec{k}),a_a^\dagger(t,\vec{k}')\right] = 0\end{gathered} \qquad (4.76)$$

We can also construct in the asymptotic limit an operator H'_A from these creation and destruction operators. This is defined as,

$$H'_A = \int\frac{d^3k}{(2\pi)^3 2E_k}E_k a_a^\dagger(t,\vec{k})a_a(t,\vec{k}) \qquad (4.77)$$

This has the same form as the free Hamiltonian constructed from a and $a^\dagger$ operators and correspond to the Hamiltonian of the asymptotic field when $t \to \pm\infty$[2]. So we have,

$$\lim_{t\to\pm\infty} H'_A|p\rangle = E_p|p\rangle \tag{4.78}$$

Using the asymptotic limit Eq.(4.69) then the $t \to \pm\infty$ limit of the asymptotic creation and destruction operators becomes,

$$U_A^\dagger(t,t_0)a(t,\vec{x})U_A(t,t_0) \to Y^{1/2}a(t,\vec{x}) \tag{4.79}$$

Therefore Eq.(4.70) can be written at asymptotic times as,

$$\Xi(t,\vec{x}) = \int \frac{d^3k}{(2\pi)^3 2E_k}\left(a_a(t,\vec{k})e^{i\vec{k}\vec{x}} + a_a^\dagger(t,\vec{k})e^{-i\vec{k}\vec{x}}\right) \tag{4.80}$$

where $E_k = Y^{-1}\omega_k$ and $a_a(t,\vec{k}) = Y^{-1/2}a(t,\vec{k})$, we will justify both of these statements in the next subsection. The conjugate momenta for the field in Eq.(4.80) at asymptotic times is given by,

$$\begin{aligned}
\pi_\Xi(t,\vec{x}) &= \int \frac{d^3k}{(2\pi)^3 2E_k}\left(\partial_0 a_a(t,\vec{k})e^{i\vec{k}\vec{x}} + \partial_0 a_a^\dagger(t,\vec{k})e^{-i\vec{k}\vec{x}}\right) \\
&= i\int \frac{d^3k}{(2\pi)^3 2E_k}\left(\left[H_A, a_a(t,\vec{k})\right]e^{i\vec{k}\vec{x}} + \left[H_A, a_a^\dagger(t,\vec{k})\right]e^{-i\vec{k}\vec{x}}\right) \\
&= -i\int \frac{d^3k}{(2\pi)^3 2E_k}E_k\left(a_a(t,\vec{k})e^{i\vec{k}\vec{x}} - a_a^\dagger(t,\vec{k})e^{-i\vec{k}\vec{x}}\right)
\end{aligned} \tag{4.81}$$

where we assume $H_A \to H'_A$ in the asymptotic limit. These solutions of the field operator Eq.(4.80) and conjugate momenta Eq.(4.81) satisfy the usual equal time commutation relations,

$$[\Xi(t,\vec{x}), \pi_\Xi(t,\vec{y})] = i\delta(\vec{x}-\vec{y}) \tag{4.82}$$

[2]We assume here that the solution of the asymptotic field Ξ means that we can treat any interaction terms as vanishing safely at asymptotic times without introducing any infrared singularities

From Eq.(4.80) and Eq.(4.81) we can then derive in the asymptotic limit,

$$\begin{aligned} a_a(t,\vec{k}) &= \int d^3x e^{-i\vec{k}\vec{x}}(E_k\Xi(t,\vec{x})+i\pi_\Xi(t,\vec{x})) \\ a_a^\dagger(t,\vec{k}) &= \int d^3x e^{i\vec{k}\vec{x}}(E_k\Xi(t,\vec{x})-i\pi_\Xi(t,\vec{x})) \end{aligned} \tag{4.83}$$

The asymptotic states

Using the asymptotic weak operator limit Eq.(4.69) we will now investigate the structure of the asymptotic states in the asymptotic limit in more detail. Eq.(4.80) in this limit is related to the free field as,

$$\Xi = Y^{1/2}\phi \Rightarrow \int \frac{d^3k}{(2\pi)^3(2E_k)}a_a^\dagger(t,\vec{k}) = \int \frac{d^3k}{(2\pi)^3(2w_k)}Y^{1/2}a^\dagger(t,\vec{k}) \tag{4.84}$$

therefore,

$$a_a^\dagger(t,\vec{k}) = \frac{E_k}{w_k}Y^{1/2}a^\dagger(t,\vec{k}) \tag{4.85}$$

Using this we can then investigate the four-momenta of the asymptotic state. We take the operator [1],

$$P_a^\mu = \int \frac{d^3k}{(2\pi)^3 2E_k}k^\mu a_a^\dagger(t,\vec{k})a_a(t,\vec{k}) \tag{4.86}$$

which measures the four-momentum of an asymptotic state in the asymptotic limit. We require that,

$$P_a^\mu|p\rangle = p_a^\mu|p\rangle \tag{4.87}$$

if we now use Eq.(4.86) and Eq.(4.85) in this we get,

$$\begin{aligned} &\int \frac{d^3k}{(2\pi)^3 2E_k}k^\mu a_a^\dagger(t,\vec{k})a_a(t,\vec{k})a_a(t,\vec{p})|0\rangle \\ &= \int \frac{d^3k}{(2\pi)^3 2E_k}k^\mu \frac{E_kE_p}{\omega_k\omega_p}Y^{1/2}Y^{1/2}2\omega_k\delta(\vec{p}-\vec{k})a_a(t,\vec{k})|0\rangle \end{aligned}$$

$$= \quad p_a^\mu \frac{E_p}{\omega_p} Y|p\rangle \tag{4.88}$$

where we have $p_a^\mu = (E_p, \vec{p})$. We can relate this result to Eq.(4.87) to get,

$$p_a^\mu = p_a^\mu \frac{E_p}{\omega_p} Y \Rightarrow E_p = \omega_p Y^{-1} \tag{4.89}$$

So we get the usual free field energy multiplied by a factor. From this we see that the operator H'_A is related to the Hamiltonian of the free fields by,

$$H'_A \quad \rightarrow \quad Y^{-1} H_0 \tag{4.90}$$

For the three momentum we have,

$$\begin{aligned} P'^i_A \quad &\rightarrow \quad \int \frac{d^3k}{(2\pi)^3 2w_k} k^i \left(Y \frac{E_k}{\omega_k} \right)^2 a^\dagger(t, \vec{k}) a(t, \vec{k}) \\ &= \quad \int \frac{d^3k}{(2\pi)^3 2w_k} k^i a^\dagger(t, \vec{k}) a(t, \vec{k}) = P_0^i \end{aligned} \tag{4.91}$$

where P_0^i is the free field three-momentum operator. So at asymptotic times the three momentum remains the same as in the free case. Finally we can use these results to simplify Eq.(4.85),

$$a_a^\dagger(t, \vec{k}) = Y^{-\frac{1}{2}} a^\dagger(t, \vec{k}) \tag{4.92}$$

We will see in Section 4.3.5 that Y is related to the propagator of the asymptotic fields.

From this discussion we can interpret this result as telling us that an asymptotic state is one in which the three-momentum of the state remains the same as a free state whilst the energy of the state is altered from the usual free field result by a factor depending upon the soft and collinear contributions to the asymptotic propagator. The factor Y is a c-number and so the asymptotic states behave in the same way as free states apart from this extra factor. We should therefore be able to interpret such states in a similar way to the free states, this includes importantly a modified LSZ formalism.

As stated in Section 4.2.1 our split of the hard and soft regions of the Lagrangian does not give us the actual asymptotic Lagrangian of the fields of the system. The true asymptotic Lagrangian comes from taking explicitly the limit $t \to \pm\infty$ of the full Lagrangian. Our asymptotic Lagrangian differs by a finite amount from the real asymptotic Lagrangian. The asymptotic states defined above come form our $\mathcal{L}_{asym}$ and therefore the parameter Δ contained in our asymptotic Lagrangian will become part of the definition of our asymptotic states. This dependence appears in the factor Y in the relations above. The question now is how are such states related to the states measured in an experimental situation.

We suspect that the amplitudes themselves may be independent of Δ. We can see this by investigating the matrix elements in the asymptotic interaction picture. Now we have,

$$\langle \Xi_\beta(\Delta)|S_A(\Delta)|\Xi_\alpha(\Delta)\rangle \tag{4.93}$$

where we have written the explicit dependence on Δ of all the quantities. We are free though to pick any Δ and so we could equally as well have written,

$$\begin{aligned}\langle \Xi_\beta(2\Delta)|S_A(2\Delta)|\Xi_\alpha(2\Delta)\rangle &= \langle \Xi_\beta(\Delta)|\Omega_d^{(-)\dagger}\Omega_d^{(-)}S_A(\Delta)\Omega_d^{(-)\dagger}\Omega_d^{(-)}|\Xi_\alpha(\Delta)\rangle \\ &= \langle \Xi_\beta(\Delta)|S_A(\Delta)|\Xi_\alpha(\Delta)\rangle \end{aligned}\tag{4.94}$$

where $\Omega_d^{(-)}$ is a unitary operator relating the two pictures. We know $\Omega_d^{(-)}$ is a unitary operator because the two different pictures should only differ by a finite amount. From this we see that the two results are the same, this suggests that the amplitudes are therefore independent of our choice of Δ. In explicit calculations though this Δ independence may not hold because as we will see in Section 4.3.5, we cannot calculate the asymptotic propagators to all orders and instead we can only define them perturbatively. This may produce a dependence on Δ in the amplitudes which is related to the order in the perturbation series to which we calculated to.

The use of these states instead of the usual free states also suggests that the physical observable definitions, such as those in Eq.(1.1), may also have to be altered to match how these states behave. Of course the usual choice of

H_0 states asymptotically is also not the same as the true asymptotic states and so this problem is not unique to the asymptotic interaction picture. The form of any such alterations and a deeper understanding of the form of these states is left to future work.

The modified LSZ reduction formula

Now that we have some understanding of the asymptotic states let us give the outline for a modified LSZ reduction formula, this will allow us to relate the time ordered correlation functions of Eq.(4.39) to S_A-Matrix elements calculated on the asymptotic states. As in the standard case we start by extracting an asymptotic creation operator from the initial state,

$$\begin{aligned} \mathcal{A} &= {}_{out}\langle p_1, ..., p_n | q_1, ..., q_m \rangle_{in} \\ &= \lim_{q_1^0 \to -\infty} {}_{out}\langle p_1, ..., p_n | a_{in}^\dagger(q_1) | q_2, ..., q_m \rangle_{in} \end{aligned} \tag{4.95}$$

where $a_{in}^\dagger$ is an asymptotic creation operator $a_a^\dagger$. Now we rewrite the creation operator as an asymptotic *in* field in the usual way using Eq.(4.83),

$$\begin{aligned} &\lim_{q_1^0 \to -\infty} {}_{out}\langle p_1, ..., p_n | a_{in}^\dagger(q_1) | q_2, ..., q_m \rangle_{in} \\ &= \lim_{t \to -\infty} \int d^3x e^{i\vec{q}_1\vec{x}} \langle p_1, ..., p_n | E_{q_1} \Xi_{in}(t, \vec{x}) - i\pi_\Xi(t, \vec{x}) | q_2, ..., q_m \rangle \end{aligned} \tag{4.96}$$

where we have dropped the *in* and *out* labels from the *in* and *out* states. At $t \to -\infty$ we have,

$$\Xi_{in} = Z_{asym}^{-1/2}\psi, \;\; \phi = Z_0^{-1/2}\psi \tag{4.97}$$

Also in the asymptotic limit the real asymptotic Hamiltonian approaches the operator H_A' which in turn is related to the free Hamiltonian by Eq.(4.90),

$$H_A \to H_A' = Y^{-1} H_0 \tag{4.98}$$

Using this we can rewrite the Heisenberg picture operators $\Xi(t,\vec{x})$ and $\pi_\Xi(t,\vec{x})$ in the asymptotic limit as,

$$\begin{aligned}\lim_{t\to-\infty}\Xi(t,\vec{x}) &\to \int\frac{d^3k}{(2\pi)^3 2\omega_k}Y^{1/2}\left(a(0,\vec{k})e^{i\vec{k}\vec{x}}+a^\dagger(0,\vec{k})e^{-i\vec{k}\vec{x}}\right)\\ &= Y^{1/2}\phi(t,\vec{x})\\ \lim_{t\to-\infty}\pi_\Xi(t,\vec{x}) &\to -i\int\frac{d^3k}{(2\pi)^3 2\omega_k}Y^{-1/2}\omega_k\left(a(0,\vec{k})e^{i\vec{k}\vec{x}}-a^\dagger(0,\vec{k})e^{-i\vec{k}\vec{x}}\right)\\ &= Y^{-1/2}\pi_\phi(t,\vec{x}) \end{aligned} \tag{4.99}$$

Then in the asymptotic limit we have,

$$\begin{aligned} iE_k\Xi(t,\vec{x})+\pi_\Xi(t,\vec{x}) &= Y^{-\frac{1}{2}}\left(i\omega_k\phi(t,\vec{x})+\pi_\phi(t,\vec{x})\right)\\ &= iY^{-\frac{1}{2}}\left(e^{-ik_0t}\overleftrightarrow{\partial_0}\,\phi(t,\vec{x})\right)\\ &= iZ_0^{-\frac{1}{2}}Y^{-\frac{1}{2}}\left(e^{-ik_0t}\overleftrightarrow{\partial_0}\,\psi(t,\vec{x})\right) \end{aligned} \tag{4.100}$$

So Eq.(4.96) becomes,

$$\lim_{t\to-\infty}(-i)Z_{asym}^{-1/2}Y^{-1}\int d^3x e^{iq_1x}\overleftrightarrow{\partial_0}\,\langle p_1,...,p_n|\psi(t,\vec{x})|q_2,...,q_m\rangle \tag{4.101}$$

Now as usual we add and subtract the following term,

$$\lim_{t\to\infty}\;{}_{out}\langle p_1,...,p_n|a^\dagger_{out}(q_1)|q_2,...,q_m\rangle_{in} \tag{4.102}$$

So that we can write Eq.(4.101) as,

$$iZ_{asym}^{-1/2}Y^{-1}\int d^4x\partial_0\left(e^{-iq_1x}\overleftrightarrow{\partial_0}\,\langle p_1,...,p_n|\psi(t,\vec{x})|q_2,...,q_m\rangle\right) \tag{4.103}$$

after we have used,

$$\left(\lim_{t\to\infty}-\lim_{t\to-\infty}\right)\int d^3xF(x,t)=\lim_{t_f\to\infty,t_i\to-\infty}\int_{t_i}^{t_f}dt\frac{\partial}{\partial t}\int d^3xF(x,t) \tag{4.104}$$

We have dropped any terms that correspond to disconnected pieces and hence give no contribution to the scattering. Next we rewrite Eq.(4.103) as,

$$iZ_{asym}^{-1/2}Y^{-1}\int d^4x\langle p_1,...,p_n|e^{-iq_1x}\left(\partial_0^2\psi(t,\vec{x})\right)-\left(\partial_0^2e^{-iq_1x}\right)\psi(t,\vec{x})|q_2,...,q_m\rangle \tag{4.105}$$

Now we know that,

$$\Box_x e^{-iq_1x}=0 \tag{4.106}$$

So this then leads to,

$$\begin{aligned} iZ_{asym}^{-1/2}Y^{-1}\int d^4x\langle p_1,...,p_n|-\left(\nabla e^{-iq_1x}\right)\psi(t,\vec{x}) \\ +e^{-iq_1x}\left(\partial_0^2\psi(t,\vec{x})\right)|q_2,...,q_m\rangle \end{aligned} \tag{4.107}$$

After we have use integration by parts to swap the space integrals in the first term this becomes,

$$iZ_{asym}^{-1/2}Y^{-1}\int d^4xe^{-iq_1x}\langle p_1,...,p_n|\Box_x\psi(t,\vec{x})|q_2,...,q_m\rangle \tag{4.108}$$

with $q_1=(\omega_{q_1},\vec{q}_1)$. We can then go on as in the usual LSZ reduction formula to extract all the in and out states to get,

$$\begin{aligned} {}_{out}\langle p_1,...,p_n|q_1,...,q_m\rangle_{in} \equiv\ & (iZ_{asym}Y^2)^{-\frac{n+m}{2}}\int d^4x_1...d^4x_nd^4y_1...d^4y_m \\ & e^{i\sum p_i.y_i}e^{-i\sum q_i.x_i}\times\Box_{y_1}...\Box_{y_n}\Box_{x_1}...\Box_{x_m} \\ & \times\langle 0|T\{\psi(y_1)...\psi(y_n)\psi(x_1)...\psi(x_m)\}|0\rangle \end{aligned} \tag{4.109}$$

From this we can see that the S_A-Matrix elements are given by the residue of the pole when all the external legs go on-shell as in the free field case. We have though as well as just the usual inverse free field propagator an extra factor Y for each external leg, which we will see cancels a similar factor in the external leg propagators exactly. This result can be extended to include spinor and vector fields in the usual way. So we can relate the correlation functions of Eq.(4.39) to S_A-Matrix elements calculated on the asymptotic states.

4.3.5 Calculating amplitudes

Wicks theorem

We now wish to calculate the amplitudes generated by Eq.(4.43). These consist of time ordered products of asymptotic fields multiplied by hard vertex factors,

$$\langle 0|\Xi(x_1)\Xi(x_2)...\Xi(x_n)|0\rangle f_h(q_1, q_2, q_3; \Delta)...f_h(q_{m-2}, q_{m-1}, q_m; \Delta) \quad (4.110)$$

We can use the following identity [1],

$$T\left\{\exp\left(-i\int d^4x\Xi(x).j(x)\right)\right\} =: \exp\left(-i\int d^4x\Xi(x).j(x)\right): \\ \times\exp\left(-\frac{1}{2}\int\int d^4xd^4y\langle 0|T\{\Xi(x).j(x)\Xi(y).j(y)\}|0\rangle\right) \quad (4.111)$$

to derive Wicks theorem for the asymptotic fields. We expand the exponentials in this identity and identify the coefficients of $j(x)$ to generate identities order by order. If we then calculate the vacuum expectation of these identities we get the following [1],

$$\langle 0|T\{\Xi(x_1)...\Xi(x_n)\}|0\rangle \\ = \begin{cases} 0 & : \text{odd n} \\ \sum_P\langle 0|T\{\Xi(x_1)\Xi(x_2)\}|0\rangle...\langle 0|T\{\Xi(x_{n-1})\Xi(x_n)\}|0\rangle & : \text{even n} \end{cases} \quad (4.112)$$

where P is a sum over all permutations of the x_i such that we only count $\langle 0|T\{\Xi(x_1)\Xi(x_2)\}|0\rangle$ and $\langle 0|T\{\Xi(x_2)\Xi(x_1)\}|0\rangle$ as a single contributing term. So we see that we get the sum over all possible contractions of the asymptotic fields in the same way as for the usual free field case except we must multiply by these by the hard factors from each vertex. So to derive the amplitude we need only the propagator of the asymptotic fields

The fermion propagator

Unlike in the standard case we cannot solve the propagator exactly. Instead we will have to calculate it perturbatively. To do this we take the full Heisenberg picture of the asymptotic fields Ξ fields and make the usual transformation into the interaction picture using the following evolution operator also in the interaction picture,

$$U_{\Delta}(t,t') = T\left\{\exp\left(-i\int_{t'}^{t} dt'' H_{IR}(t'')\right)\right\} \tag{4.113}$$

The fields in H_{IR} are now in the interaction picture. The propagator is given by the two point correlation function of the asymptotic fields. In the case of a fermionic propagator this gives,

$$\begin{aligned} S_{\Xi}(x_1-x_2) &= \langle 0|T\{\Xi(x_1)\overline{\Xi}(x_2)\}|0\rangle \\ &= \langle 0|T\left\{\phi(x_1)\overline{\phi}(x_2)\exp\left(-i\int_{-\infty}^{\infty} d^4x\mathcal{L}_{IR}(x)\right)\right\}|0\rangle \end{aligned} \tag{4.114}$$

The first order of Eq.(4.114) that contributes is at zero order in the coupling,

$$S_{\Xi,0}(x_1-x_2) = i\int \frac{d^4p}{(2\pi)^4}\frac{\not{p}}{p^2+iO_+}e^{-ip(x_1-x_2)} \tag{4.115}$$

which is the usual free field propagator. Higher order terms will then apply corrections to this. We split up all the higher order terms into the 1PI diagrams Σ_{Ξ}. To get the "complete" solution we would then sum the perturbation series to all orders,

$$S_{\Xi} = S_{\Xi,0} + S_{\Xi,0}\Sigma_{\Xi}S_{\Xi,0} + S_{\Xi,0}\Sigma_{\Xi}S_{\Xi,0}\Sigma_{\Xi}S_{\Xi,0} + \ldots \tag{4.116}$$

Which gives,

$$S_{\Xi} = S_{\Xi,0}\left(1+\Sigma_{\Xi}\left(S_{\Xi,0}+S_{\Xi,0}\Sigma_{\Xi}S_{\Xi,0}+\ldots\right)\right)$$

$$S_\Xi = S_{\Xi,0}\left(1+\Sigma_\Xi S_\Xi\right) \tag{4.117}$$

This can be rewritten as,

$$S_\Xi = \frac{S_{\Xi,0}}{1-S_{\Xi,0}\Sigma_\Xi} \tag{4.118}$$

To derive an explicit form for this we need to calculate Σ_Ξ. We will do this perturbatively order by order in the coupling.

We will consider the case of the fermion propagator in QED. This will contain a single three point fermion-antifermion-photon vertex. We calculate Σ_Ξ using standard field theory techniques. From Eq.(4.114) we see that there is no first order term and so the first contribution to Σ_Ξ will be at second order and is given by,

$$\begin{aligned}
\Sigma_\Xi\Big|_2 &= \frac{1}{2!}\int_{-\infty}^{\infty} d^4x d^4y \langle 0|T\left\{\phi(x_1)\overline{\phi}(x_2)\mathcal{L}_{IR}(x)\mathcal{L}_{IR}(y)\right\}|0\rangle \\
&= (-ig^2)\int \frac{d^4k}{(2\pi)^4}\frac{\gamma^\mu(\not{p}+\not{k})\gamma_\mu}{(k^2+iO_+)\left((p+k)^2+iO_+\right)} f_s^2(p+k,k,p;\Delta) \\
&= (D-2)ig^2\int \frac{d^4k}{(2\pi)^4}\frac{(\not{p}+\not{k})f_s^2(p+k,k,p;\Delta)}{(k^2+iO_+)\left((p+k)^2+iO_+\right)}
\end{aligned} \tag{4.119}$$

where k and p are both off-shell. IR divergences will only appear in this integral when p goes on-shell and our f_s functions will cut off the higher energy regions of the integrals. Therefore we can perform this integral in $D=4$ dimensional space without any UV or IR regulators. We will see later that the possible IR divergence coming from this diagram when p goes on-shell will not be a problem.

We can perform the majority of the integrals of Eq.(4.119) analytically, this gives the result,

$$\begin{aligned}
\Sigma_\Xi\Big|_2 &= \frac{2ie^2\not{p}}{(2\pi)^4}\int_0^\infty dx \frac{\pi^{5/2}}{\sqrt{(1+x)^3(p^2/\Delta)}}\exp\left(-(3+x)\frac{p^2}{\Delta}\right) \\
&\quad \times \mathrm{Erfi}\left(\frac{x}{\sqrt{1+x}}\sqrt{\frac{p^2}{\Delta}}\right) \\
&= ie^2\not{p}F_\Xi(p^2/\Delta)
\end{aligned} \tag{4.120}$$

where,

$$\mathrm{Erfi}(z) = \frac{-2i}{\sqrt{\pi}} \int_0^{iz} dt e^{-t^2} \tag{4.121}$$

We see that this result only depends upon the single scale p^2/Δ. The remaining integral would have to be done numerically.

Checking the limits

We will now investigate this result by checking that we get the expected results when we take the $\Delta \to 0$ and $p^2 \to 0$ limits. We know from Eq.(4.120) that the integral only depends upon the ratio of p^2 and Δ and therefore we must always take these limits simultaneously. We will assume that we can swap the order of the integration and these limits, although this is not entirely rigorous. Taking p^2 fixed to be finite and non-zero then the $\Delta \to 0$ limit gives,

$$\begin{aligned}\int_0^\infty dx \lim_{\Delta\to 0} \frac{\pi^{5/2}}{\sqrt{(1+x)^3(p^2/\Delta)}} \exp\left(-(3+x)\frac{p^2}{\Delta}\right) \mathrm{Erfi}\left(x\sqrt{\frac{(p^2/\Delta)}{1+x}}\right) \\ \to 0 \end{aligned}\tag{4.122}$$

Which is the expected result as the asymptotic propagator should become the free propagator as we shrink the soft region down to zero. Therefore all the correction terms need to vanish.

For the limit $p^2 \to 0$ we take Δ fixed to be finite and non-zero and get,

$$\begin{aligned}&\int_0^\infty dx \lim_{p^2\to 0} \frac{\pi^{5/2}}{\sqrt{(1+x)^3(p^2/\Delta)}} \exp\left(-(3+x)\frac{p^2}{\Delta}\right) \mathrm{Erfi}\left(x\sqrt{\frac{(p^2/\Delta)}{1+x}}\right) \\ &\to \int_0^\infty dx \frac{2\pi^2 x}{(1+x)^2} \to \infty\end{aligned}\tag{4.123}$$

Now this integral diverges and so we have found the expected return of the infrared divergences when the propagator goes on-shell.

The fermion propagator

Now that we have calculated the one-loop 1PI term we can give the form for the asymptotic fermion propagator in QED at one-loop. We start from Eq.(4.117),

$$S_\Xi(p) \quad = \quad S_{\Xi,0}(p)\left(1+\Sigma_\Xi S_\Xi(p)\right) = \frac{i\not{p}}{p^2+iO_+}\left(1+ie^2\not{p}F_\Xi(p^2,\Delta)S_\Xi(p)\right) \tag{4.124}$$

We can then rearrange this to get,

$$S_\Xi(p) = \frac{i\not{p}}{p^2+iO_+}\frac{1}{1+e^2F_\Xi(p^2/\Delta)} \tag{4.125}$$

This one-loop propagator is all we need to calculate the one-loop amplitudes from Eq.(4.43). This can be seen by expanding the propagator in terms of e, we see that two-loop contributions will only appear at order e^4. The only order below one-loop, is lower in order by e^2 at the most. Therefore this propagator will give the correct answer perturbatively only up to one-loop. For two-loop results we would need to include two loop contributions to the propagator Eq.(4.125).

We can also investigate the behaviour of this propagator as it goes on-shell. We see that,

$$\lim_{p^2\to 0} F_\Xi(p^2/\Delta) \to \infty \tag{4.126}$$

and therefore the propagator will approach zero and not diverge as it goes on-shell, unlike in the normal case. Therefore we avoid any possible IR divergences coming from the propagator. This occurs because we have re-summed all the one-loop 1PI diagrams into the propagator.

The S_A-Matrix elements

Once we have calculated an amplitude from Eq.(4.43) we need to relate this to an S_A-Matrix element. This can be done using the modified LSZ reduction formula from Section 4.3.4. The external legs from the amplitudes generated by Eq.(4.43) will all have propagators of the type given in Eq.(4.125) attached to them.

We know that in the asymptotic limit $\Xi \to Y^{1/2}\phi$ and so we expect,

$$\langle 0|T\{\Xi(x_1)\overline{\Xi}(x_2)\}|0\rangle \to Y\langle 0|T\{\phi(x_1)\overline{\phi}(x_2)\}|0\rangle \tag{4.127}$$

If we compare this with Eq.(4.125) then we see that we can associate in the asymptotic limit,

$$Y(p^2/\Delta) = \frac{1}{1 + e^2 F_\Xi(p^2/\Delta)} \tag{4.128}$$

Now Eq.(4.109) contains a factor Y^{-1} for each external line. Therefore in the same way as the usual case the LSZ reduction formula removes any external leg propagators. The S_A-Matrix elements are then just the residue of the multi-particle pole when the external legs go on-shell as in the standard case. From these S_A-Matrix elements we should then be able to go on and calculate physical observables.

4.4 Conclusion

In this chapter we have demonstrated the difficulties associated with the use of dressed states in the interaction picture. We started by defining the Møller operators $\Omega_A^{(\pm)}$ in the interaction picture. Then when we derived the S_A operator from these Møller operators we ran into inconsistencies in the interaction picture. The amplitudes were all derived in time ordered perturbative theory, which produces many diagrams. To reduce the number of diagrams we then attempted to combine these time ordered diagrams into reduced numbers of covariant diagrams. We saw that this was impossible though we could combine them into an almost covariant form. This required the choice of a suitable asymptotic Hamiltonian, the form of which would unfortunately mix the soft and hard regions together.

The problem with the overall delta function factors is more difficult to solve. Attempting to use the true asymptotic basis of states when performing interaction picture calculations would force us to relate the asymptotic states to the free states. The only operator which can do this though is infrared divergent itself and so is of little practical benefit.

These difficulties when working in the interaction picture then motivated us to instead suggest the use of the asymptotic interaction picture. We then gave a brief overview of how we can modify the usual covariant field theory techniques to produce covariant Feynman diagrams from correlation functions of asymptotic fields in the asymptotic interaction picture. We were then able to prove that such amplitudes are infrared finite. To work in the asymptotic interaction picture we needed a solution for the asymptotic field propagator. We were able to outline how this could be done perturbatively and then derived a form for a fermion propagator in QED. Also we gave a heuristic derivation of a modified LSZ reduction formula which would take these correlation functions and relate them to S_A matrix elements calculated on the asymptotic states. This lead on to a discussion of the asymptotic states and their dependence upon Δ. These discussions on the asymptotic interaction picture did not attempt to be completely rigorous and instead gave an outline of how calculations in the asymptotic interaction picture could proceed.

Chapter 5

Conclusions and Outlook

In this thesis we have discussed various different methods of producing scattering amplitudes for massless quantum field theories which are entirely free of infrared divergences. The motivation for deriving a formalism to produce such amplitudes was outlined in Chapter 1. Currently general techniques exist to calculate physical observables at the NLO level using amplitudes that contain infrared divergences. One of the main difficulties with proceeding to calculate physical observables at NNLO is the proliferation of infrared divergences in higher order amplitudes. General techniques do not exist for calculating such amplitudes and therefore amplitudes without infrared divergences in would be of great benefit.

In chapter 2 we gave an overview of the scattering theory that we would use throughout the rest of this thesis. Starting from the overlap of the initial and final states of the process being calculated we showed how amplitudes could be derived in time ordered perturbation theory instead of the usual covariant perturbation theory. During this derivation the fundamental source of infrared singularities became apparent. In the usual field theory approach the standard assumption that the asymptotic Hamiltonian is equivalent to the free field Hamiltonian leads to Møller operators which are not isometric. This is one of the fundamental requirements of a Møller operator and this broken requirement manifests itself as the infrared singularities that appear in the usual scattering amplitudes.

From this we were able to suggest two different directions to take to produce amplitudes which were free of infrared singularities. The method we looked at first and in the greatest detail was that of *dressed* states. In Chapter 3 we showed how such amplitudes can be constructed by separating the interaction Hamiltonian into two parts. One part contained all the hard interactions of the theory and the other part, which we called the asymptotic interaction, contained all the soft and collinear parts of the interaction. Using this asymptotic Hamiltonian we derived an operator which "dressed" the initial and final states of the usual S-Matrix to produce new scattering amplitudes. In doing this we removed any infrared singularities from the amplitudes. We then went on to give an example calculation using these amplitudes to produce the total cross section for $e^+e^- \to 2$ jets at NLO. This demonstrated the complete cancellation of the infrared singularities at the amplitude level with the final answer the same as that produced using standard techniques. Thus showing that these dressed amplitudes gave the same results as the standard methods.

The construction used in Chapter 3 to produce the dressed state amplitudes was rather cumbersome. In order to exploit the advantage of the infrared finiteness in higher order calculations we would need a more streamlined approach. So in Chapter 4 we focused on fixing the two distinct problems that the formalism suffered from. The first was that the amplitudes were constructed from separate pieces which were themselves infrared divergent. So although the final amplitude was infrared finite the intermediate steps were not necessarily so, this would mean that a purely numerical approach would be difficult to implement. The second problem was that the pieces once combined were not all multiplied by the same energy delta function. Instead separate pieces of the amplitude were multiplied by different energy delta functions which differed by a soft/collinear energy difference. This means that the calculation of physical observables from these amplitudes becomes difficult due to the need to "square" the different delta functions in the amplitude.

To solve the first of these problems we looked at calculating all the separate infrared finite pieces of the amplitude together using a new S operator, the asymptotic S_A operator. The amplitudes would then be infrared finite at every step of the calculation. The difficulty with this was that such amplitudes were described in terms of time ordered perturbation theory. This meant that we would generate large numbers of diagrams even for simple processes. To avoid this problem we then attempted to combine the time ordered diagrams into a reduced number of completely covariant amplitudes. The difficulties with this were related to the way in which we split the hard from the soft region in the Hamiltonian. We found that it was impossible to choose a splitting such that we could produce a covariant amplitude. It was though possible to reduce the time ordered diagrams down to a reduced number of almost covariant diagrams.

After this there was the second problem of the different delta functions within each amplitude. The root cause of which was that the S_A operator does not commute with H_0 which defines the basis of free states $|\phi_\alpha\rangle$ which we calculated on. Solving this problem would require the use of the eigenstates of the asymptotic Hamiltonian as our basis of states. Unfortunately it can be shown that the only way of perturbatively relating the asymptotic states to the free states in the interaction picture is itself infrared divergent and therefore of no practical benefit.

These difficulties lead us to abandoning the use of the interaction picture entirely and to instead investigate the use of the asymptotic interaction picture. The remainder of the thesis then focused on giving an indication of how such a formalism could be constructed. We defined the asymptotic interaction picture and presented an overview of how calculations could be performed. We showed how we could construct correlation functions from asymptotic fields rather than the usual free fields. We showed that we could use Wicks theorem to reduce these correlation functions to products of two point correlations functions. We then derived a perturbative form for the asymptotic fermion propagator in QED to the one-loop level. We then showed that this was infrared finite in the limit that the propagator momentum goes on-shell.

In order to relate the asymptotic field correlation functions to S_A-Matrix elements calculated using the S_A operator on the asymptotic states we needed a modified LSZ reduction formalism, for which we gave a brief overview of a derivation. The exact form of these asymptotic states was discussed briefly. The asymptotic Hamiltonian that we use throughout this thesis depends upon a parameter Δ that defines the splitting of the hard from the soft region. The real asymptotic Hamiltonian of the theory contains no such parameter, so an important question is how do our asymptotic states relate to the detected states in an experiment. We would expect any physical process to not depend upon any internal parameter. On closer examination it appears that the amplitudes should be independent of Δ. This dependence though may return because we cannot calculate the asymptotic propagators to all orders. The amplitudes may then depend on to which perturbative order we calculated the propagators to. As well as this we also suspect that the definitions of measurement functions for physical observables may differ from those used in the asymptotic free field case. Defining these though should not present any fundamental difficulties as the usual choice of the free external states does not match the true asymptotic Hamiltonian either. In conclusion therefore the meaning of these states remains an open question at the moment and requires much further work.

The aim of future work will, as well as focusing on the definition of these states and their consequences to the calculation of physical observables, also look at producing the amplitudes themselves in the asymptotic interaction picture. This will require a rigorous derivation of a modified LSZ reduction formula along with a much deeper understanding of the asymptotic states themselves. We will need to derive forms for the propagators initially at the one-loop level but for further work at the two-loop level. The amplitudes themselves will have to be numerically integrated due to the difficulty of analytically performing the loop integrals in the amplitudes. Although there would appear to be no fundamental difficulties in doing this we would have to set up the numerical cancellation of UV divergences as in [12]. Most importantly of all, explicit checks on the results produced by these amplitudes are required. Initially this would involve the calculation in this formalism of the total cross section for $e^+e^- \to 2$ jets at NLO. Afterwards more challenging process and observables would need to be investigated. Until we have compared such results against known data this whole technique must remain as only a possible solution to the infrared problem.

Acknowledgements

Firstly my deepest thanks must go to my supervisor Adrian Signer for all his help and guidance throughout the three years of my PhD. I would also like to thank Mark who has also worked in the world of infrared singularities with me for the last year and a half and also Gareth who has recently just started as well.

Next I would like thank Michael, who proofread chapter 4 of this thesis and so any mistakes in there are clearly his fault! Also I would like to thank everyone else in my office including James, Graeme and George for many conversations related to and not related to physics.

Finally I should like to thank everyone else in the IPPP for making this an enjoyable place to work in for the last three years.

Appendix A

A Dressed State Example Calculation

In this Appendix we give some details concerning the evaluation of the diagrams mentioned in Section 3.2.4.

We consider first with the self-interaction term $a_{15}^{\{2,0\}}$ of Section 3.2.4. We start from Eq. (3.49), substitute $\not{p}_1 - \not{q}_3 + \not{r}$ for $\{\not{p}_1 - \not{q}_3\}$, where $r = (r_0, \vec{0})$ with $r_0 = \rho(\vec{q}_3, \vec{p}_1 - \vec{q}_3)$ and then expand the numerator to obtain

$$\begin{aligned} a_{15}^{\{2,0\}} &= \frac{(-ie)\, g^2}{4} T^a_{ik} T^a_{kj}\, (2\pi)^D \delta^{(D)}(P - p_1 - p_2) \int \mathrm{d}\widetilde{q}_3\ \Theta(\Delta - |r_0|) \\ & \left((D-2)((p_1 q_3) - (p_1 r)) - \frac{4(p_1 q_3)(p_1 \overline{q}_3)}{(q_3 \overline{q}_3)} - \frac{2 r_0 (p_1 q_3)(p_2 q_3)}{\omega(\vec{p}_1)(q_3 \overline{q}_3)} \right) \\ & \frac{\langle p_1 | \gamma^\alpha | p_2 \rangle}{\omega(\vec{p}_1)\, \omega(\vec{p}_1 - \vec{q}_3)\, r_0^2} \end{aligned} \tag{A.1}$$

This expression contains infrared singularities coming from the region where q_3 is soft and/or collinear to p_1. In order to evaluate the expression, Eq. (A.1) we choose to parameterize the momenta in the center-of-mass frame. The momenta are all on-shell and are defined as

$$\begin{aligned} P &= \sqrt{s}(1, \mathbf{0}, 0), \\ p_1 &= \frac{\xi_{p_1}}{2}(1, \mathbf{0}, 1), \end{aligned}$$

$$
\begin{aligned}
p_2 &= \frac{\xi_{p_1}}{2}(1, \mathbf{0}, -1), \\
q_3 &= \frac{\xi_{p_1}}{2}\, z\,(1, \sqrt{1-y^2}\,\mathbf{e}_T, y), \\
\{p_1 - q_3\} &= \frac{\xi_{p_1}}{2}(\sqrt{1-2zy+z^2}, -z\sqrt{1-y^2}\,\mathbf{e}_T, 1-zy),
\end{aligned} \tag{A.2}
$$

where $\mathbf{0}$ is the null vector in a $(2-2\epsilon)$-dimensional space, $\mathbf{e}_T$ is a unit vector in the $(2-2\epsilon)$-dimensional transverse momentum space and we have $0 \leq z \leq \infty$, $-1 \leq y \leq 1$. The singular limits are then given by the limits $z \to 0$ for soft singularities, $y \to 1$ for $q_3 \| p_1$ singularities and $y \to -1$ for $q_3 \| p_2$ singularities. As the asymptotic region does not conserve energy we find that the upper limit of z goes to ∞. This would suggest the possibility of UV singularities in the asymptotic regions. However we will see that the Θ function will restrict this upper limit to a finite value, removing the need to renormalize these regions. The integral measure is given by

$$
\begin{aligned}
&\int \mathrm{d}\widetilde{q}_3\ \Theta(\Delta - r_0) \to \\
&\quad \left(\frac{\mu^2}{s}\right)^{\epsilon} \frac{1}{2(2\pi)^{3-2\epsilon}}\, \frac{\xi_{p_1}^2}{4}\, z^{1-2\epsilon}(1-y)^{-\epsilon}\,(1+y)^{-\epsilon}\, dy\, dz\, d\Omega_{(2-2\epsilon)}
\end{aligned} \tag{A.3}
$$

where we have three separate integration regions for the z and y integrals,

$$
\begin{aligned}
0 \leq z \leq \frac{\Delta}{2}\frac{(2+\Delta)}{(1-y+\Delta)} \quad &\text{with} \quad -1 \leq y \leq \frac{2-\Delta^2}{2}, \\
0 \leq z \leq 1 \quad &\text{with} \quad \frac{2-\Delta^2}{2} \leq y \leq 1, \\
1 \leq z \leq \frac{\Delta}{2}\frac{(2+\Delta)}{(1-y+\Delta)} \quad &\text{with} \quad \frac{2-\Delta^2}{2} \leq y \leq 1.
\end{aligned}
$$

The infrared singularities are in the first two regions whereas the last region will give a finite contribution. The remaining angular integral is given by

$$
\int d\Omega_{(2-2\epsilon)} = \frac{2\pi^{1-\epsilon}}{\Gamma(1-\epsilon)}. \tag{A.4}
$$

We now turn back to Eq. (A.1) and notice that the infrared singularities q_3

soft and/or collinear to p_1 come from the region $z = 0$ and $y = 1$ but not $y = -1$. We use the subtraction method to isolate these singularities and evaluate them analytically. Writing the integrand schematically as a function $F(z, y)$ we write

$$\begin{aligned} F(z,y) &= (F(0,y) + F(z,1) - F(0,1)) \\ &+ (F(z,y) - F(0,y) - F(z,1) + F(0,1)) . \end{aligned} \tag{A.5}$$

The first term contains all the divergent pieces whereas the second term will give a finite contribution upon integration over $d\widetilde{q}_3$. Applying this method to Eq. (A.1) we obtain

$$\begin{aligned} a_{15}^{\{2,0\}} &= (-ie)\, g^2\, T^a_{ik} T^a_{kj} \left(\frac{\mu^2}{s}\right)^{\epsilon} \frac{1}{2(2\pi)^{3-2\epsilon}}\, (2\pi)^D \delta^{(D)}(\vec{P} - \vec{p}_1 - \vec{p}_2) \\ & \langle p_1|\gamma^\alpha|p_2\rangle \int d\Omega_{(2-2\epsilon)}\, dy\, dz\, z^{1-2\epsilon}\, (1-y)^{-\epsilon}\, (1+y)^{-\epsilon} \\ & \times \left(\frac{(2-D)}{4(1-y)} + \frac{(2z-1-y)}{2(1-y)z^2} + f_1(p_1, p_2, q_3) \right) \end{aligned} \tag{A.6}$$

where

$$\begin{aligned} & f_1(p_1, p_2, q_3) = \\ & \quad \frac{\omega(\vec{p}_1)^2}{2\omega(\vec{p}_1 - \vec{q}_3)\, r_0} \left(1 - \frac{(p_1 q_3)}{\omega(\vec{p}_1)\, r_0} - \frac{(p_1 q_3)(p_2 q_3)}{\omega(\vec{p}_1) r_0 (q_3 \overline{q}_3)} \left(2 - \frac{r_0}{\omega(\vec{p}_1)} \right) \right) \\ & \quad - \frac{\omega(\vec{p}_1)^2}{2(p_1 q_3)} \left(- \frac{\omega(\vec{q}_3)}{\omega(\vec{p}_1)} - \frac{(p_2 q_3)}{\omega(\vec{q}_3)^2} + 2 \right). \end{aligned} \tag{A.7}$$

Integrating the singular terms and expanding around $\epsilon = 0$ we obtain Eq. (3.51). Note that the D in the first term of Eq. (A.6) arises from the γ-matrix algebra. Thus we write it as $D = 4 - 2\epsilon + c_R 2\epsilon$ to obtain the expressions in conventional dimensional regularization ($c_R = 0$) and in dimensional reduction ($c_R = 1$).

Let us now turn to the evaluation of $a_{18}^{\{2,0\}}$ needed in Section 3.2.4. We start with the expression Eq. (3.54) and proceed in the same way as for $a_{15}^{\{2,0\}}$. We introduce the on-shell momenta $\{\not{p}_1 - \not{q}_3\} = \not{p}_1 - \not{q}_3 + \not{r}'$ and $\{\not{p}_2 + \not{q}_3\} = \not{p}_2 + \not{q}_3 - \not{r}''$, where $r' = (r'_0, \vec{0})$ with $r'_0 = \rho(\vec{q}_3, \vec{p}_2) = \omega(\vec{q}_3) + \omega(\vec{p}_2) - \omega(\vec{p}_2 + \vec{q}_3)$.

In order to proceed we subtract the soft singularity in Eq. (3.54) and add it back to produce an integrand that results in a non-singular term. In the soft limit the D-dimensional delta function becomes the usual $\delta^{(D)}(P - p_1 - p_2)$ which can be pulled out from the integral.

We use the same momentum parametrization as for the self-interacting case, but because of the extra Θ function the integration ranges change to

$$\begin{aligned} 0 \leq z \leq \frac{\Delta}{2}\frac{(2+\Delta)}{(1-y+\Delta)} \quad &\text{with} \quad -1 \leq y \leq \frac{\Delta}{2}, \\ 0 \leq z \leq -\frac{\Delta}{2}\frac{(2-\Delta)}{(1+y-\Delta)} \quad &\text{with} \quad \frac{\Delta}{2} \leq y \leq 1 \end{aligned}$$

The remaining angular integral is as given in Eq. (A.4).

Using this momentum parametrization and expanding around the soft region gives

$$\begin{aligned} a_{18}^{\{2,0\}} &= -T^a_{ik}T^a_{kj}\left(\frac{\mu^2}{s}\right)^{\epsilon}(-ie)\,g^2\,\frac{1}{2(2\pi)^{3-2\epsilon}}\,(2\pi)^D\delta^{(D-1)}(\vec{P}-\vec{p}_1-\vec{p}_2) \\ &\quad \langle p_1|\gamma^\alpha|p_2\rangle \int d\Omega_{(2-2\epsilon)}\,dy\,dz\,z^{1-2\epsilon}\,(1-y)^{-\epsilon}\,(1+y)^{-\epsilon} \\ &\quad\quad \times \left(\frac{1}{2z^2}\delta(\sqrt{s}-\omega(\vec{p}_1)-\omega(\vec{p}_2)) + f_2(p_1,p_2,q_3)\right) \end{aligned} \tag{A.8}$$

with

$$\begin{aligned} f_2(p_1,p_2,q_3) &= \frac{\omega(\vec{p}_1)^2}{2\omega(\vec{p}_1-\vec{q}_3)\,r_0\,\omega(\vec{p}_2+\vec{q}_3)\,r_0'}\Bigg((p_1p_2)+(p_1q_3)-(p_2q_3) \\ &+ \omega(\vec{p}_1)r_0 - \omega(\vec{p}_1)r_0' - \frac{r_0r_0'}{2} + \frac{(p_1q_3)r_0}{2\omega(\vec{p}_1)} + \frac{(p_2q_3)r_0'}{2\omega(\vec{p}_1)} \\ &- \frac{(p_1q_3)(p_2q_3)}{2\omega(\vec{p}_1)^2} - \frac{1}{2(q_3\overline{q}_3)}\Bigg(\frac{(p_1q_3)^3}{\omega(\vec{p}_1)^2}\left(1+\frac{r_0}{2\omega(\vec{p}_1)}\right) \\ &- \frac{(p_2q_3)^3}{\omega(\vec{p}_1)^2}\left(1-\frac{r_0'}{2\omega(\vec{p}_1)}\right) + \left(2+\frac{r_0}{\omega(\vec{p}_1)} - \frac{r_0'}{\omega(\vec{p}_1)} - \frac{r_0r_0'}{\omega(\vec{p}_1)^2}\right) \\ &\quad \left((p_1q_3)^2+(p_2q_3)^2\right)\Bigg)\Bigg)\delta(\sqrt{s}-\omega(\vec{p}_1)-\omega(\vec{p}_2)-r_0+r_0') \\ &- \frac{\omega(\vec{p}_1)^2}{2\omega(\vec{q}_3)^2}\delta(\sqrt{s}-\omega(\vec{p}_1)-\omega(\vec{p}_2)). \end{aligned} \tag{A.9}$$

Upon performing the integration of the singular terms explicitly and expanding in ϵ we get Eq. (3.56). In this case the expression is the same in conventional dimensional regularization and dimensional reduction.

Finally we turn to the evaluation of $a_1^{\{1,1\}}$ needed in Section 3.2.4, proceeding as in the previous cases. We subtract the soft and collinear singular parts and integrate them analytically. In both limits the D-dimensional delta function takes its usual form $\delta^{(D)}(P-p_1-p_2)$. Thus, the delta function is independent of the integration variables and can be taken outside the integral, as in the one-gluon exchange terms.

We can use the same momentum parametrization and integration regions as the self-interacting case as we have the same Θ function in both cases. Taking the $z \to 0$ and $y \to 1$ limits of the above terms we obtain

$$
\begin{aligned}
a_1^{\{1,1\}} \;=\; & (-ie)\, g^2\, T^a_{ik} T^a_{kj} \left(\frac{\mu^2}{s}\right)^{\epsilon} \frac{1}{2(2\pi)^{3-2\epsilon}} (2\pi)^D \delta^{(D-1)}(\vec{P}-\vec{p}_1-\vec{p}_2) \\
& \langle p_1|\gamma^\alpha|p_2\rangle \int d\Omega_{(2-2\epsilon)}\, dy\, dz\, z^{1-2\epsilon}\, (1-y)^{-\epsilon}\, (1+y)^{-\epsilon} \\
& \times \left(\frac{4-4z+(D-2)z^2}{2(1-y)z^2}\delta(\sqrt{s}-\omega(\vec{p}_1)-\omega(\vec{p}_2)) + f_3(p_1,p_2,q_3)\right)
\end{aligned}
\tag{A.10}
$$

where

$$
\begin{aligned}
f_3(p_1,p_2,q_3) = & \frac{\omega(\vec{p}_1)^2}{2\omega(\vec{p}_1-\vec{q}_3)r_0(\{p_1-q_3\}q_3)} \Bigg(r_0^2 + 2\, r_0\, \omega(\vec{p}_1) \\
& - (p_1q_3)\left(2+\frac{r_0}{\omega(\vec{p}_1)}\right) + \frac{(p_1q_3)(p_2q_3)}{(q_3\overline{q}_3)}\left(2+\frac{2r_0}{\omega(\vec{p}_1)}+\frac{r_0^2}{2\omega(\vec{p}_1)^2}\right)\Bigg) \\
& + \frac{\omega(\vec{p}_1)^2}{2\omega(\vec{p}_1-\vec{q}_3)r_0(p_2q_3)}\Bigg(2(p_1p_2)+(p_1q_3)\left(2+\frac{r_0}{\omega(\vec{p}_1)}-\frac{(p_2q_3)}{\omega(\vec{p}_1)^2}\right) \\
& - 2(p_2q_3) + 2r_0\omega(\vec{p}_1) - \frac{(p_1q_3)^2}{(q_3\overline{q}_3)}\Bigg(2+\frac{r_0}{\omega(\vec{p}_1)} \\
& + \frac{(p_1q_3)}{\omega(\vec{p}_1)^2}\left(1+\frac{r_0}{2\omega(\vec{p}_1)}\right)\Bigg)\Bigg)\delta(\sqrt{s}-\omega(\vec{p}_1)-\omega(\vec{p}_2)-r_0) \\
& - \omega(\vec{p}_1)^2\Bigg(\frac{(p_1p_2)}{(p_1q_3)(p_2q_3)} + \frac{\omega(\vec{q}_3)}{\omega(\vec{p}_1)(p_1q_3)} + \frac{(p_2q_3)}{2(p_1q_3)\omega(\vec{q}_3)^2}
\end{aligned}
$$

$$- \frac{(p_1 q_3)}{2(p_2 q_3)\omega(\vec{q}_3)^2} - \frac{2}{(p_1 q_3)}\Bigg)\delta(\sqrt{s} - \omega(\vec{p}_1) - \omega(\vec{p}_2)). \tag{A.11}$$

Integrating the singular terms with $D = 4 - 2\epsilon + c_R 2\epsilon$ and expanding around $\epsilon = 0$ we obtain Eq. (3.59).

References

[1] C. Itzykson and J. Zuber, *Quantum Field Theory* McGraw-Hill, 1980.

[2] M. E. Peskin and D. V. Schroeder, *An Introduction to Quantum Field Theory* Persus Books, 1995.

[3] S. Weinberg, *The Quantum Theory Of Fields : Vol I*, CUP, 1995.

[4] S. J. Brodsky, H. Pauli and S.S.Pinsky, Physics Reports **301** (1998) 299-486.

[5] F. Bloch and A. Nordsieck, Phys. Rev. **52**, 54 (1937).

[6] T. Kinoshita, J. Math. Phys. **3**, 650 (1962);

T. D. Lee and M. Nauenberg, Phys. Rev. **133**, B1549 (1964).

[7] R. K. Ellis, W. J. Stirling and B. R. Webber, *QCD and Collider Physics* CUP, 1996.

[8] Editor: A. H. Mueller, *Perturbative Quantum Chromodynamics* World Scientific Publishing, 1989.

[9] W. T. Giele and E. W. N. Glover, Phys. Rev. D **46**, 1980 (1992).

[10] S. Frixione, Z. Kunszt and A. Signer, Nucl. Phys. B **467**, 399 (1996) [arXiv:hep-ph/9512328];

[11] S. Catani and M. H. Seymour, Nucl .Phys. B**485** (1997) 291-419, [Erratum-ibid. B**510** (1997) 503-504],[arXiv:hep-ph/9605323].

[12] Z. Nagy and D. E. Soper, QCD matrix elements, JHEP **0309**, 055 (2003) [arXiv:hep-ph/0308127].

[13] T. Gehrmann and E. Remiddi, hep-ph/0101147.
P. Mastrolia and E. Remiddi, Nucl. Phys. Proc. Suppl. **116**, 412 (2003) [hep-ph/0211210];
V.A. Smirnov, Nucl. Phys. Proc. Suppl. **116**, 417 (2003) [hep-ph/0209295].

[14] T. Gehrmann, hep-ph/0211169; Int. J. Mod. Phys. A**19**, 851 (2004) [hep-ph/0310178];
E.W.N. Glover, Nucl. Phys. Proc. Suppl. **116**, 3 (2003) [hep-ph/0211412];
Z. Bern, Nucl. Phys. Proc. Suppl. 117, 260 (2003) [hep-ph/0212406].

[15] S. Catani, Phys. Lett. B**427** (1998) 161-171, ,[arXiv:hep-ph/9802439].

[16] G. Sterman and M. E. Tejeda-Yeomans, Phys. Lett. B**552** (2003) 48-56, [arXiv:hep-ph/0210130].

[17] Z. Bern, L. J. Dixon and D. A. Kosower, [arXiv:hep-ph/0404293].

[18] S D. Badger and E. W. N. Glover, [arXiv:hep-ph/0405236].

[19] Z. Bern,V. Del Duca and C. R. Schmidt, Phys. Lett. B**445** (1998) 168, [arXiv:hep-ph/9810409];
Z. Bern, V. Del Duca, W. B. Kilgore and C. R. Schmidt, Phys. Rev. D**60** (1999) 116001, [arXiv:hep-ph/9903516].

[20] C. Anastasiou, K. Melnikov and F. Petriello, Phys. Rev. D**69** (2004) 076010, [arXiv:hep-ph/0311311].

[21] J. M. Campbell and E. W. N. Glover, Nucl. Phys. B**527** (1998) 264, [arXiv:hep-ph/9710255].

[22] S. Catani and M. Grazzini, Phys. Lett. B**446** (1999) 143, [arXiv:hep-ph/9810389];
Nucl. Phys. B**570** (2000) 287, [arXiv:hep-ph/9908523].

[23] A. Gehrmann-De Ridder, T. Gehrmann and E. W. N. Glover, [arXiv:hep-ph/0403057].

[24] C. Anastasiou, K. Melnikov and F. Petriello, [arXiv:hep-ph/0402280].

[25] V. Chung, Phys. Rev. **140**, B1110 (1965).

[26] D. Zwanziger, Phys. Rev. D **7**, 1082 (1973);

D. Zwanziger, Phys. Rev. D **11**, 3481 (1975).

[27] H. F. Contopanagos and M. B. Einhorn, Phys. Rev. D **45**, 1291 (1992).

[28] P. P. Kulish and L. D. Faddeev, Theor. Math. Phys. **4**, 745 (1970)

[29] N. Papanicolaou, Phys. Rep. **24**, No. 4 (1976) 229-313

[30] M. Greco, F. Palumbo, G. Pancheri-Srivastava and Y. Srivastava, Phys. Lett. B **77**, 282 (1978).

[31] D. R. Butler and C. A. Nelson, Phys. Rev. D **18**, 1196 (1978);

C. A. Nelson, Nucl. Phys. B **181**, 141 (1981);

C. A. Nelson, Nucl. Phys. B **186**, 187 (1981).

[32] M. Ciafaloni, Phys. Lett. B **150**, 379 (1985);

S. Catani, M. Ciafaloni and G. Marchesini, Phys. Lett. B **168**, 284 (1986);

S. Catani, M. Ciafaloni and G. Marchesini, Nucl. Phys. B **264**, 588 (1986).

[33] S. Catani and M. Ciafaloni, Nucl. Phys. B **249**, 301 (1985).

[34] J. Frenkel, J. G. Gatheral and J. C. Taylor, Nucl. Phys. B **194**, 172 (1982).

[35] G. Giavarini and G. Marchesini, Nucl. Phys. B **296**, 546 (1988).

[36] F. N. Havemann, PHE-85-14.

[37] V. Del Duca, L. Magnea and G. Sterman, Nucl. Phys. B **324**, 391 (1989).

[38] L. V. Prokhorov, Phys. Usp. **42**, 1099 (1999) [Usp. Fiz. Nauk **169**, 1199 (1999)].

[39] M. Lavelle and D. McMullan, Phys. Rept. **279**, 1 (1997) [arXiv:hep-ph/9509344].

[40] E. Bagan, M. Lavelle and D. McMullan, Annals Phys. **282**, 471 (2000) [arXiv:hep-ph/9909257].

[41] R. Horan, M. Lavelle and D. McMullan, J. Math. Phys. **41**, 4437 (2000) [arXiv:hep-th/9909044].

[42] R. G. Newton, *Scattering Theory of Waves and Particles*, McGraw-Hill, 1966.

[43] Golberger and Watson, *Collision Theory*, Wiley, 1964.

[44] G. Sterman, *An Introduction to Quantum Field Theory* CUP, 1993.

[45] T. Morota, Prog. Theor. Phys. **24** (1960) 1109

[46] G. Sterman, Phys. Rev. D, **17**, 2773 (1978) [arXiv:hep-th/9909044];
S. B. Libby and G. Sterman, Phys. Rev. D, **18**, 4737 (1978) [arXiv:hep-th/9909044].